UNIVERSITY OF CALIFORNIA SAN DIEGO

Design and Analysis of Interconnected Systems: Optimization Algorithms and Linear-Threshold Brain Networks

A dissertation submitted in partial satisfaction of the
requirements for the degree
Doctor of Philosophy

in

Engineering Sciences (Mechanical Engineering)

by

Ahmed Allibhoy

Committee in charge:

Professor Jorge Cortés, Chair
Professor Robert Bitmead
Professor Melvin Leok
Professor Sylvia Herbert
Professor Fabio Pasqualetti

2023

The dissertation of Ahmed Allibhoy is approved, and it is acceptable in quality and form for publication on microfilm and electronically.

University of California San Diego

2023

TABLE OF CONTENTS

LIST OF FIGURES

LIST OF TABLES

ACKNOWLEDGEMENTS

First and foremost I want to extend my deepest gratitude to my advisor, Prof. Jorge Cortés. I am truly astonished by the level of commitment he has toward his students, his meticulous attention to detail, and the sheer breadth and ambitiousness of his research program. I sincerely thank him for his patience, and for taking the time to meet with me 1-1 nearly every week during this $5^1/_2$ year long journey. Jorge represents everything that I aspire to be as a scholar, and I would not be the researcher I am today without his mentorship and support.

I also want to express my appreciation for the rest of my dissertation committee, Prof. Robert Bitmead, Prof. Melvin Leok, Prof. Sylvia Herbert, and Prof. Fabio Pasqualetti. I thank them for the taking the time to serve on my committee and the helpful suggestions and feedback they have provided on this dissretation.

I had the pleasure of collaborating with Federico Celi and Prof. Fabio Pasqualetti for nearly two years on modeling and controlling brain networks. This project opened my eyes to the possibilities of applying control theory to neuroscience, and biological systems more generally. The two years we worked together was one of the most intellectually stimulating periods of my PhD. I thank Fabio for introducing me to what I consider to be the next and greatest frontier in control theory, and Federico for not only being a wonderful collaborator, but also a friend who I always looked forward to catching up with during the SoCal Control Workshops.

I would also like to thank all the current and former members in the research group of Prof. Jorge Cortés and Prof. Sonia Martínez. I consider it an honor to have been a part

of this highly dynamic and accomplished group, and especially want to thank Pio, Priyank, Jaap, Masih, Pol, Paul, Michael, Parth, Nirabhra, Neilabh, Mohammed A., Mohammad K., Scott A., Scott B., Azra, and Dhruv for the discussions during group meetings and numerous incidental interactions which have had an intangible impact on me as a scholar.

My time at UCSD coincided with the Fall 2022 UC-UAW strike, which was the largest academic workers strike in history, and kicked off a wave of academic worker unionization across the country. I had the privilege of being among the thousands of individuals across the state who organized the strike, and while I only had a marginal impact on the ultimate outcome, the experience had a profound effect on me personally. I thank Allie for starting me on my journey as a labor organizer, and Kelvin for his guidance and endless patience while I was inexperienced and just beginning to build up my confidence. I also thank the rest of the UCSD-UAW strike staff: (other) Ahmed, Amy, Adu, Aidee, Laura, and Natalie. I would not have survived those six weeks without them. Next, I thank the rest of the San Diego Joint Council and Organizing Committee, especially Beatrice, Udayan, Hiya, Adam H., Abhik, Maya, Gwen, Danea, and Casey. I could not have asked for a better group of people with whom to experience the highs and lows of organizing. Finally, I thank the other organizers in MAE / MATS, NanoEngineering, and Structural Engineering, including Bill, Jennifer, Evelia, Natalia, Jayden, Robert, Alex, Adam C., Elide, Anna, and Lucas, who ultimately made all of our big wins over the last two years possible.

My experience in grad school was enriched by the other grad students I met during my time here at UCSD. First, I thank Ryan, Anne, and Aditya for being my first real friends I made after moving to San Diego. I also want to shout out the rest of the allium caucus,

Abhik, Anna, Anya, Beatrice, Gwen, Jayden, Jennifer, and Lucas. Though the name and purpose of the group went through many iterations, my friendship with them kept me sane during the final days of the strike and my final year of grad school.

My intellectual journey would not have been possible without the advice and encouragement I received from the late Dr. Alaudin Bhanji. I am eternally indebted to him for his guidance and mentorship through every step of my journey as I progressed from high school, enrolled in community college, transferred to UCLA, and finally applied to PhD programs. Everything that I have accomplished, I owe to him.

Finally I want to extend my appreciation to my entire family for their unconditional love and support over the years, in particular my parents, my grandparents, my sisters Sarah and Sahar, and my cousins, Safia, Samar, and Adam. I would not have made it this far without them.

The research reported in this dissertation was supported in part by the National Science Foundation under Awards IIS-2007141 and CMMI-2044900, the Air Force Office of Scientific Research under Award FA9550-19-1-0235, and the Army Research Office under Grant W911NF-18-1-021.

Chapter 3, in part, is a reprint of the material [AC24] where it appears as "Control-Barrier-Function-Based Design of Gradient Flows for Constrained Nonlinear Programming" by Ahmed Allibhoy and Jorge Cortés in IEEE Transactions on Automatic Control. The dissertation author is the primary investigator and author of this paper.

Chapter 4, in full, is a reprint of material submitted for publication where it may appear as "Anytime Solvers for Variational Inequalities: the (Recursive) Safe Monotone

Flows" by Ahmed Allibhoy and Jorge Cortés in Automatica. The dissertation author is the primary investigator and author of this paper.

Chapter 6, in full, is a reprint of the material [CAPC21] where it appears as "Linear-Threshold Dynamics for the Study of Epileptic Events" by Federico Celi, Ahmed Allibhoy, Fabio Pasqualetti, and Jorge Cortés in IEEE Control Systems Letters. The dissertation author is one of the primary investigators and authors of this paper.

Chapter 7, in full, is a reprint of the material [ACPC22] where it appears as "Optimal Network Interventions to Control the Spreading of Oscillations" by Ahmed Allibhoy, Federico Celi, Fabio Pasqualetti, and Jorge Cortés in IEEE Open Journal of Control Systems. The dissertation author is one of the primary investigators and authors of this paper.

VITA

2018	Bachelor of Science in Mathematics Bachelor of Science in Electrical Engineering University of California, Los Angeles
2020	Master of Science in Engineering Sciences (Mechanical Engineering) University of California San Diego
2023	Doctor of Philosophy in Engineering Sciences (Mechanical Engineering) University of California San Diego

PUBLICATIONS

Journal Publications:

[J1] P. Mestres, **A. Allibhoy**, and J. Cortés, "Robinson's Counterexample and Regularity Properties of Optimization-based Controllers," *Systems & Control Letters*. Submitted.

[J2] **A. Allibhoy** and J. Cortés, "Anytime Solvers for Variational Inequalities: the (Recursive) Safe Monotone Flows," *Automatica*. Submitted.

[J3] **A. Allibhoy** and J. Cortés, Control Barrier Function Based Design of Gradient Flows for Constrained Nonlinear Programming, *IEEE Transactions on Automatic Control*, vol. 69, no. 6, 2024, to appear.

[J4] **A. Allibhoy**, F. Celi, F. Pasqualetti, and J. Cortés, Optimal Network Interventions to Control the Spreading of Oscillations, *IEEE Open Journal of Control Systems*, vol. 1, pp. 141–151, 2022.

[J5] F. Celi, **A. Allibhoy**, F. Pasqualetti, and J. Cortés, Linear-Threshold Dynamics for the Study of Epileptic Events, *IEEE Control Systems Letters*, vol. 5, no. 4, pp. 1405–1410, 2021.

[J6] **A. Allibhoy** and J. Cortés, Data-Based Receding Horizon Control of Linear Network Systems, *IEEE Control Systems Letters*, vol. 5, no. 4, pp. 1207–1212, 2021.

Conference Publications:

[C1] **A. Allibhoy** and J. Cortés, Safety-Critical Control as a Design Paradigm of Anytime Solvers of Variational Inequalities, in *IEEE Conference on Decision and Control*, (Cancun, Mexico), pp. 6211–6216, Dec. 2022.

[C2] **A. Allibhoy** and J. Cortés, Anytime Solution of Constrained Nonlinear Programs via Control Barrier Functions, in *IEEE Conference on Decision and Control*, (Austin, Texas), pp. 6520–6525, Dec. 2021.

[C3] **A. Allibhoy** and J. Cortés, Data-Driven Distributed Predictive Control via Network Optimization, in *Conference on Learning for Dynamics and Control*, vol. 120 of *Proceedings of Machine Learning Research*, pp. 838–839, June 2020.

ABSTRACT OF THE DISSERTATION

Design and Analysis of Interconnected Systems:
Optimization Algorithms and Linear-Threshold Brain Networks

by

Ahmed Allibhoy

Doctor of Philosophy in Engineering Sciences (Mechanical Engineering)

University of California San Diego, 2023

Professor Jorge Cortés, Chair

From the electric power grid, to social networks, to the human brain, many systems of engineering and scientific interest are obtained by interconnecting simpler subsystems. This interconnection can be as simple as a feedback loop, or have a complicated network structure. However, in each case, the dynamic coupling results in complicated behaviors that cannot be explained simply by looking at the constituent components in isolation. This poses two major challenges: first, in terms of developing mathematical models to gain insight into the behavior of complex systems, and second, in terms of optimizing their operation

or controlling them. The goal of this thesis is to develop a mathematical framework to tackle these challenges using tools from nonlinear dynamics, control theory, optimization, and network science.

This thesis is divided into two parts, each focusing on a specific class of interconnected system arising in real world applications. In the first part, we focus on developing a "systems theory" of optimization algorithms, in order to understand their properties and study their interconnection with physical processes. We demonstrate that tools from safety-critical control can be used to synthesize flows solving constrained nonlinear optimization problems, with safety, stability and robustness guarantees that make them ideal for online implementation when interconnected with physical processes. The second part of this thesis discusses mathematical modeling of interconnected neurological systems, in order to understand and control epileptic seizures. We model the epileptic brain with Linear Threshold Networks (LTNs), and analyze the interplay between the network structure and the dynamical properties they exhibit. We characterize conditions on the network structure under which oscillations spread in LTNs, and develop strategies to optimally modify networks to prevent the spread of epileptic seizures.

Chapter 1

Introduction

Engineering interconnected systems are increasingly important in the 21st century, but introduce a number of practical challenges. For example, advances in green technology have resulted in renewable energy resources distributed across the electric power grid, thus reducing our carbon footprint, but it is difficult to coordinate these resources while ensuring reliable operation of the power grid that was designed for a paradigm where energy is generated centrally. Autonomous vehicles promise to make our transportation system safer and more efficient, but initial roll-outs of this technology have exposed deficiencies in their ability to navigate safely while ensuring smooth traffic flow. And in synthetic biology, engineered genetic circuits are on the verge of revolutionizing biotechnology, but circuits designed *in vitro* often do not behave predictably and reliably when embedded within a host cell. Despite the sheer breadth covered by these examples, the fundamental challenge is the same: engineering systems considered in isolation are not enough, one must consider their interactions with other systems.

By interaction we refer to any situation where multiple systems are dynamically coupled, meaning the state of one influences the other and vice versa. This interaction can manifest in many ways, e.g., as a simple feedback loop between two systems, or through a complex network with thousands of nodes. In the network case, a large number of nodes, a lack of full knowledge of the network topology, and heterogeneity contribute to engineering challenges. However, even when the interconnection structure is simple, the dynamical nature of the interactions between components can still cause problems. For example, given two systems which are individually stable, it is possible to couple them in a way such that the aggregate system as a whole is unstable. Other sources of challenges arising from the dynamic aspects of interactions include unknown dynamics, parametric uncertainties, and stochastic noise.

The goal of this dissertation is to build a mathematical framework to tackle challenges that arise in modeling, optimization, and control of interconnected systems. While the tools we develop are broadly applicable, we focus our attention on two specific classes of interconnected systems: online optimization algorithms used to control physical processes and the human brain. Despite the differences in these applications, the mathematical tools we use are remarkably similar. In both cases, the underlying task can be formalized using notions from control theory, we can obtain a set of conditions on the structure and dynamic properties of the interconnection that ensure correct performance, and we can use these conditions to develop a set of design principles for these systems.

1.1 Organization of Thesis

This thesis is divided into two parts. The first part is devoted to the study of the "systems theoretic" properties of optimization algorithms. This perspective allows us to understand the qualitative and quantitative properties of algorithms, study their interconnection with physical processes, and systematically design novel algorithms. Using tools from safety-critical control, we synthesize continuous-time flows solving constrained nonlinear optimization problems, while ensuring the constraint set is forward invariant. This ensures that in real-time applications, feasibility is maintained even when the algorithm is terminated early. We show that these flows have safety and stability properties that make them ideal for their implementation in online feedback optimization problems.

The second part of this thesis discusses mathematical modeling of neurological systems, in order to understand and control epileptic seizures. We model the epileptic brain using a class of network dynamical system called Linear Threshold Networks (LTNs). After performing a detailed bifurcation analysis of planar LTNs, we associate behaviors originating from these bifurcations to prototypical waveforms observed in EEG signals during epileptic seizures. This provides a mathematical characterization of biomarkers associated with epilepsy. Next, we discuss conditions on the network structure under which oscillations spread in LTNs, and develop an optimization-based framework to design networks that are robust to oscillations spreading, providing a path toward effective interventions to mitigate epileptic seizures.

1.2 Statement of Contributions

The unifying theme of this thesis is understanding and controlling interconnected systems that arise in engineering applications, with each part looking at this challenge from a different angle. Part I focuses on the systems-theoretic aspects of optimization algorithms with a view toward interconnecting them with physical properties. Part II considers the brain as a complex networked dynamical system in an effort to model and control epileptic seizures. We describe next in detail our contribution in each chapter.

Chapter 2: We introduce the reader to the idea of analyzing optimization algorithms from a systems-theoretic perspective, and review in detail the literature in this area. We then recall preliminary notions from variational analysis, optimization theory, and safety-critical control which will be used to develop our results in later chapters.

Chapter 3: We consider the synthesis of continuous-time dynamical systems that solve constrained optimization problems while making the feasible set forward invariant and asymptotically stable. Our solution to the problem is a novel continuous-time flow, which we call the *safe gradient flow*. We discuss two equivalent derivations of the system: the first as a gradient flow controlled with a feedback controller implemented as a control barrier function based quadratic program, and the second as as a continuous modification of the projected gradient flow, based on a design parameter. We show that equilibria correspond exactly with critical points of the original optimization problem, and conduct a thorough stability analysis. We provide a suite of constraint qualification-based conditions under which isolated local minimizers are either locally asymptotically stable with respect to the feasible set,

locally asymptotically stable with respect to the global state space, or locally exponentially stable. We also characterize conditions for semistability of nonisolated local minimizers and establish global convergence to critical points of the optimization problem. We compare the safe gradient flow with other continuous-time methods in optimization on a numerical example to illustrate its advantages.

Chapter 4: We extend the framework we developed in Chapter 3 to synthesize continuous-time dynamical systems that solve monotone variational inequalities. We discuss three dynamical systems that solve this problem. The first, the projected monotone flow, is already known, but we discuss a novel reinterpretation of it through the lens of control theory. The second is the safe monotone flow, which analogous to the safe gradient flow, can either be interpreted as a system controlled with a feedback controller synthesized using techniques from safety critical control, or as an approximation of the projected monotone flow. We show that equilibria correspond exactly with critical points of the original problem, and derive global stability guarantees under the additional assumption of convexity and monotonicity. In the case where the constraint set is polyhedral, we establish that the system is contracting. The third flow is the recursive safe monotone flow, which is derived by interconnecting two dynamical systems evolving on different time scales. Using tools from singular perturbation theory for contracting systems, we show that for variational inequalities with polyhedral constraints, the KKT points are locally exponentially stable and globally attracting, and obtain practical stability guarantees. We compare the three flows on a simple example problem. We also demonstrate that the safe monotone flow can be interconnected with dynamical

processes using an example of a receding horizon linear quadratic dynamic game.

Chapter 5: In this chapter we motivate our analysis of brain networks by discussing challenges in the treatment of epilepsy. We discuss how the brain can be interpreted as a network dynamical system and review in detail various models that exist on different spatial scales. Next, we review properties of Linear Threshold Networks, to set the stage for our contributions in the following chapters.

Chapter 6: In this chapter we focus our attention on a specific type of planar Linear Threshold Network, referred to as an excitatory-inhibitory pair (EI pair). We fully characterize the dynamical properties of EI pairs, including computing the equilibrium points, deriving necessary and sufficient conditions for the existence of stable limit cycles, as well as providing a full topological characterization of the possible bifurcation diagrams with the input as the bifurcation parameter. This analysis allows us to show that the behavior of the system in different dynamical regimes approximates prototypical patterns of EEG activity observed before, during, and after epileptic seizures, and relate the transition between different states corresponds to the bifurcations in EI pairs. Our result pave the way to designing control systems that suppress the spread of epileptic seizures.

Chapter 7: In this chapter, we build on results from Chapter 6 to characterize conditions for the spreading of oscillations in brain networks and to formulate and solve optimization problems for the design of networks that are robust to oscillation spreading. In particular, we model the excitatory and inhibitory activity of a small brain tissue (micro-domain) using

networks of coupled EI Pairs. Using these networks, we model the complex interactions among domains of the human brain. Our goal is to exploit the known properties of the single EI pairs to infer global properties of the brain network. Once formal conditions on the spreading of oscillations are derived, we develop and solve a series of optimization problems through which we can efficiently compute conditions to isolate localized oscillations from the rest of the network. We show how these optimization problems are computationally efficient and practically effective. We conclude the discussion with extensive numerical simulations on synthetically generated networks.

Chapter 8: We summarize the contributions of the thesis and propose future directions to extend our work.

Part I

On the Systems Theory of Optimization Algorithms

Chapter 2

On the Systems Theory of Optimization Algorithms

The first part of this thesis concerns progress toward a "systems theory" for optimization algorithms. The idea is to interpret iterative algorithms solving optimization problems – either in continuous time or discrete time – as dynamical systems, and to use tools from control and systems theory to understand them.

There are two primary motivations for this perspective. First, the systems approach opens the door for understanding both qualitative and quantitative properties of algorithms themselves. In practical applications, one seeks guarantees that the algorithm converges to the optimizer, as well as estimates of the convergence rate. Furthermore, the real world is full of uncertainties, which manifest themselves in problems in a myriad of ways, e.g., stochastic noise, parametric uncertainties, unmodeled disturbances. Thus, when deploying optimization algorithms, one needs assurances that their performance would be robust to

these uncertainties. Control theory offers a structured way to reason about the dynamical properties of algorithms and provides tools for quantifying the effects of uncertainty, making this perspective useful for analysis. However, the systems theoretic approach also holds value for the *design* of algorithms, since at its core, control theory is the study of synthesizing dynamical systems with desired properties. The ultimate promise of a "systems theory" for optimization algorithms is to provide a design methodology enabling a user to obtain an algorithm that can handle the specific challenges inherent to their intended application.

The second motivation stems from the interconnection of optimization algorithms with physical processes, a set-up often referred to as *online feedback optimization*. Feedback optimization is required when information relevant to the optimization problem cannot be known a priori, thus necessitating an online approach. This approach also presents an opportunity in situations where the objective function or the constraints of the optimization problem are not known in closed form: solving the optimization problem online allows the evolution of the physical process to "compute" these functions.

Feedback optimization problems arise in many engineering applications e.g., power grids, transportation systems, robotics, and communication networks. A shared feature in all of these examples is that the optimization algorithm is in a feedback loop with a dynamically varying plant, and thus the analysis of the system as a whole is done naturally within a control-theoretic framework. The feedback is due to the fact that the estimate of the solution to the optimization problem is used to influence the state of the plant (e.g., by providing a set-point, specifying the input using an optimization-based feedback controller, steering the plant toward an optimal steady-state), and in turn the state of the plant modifies

the parameters of the optimization problem. The optimization algorithm, when deployed, progresses in parallel to the time evolution of the plant.

We illustrate this set-up diagrammatically in Figure 2.1. On the left, we depict the ideal situation, where the exact solution to the optimization problem is used to regulate the plant. On the right we show the actual implementation, where the optimization problem is solved using a flow that evolves alongside the plant dynamics. The principal challenge in feedback optimization is ensuring the interconnected system behaves optimally, which leads one to consider questions such as: does the trajectory $u(t)$ track the time-varying optimizer? Are the constraints satisfied for all time? Is the interconnected system stable? Answering these questions is nontrivial, even when stability and convergence can be verified for both the plant and the optimizing flow individually, and requires the full battery of controls and systems theoretic tools.

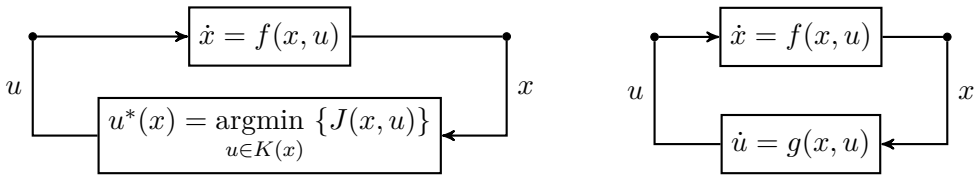

Figure 2.1: Diagram depicting a typical instance of an online feedback optimization problem. (Left) The ideal case, where the input to the plant is determined by the exact solution to a parametric optimization problem, where the parameter is the system state. (Right) A real-time implementation of feedback optimization. Here the flow $\dot{u} = g(x, u)$ is used to solve the optimization problem on the left, and evolves in parallel to the plant dynamics.

Finally, we mention the utility of the systems theoretic approach to optimization in the network setting. For distributed optimization problems, care must be taken to ensure that nodes can solve the problem using only information that is available to them locally. Recent advances in consensus dynamics and distributed control provide a path to solving difficult

network optimization problems in real-time. As computing power increases and becomes distributed over large-scale networks, we can expect online and distributed optimization to play a more prominent role in the future, so systems and control theory will continue to be indispensible in the development and analysis of optimization algorithms.

2.1 Related Work

Here we review the literature that connects systems-theoretic concepts with optimization. Early works include the study of dynamical systems solving optimization and saddle point problems [AHU58], and demonstrating that certain combinatorial optimization problems can be solved using continuous-time flows on manifolds [Bro91, HM94]. More recent work has focused on uncovering the phenomenon of acceleration in first-order optimization, synthesizing flows solving constrained optimization problems, understanding the theoretical properties of projected systems, studying saddle flows, and connecting optimization algorithms with plants in a feedback loop. We now discuss in detail each of these areas in the literature.

A Extremum Seeking Control

We begin by reviewing extremum seeking control. This refers to a class of feedback controllers which steer a dynamical system to the optimizer of an unknown map. These methods are widely used in real-time applications where the model being controlled is unknown and is used in applications as varied as automotive control, bioreactors, formation flight, and gas turbines (c.f. [AK03] and references therein). Extremum seeking control

methods were first introduced in the 1920s [Leb22], and although these methods are related to those in adaptive control, the historical development proceeded in parallel to developments in control theory until being rediscovered by the community in the 2000s [KW00]. Recently, there has been a resurgence of interest in extremum seeking control after it was discovered that extremum-seeking feedback can be studied using Lie-algebraic methods in nonlinear control [DSEJ13, GZE18]. These methods have been extended to nonsmooth optimization [FZE18, FBE21], and have been applied to safety critical applications [WKS23], game theory [KG21], power systems [CPL22], and particle accelerators [WSH$^+$23].

B Accelerated Optimization

The dynamical systems approach to optimization has also been fruitful for gaining insight into the phenomenon of acceleration in optimization, where certain first-order descent algorithms achieve super-linear convergence rates. An example of this is the celebrated Nesterov's method [Nes83]. Similar to how gradient descent can be viewed as a discretization of the gradient flow, recent work has uncovered that Nesterov acceleration can be viewed as discretization of an ordinary differential equation (ODE) [SBC16]. This connection has enabled the use of control-theoretic methods in analyzing acceleration, such as Lyapunov-based convergence estimates [WRJ21], and analysis of discretization and stability [MJ21]. These continuous-time flows can be derived using variational methods in mechanics [WWJ16], and recent work has focused on developing rate-matching discretizations, either using the notion of "high-resultion" differential equations [SDJS22], or symplectic integrators [SDSJ19, FSRV20].

C Flows Solving Equality Constrained Problems

We now discuss the dynamical systems approach for solving problems involving only equality constraints. The works [Tan80, Yam80] employ differential geometric techniques to design a vector field that maintains feasibility along the flow, makes the constraint set asymptotically stable, and whose solutions converge to critical points of the objective function. Recently [SS00] introduces a generalized form of this vector field to deal with inequality constraints in the form of a differential algebraic equation and explores links with sequential quadratic programming. Recently, this work has been extended in [FZL20] to study the region of attraction of local minima, showing that the introduction of a stochastic perturbation allows solutions to escape sharp local minimizers.

D Projected Dynamical Systems

A particularly fruitful area of research is in the area of projected dynamical systems, which are commonly employed to solve optimization problems [NZ96]. Typically, this approach proceeds by projecting the gradient of the objective function onto the cone of feasible descent directions. Projected systems are closely related to differential inclusions [AC84], and have also been shown to be equivalent to complementary systems [HSW00, BDLA06]. These systems are, in general, discontinuous, which from an analysis viewpoint requires properly dealing with notions and existence of solutions, cf. [Cor08]. The discontinuous methods also introduce challenges in the computation implementation of these systems [AB08]. Projected systems have been employed to solve problems arising in power systems applications [HSB$^+$18, DSSPG19], coverage control in robotics [GCB06], and control of transportation

systems [NZ96].

Several modifications and extensions to projected dynamical systems have been proposed in recent years. The work [HBD21] discuss projected dynamical systems on non-Euclidean manifolds. A continuous modification of the projected gradient method was introduced in [FBM+94] and its stability was analyzed in [XW00]. However, this method projects onto the constraint set itself, rather than the tangent cone, and may fail when it is nonconvex. Another modification is the "constrained gradient flow" proposed in [MJ22], derived using insights from nonsmooth mechanics, and is well-defined outside the feasible set. The resulting method is related to the one we present in Chapter 3, though unlike the flow we discuss, this one is discontinuous and stability guarantees are only provided in the case of convexity.

E Saddle-Point Dynamics

A common method for solving convex optimization problems is by searching for saddle points of the associated Lagrangian. This can be done via a primal-dual dynamics, consisting of a gradient descent in the primal variable and a gradient ascent in the dual one. The analysis of stability and convergence of this method has a long history [AHU58, Kos56], however, because they are particularly well suited for distributed implementation on network optimization problems, they have been the subject of intense research in recent years. Stability of these methods has been analyzed both for discrete-time implementations [LJJ20], and continuous-time ones [FP10, CGC17, CMLC18]. Recent work has also extended these methods for nonsmooth optimization problems [CN19], and explored their contraction properties

[CVJB21].

F Online Feedback Optimization

Here we review the literature analyzing applications where the solution to the optimization problem used to regulate the behavior of a physical plant [JLvdB09, CDB20, LSPM21]. Feedback optimization problems arise in a number of advanced engineering applications, including power systems [CDB20, LSPM21], network congestion [LPD02], and transportation [BCPD22]. We refer the reader to [HBHD21] for a review on both theoretical methods and applications in this line of research. One particularly interesting example of feedback optimization is model predictive control (MPC), where an optimal control problem is solved in a receding horizon manner. While stability and robustness guarantees for MPC can be provided [RM09], recent work has explored the case where the optimization problem is embedded in a feedback loop with a continuous-time plant [NLMK18], or solved only approximately and warm-started on each iteration [LMNK20]. In these settings, understanding the convergence and robustness properties of the optimization algorithm is of key importance, and necessitates a systems-theoretic approach.

2.2 Mathematical Preliminaries

We now discuss various mathematical preliminaries, included Variational Analysis, nonlinear programming, variational inequalities, stability notions for dynamical systems, and safety-critical control.

2.2.1 Notation

We let $\mathbb{R}$ denote the set of real numbers. For $v, w \in \mathbb{R}^n$, $v \leq w$ denotes $v_i \leq w_i$ for $i \in \{1, \ldots, n\}$. We let $\|v\|$ denote the Euclidean norm and $\|v\|_\infty = \max_{1 \leq i \leq n} |v_i|$ the infinity norm. For $y \in \mathbb{R}$, we denote $[y]_+ = \max\{0, y\}$, and $\operatorname{sgn}(y) = 1$ if $y > 0$, $\operatorname{sgn}(y) = -1$ if $y < 0$ and $\operatorname{sgn}(y) = 0$ if $y = 0$. We let $\mathbf{1}_m \in \mathbb{R}^m$ denote the vector of all ones. For a matrix $A \in \mathbb{R}^{n \times m}$, we use $\rho(A)$ and $A^\dagger$ to denote its spectral radius and its Moore-Penrose pseudoinverse, respectively. We write $A \succeq 0$ (resp., $A \succ 0$) to denote A is positive semidefinite (resp., A is positive definite). Given a symmetric matrix Q, let $\lambda_{\min}(Q)$ and $\lambda_{\max}(Q)$ denote the minimum eigenvalue and maximum eigenvalue of Q respectively. For a matrix $Q \succ 0$ and $x \in \mathbb{R}^n$, let $\|x\|_Q = \sqrt{x^\top Q x}$. Given a subset $\mathcal{C} \subset \mathbb{R}^n$, the distance of $x \in \mathbb{R}^n$ to $\mathcal{C}$ is $\operatorname{dist}_{\mathcal{C}}(x) = \inf_{y \in \mathcal{C}} \|x - y\|$. We let $\overline{\mathcal{C}}$, $\operatorname{int}(\mathcal{C})$, and $\partial \mathcal{C}$ denote the closure, interior, and boundary of $\mathcal{C}$, respectively. Given $g : \mathbb{R}^n \to \mathbb{R}$, we denote its gradient by ∇g and its Hessian by $\nabla^2 g$. For $g : \mathbb{R}^n \to \mathbb{R}^m$, $\frac{\partial g(x)}{\partial x}$ denotes its Jacobian. For $I \subset \{1, 2, \ldots, m\}$, we denote by $\frac{\partial g_I(x)}{\partial x}$ the matrix whose rows are $\{\nabla g_i(x)^\top\}_{i \in I}$.

2.2.2 Variational Analysis

We review basic notions from variational analysis following [RW98]. The *extended real line* is $\overline{\mathbb{R}} = \mathbb{R} \cup \{\pm\infty\}$. Given $f : \mathbb{R}^n \to \overline{\mathbb{R}}$, its *domain* is $\operatorname{dom}(f) = \{x \in \mathbb{R}^n \mid f(x) \neq \infty, -\infty\}$. The *graph* of f is $\operatorname{graph}(f) = \{(x, f(x)) \mid x \in \mathbb{R}^n\}$. Similarly, given a set-valued map $\mathcal{F} : X \rightrightarrows \mathbb{R}^m$, its graph is $\operatorname{graph}(\mathcal{F}) = \{(x, y) \mid x \in X, y \in \mathcal{F}(x)\}$.

Consider a subset $\mathcal{C} \subset \mathbb{R}^n$. The *indicator function of* $\mathcal{C}$ is $\delta_{\mathcal{C}} : \mathbb{R}^n \to \overline{\mathbb{R}}$,

$$\delta_{\mathcal{C}}(x) = \begin{cases} 0 & \text{if } x \in \mathcal{C}, \\ \\ \infty & \text{if } x \notin \mathcal{C}. \end{cases}$$

Note that $\mathrm{dom}(\delta_{\mathcal{C}}) = \mathcal{C}$. For $x \in \mathrm{dom}(f)$ and $d \in \mathbb{R}^n$, consider the following limits

$$f'(x;d) = \lim_{(h,y)\to(0^+,x)} \frac{f(y+hd) - f(x)}{h}, \tag{2.1a}$$

$$f''(x;d) = \lim_{(h,y)\to(0^+,x)} \frac{f(y+hd) - f(x) - hf'(y;d)}{h^2}. \tag{2.1b}$$

If the limit in (2.1a) (resp. (2.1b)) exists, f is *directionally differentiable in the direction* d (resp. *twice directionally differentiable in the direction* d). By definition, $f'(x;d) = \nabla f(x)^\top d$ if f is continuously differentiable at x and $f''(x;d) = d^\top \nabla^2 f(x) d$ if f is twice continuously differentiable at x.

Given a dynamical system $\dot{x} = \mathcal{G}(x)$ and a function $V : \mathbb{R}^n \to \mathbb{R}$, the *upper-right Dini derivative* of V along solutions of the system is

$$D^+_{\mathcal{G}} V(x) = \limsup_{h\to 0^+} \frac{1}{h} \left[V(\Phi_h(x)) - V(x) \right],$$

where Φ_h is the flow map of the system. If V is directionally differentiable then $D^+_{\mathcal{G}} V(x) = V'(x; \mathcal{G}(x))$, and if V is differentiable then $D^+_{\mathcal{G}} V(x) = \nabla V(x)^\top \mathcal{G}(x)$.

The *tangent cone* to $\mathcal{C} \subset \mathbb{R}^n$ at $x \in \mathbb{R}^n$ is

$$T_{\mathcal{C}}(x) = \Bigg\{ \xi \in \mathbb{R}^n \mid \exists \{t^\nu\}_{\nu=1}^{\infty} \subset (0,\infty), \{x^\nu\}_{\nu=1}^{\infty} \subset \mathcal{C} \\ t^\nu \to 0^+, x^\nu \to x, \frac{x^\nu - x}{t^\nu} \to \xi \text{ as } \nu \to \infty \Bigg\},$$

and the *normal cone* to $\mathcal{C}$ at $x \in \mathbb{R}^n$ is

$$\mathcal{N}_{\mathcal{C}}(x) = \Bigg\{ w \in \mathbb{R}^n \mid \exists (x^\nu)_{\nu=1}^{\infty} \subset \mathcal{C}, \\ x^\nu \to x, \frac{w^\top (x^\nu - x)}{\|x^\nu - x\|} \to 0 \text{ as } \nu \to \infty \Bigg\}.$$

When $\mathcal{C}$ is convex, then the normal and tangent cones simplify to

$$\mathcal{N}_{\mathcal{C}}(x) = \left\{ w \in \mathbb{R}^n \mid w^\top (y - x) \leq 0 \ \ \forall y \in \mathcal{C} \right\},$$
$$T_{\mathcal{C}}(x) = \left\{ \xi \in \mathbb{R}^n \mid d^\top w \leq 0 \ \ \forall w \in \mathcal{N}_{\mathcal{C}}(x) \right\}.$$

If $\mathcal{C}$ is an embedded submanifold of $\mathbb{R}^n$, then the tangent cone coincides with the usual differential geometric notion of tangent space. Let $\Pi_{\mathcal{C}} : \mathbb{R}^n \rightrightarrows \overline{\mathcal{C}}$, with

$$\Pi_{\mathcal{C}}(x) = \left\{ y \in \overline{\mathcal{C}} \mid \|x - y\| = \operatorname{dist}_{\mathcal{C}}(x) \right\},$$

be the projection map onto $\overline{\mathcal{C}}$. The *proximal normal cone* to $\mathcal{C}$ at x is

$$\begin{aligned}\mathcal{N}_{\mathcal{C}}^{\text{prox}}(x) = \Big\{ d \in \mathbb{R}^n \mid \exists \{t^\nu\}_{\nu=1}^{\infty} \subset (0,\infty), \\ \{(x^\nu, y^\nu)\}_{\nu=1}^{\infty} \subset \text{graph}(\Pi_{\mathcal{C}}), \\ t^\nu \to 0^+, x^\nu \to x, \frac{x^\nu - y^\nu}{t^\nu} \to d \text{ as } \nu \to \infty \Big\}.\end{aligned}$$

When $\mathcal{C}$ is convex, the proximal normal cone coincides with the usual notion of normal cone.

2.2.3 Nonlinear Programming

We present the basic background on necessary conditions for optimality [Ber99]. Consider a nonlinear program of the form

$$\begin{aligned} \underset{x \in \mathbb{R}^n}{\text{minimize}} \quad & f(x) \\ \text{subject to} \quad & g(x) \leq 0 \\ & h(x) = 0, \end{aligned} \tag{2.2}$$

where $f : \mathbb{R}^n \to \mathbb{R}$, $g : \mathbb{R}^n \to \mathbb{R}^m$, and $h : \mathbb{R}^n \to \mathbb{R}^k$ are continuously differentiable. Let $\mathcal{C} = \{x \in \mathbb{R}^n \mid g(x) \leq 0, h(x) = 0\}$ denote its feasible set. Necessary conditions for optimality can be derived provided that the feasible set satisfies appropriate constraint qualification

conditions. Let the active constraint, constraint violation, and inactive constraint sets be

$$I_0(x) = \{1 \leq i \leq m \mid g_i(x) = 0\}, \tag{2.3a}$$

$$I_+(x) = \{1 \leq i \leq m \mid g_i(x) > 0\}, \tag{2.3b}$$

$$I_-(x) = \{1 \leq i \leq m \mid g_i(x) < 0\}, \tag{2.3c}$$

respectively. We say that the constraint set $\mathcal{C}$ satisfies

- the Constant Rank Constraint Qualification (CRCQ) condition at x if there there exists an open neighborhood U containing x such that for all $y \in U$, and all $I \subset \{1, \ldots, m\}$ the set $\{\nabla g_i(y)\}_{i \in I} \cup \{\nabla h_j(y)\}_{j=1}^k$ has constant rank.

- the Mangasarian-Fromovitz Constraint Qualification (MFCQ) at x if $\{\nabla h_j(x)\}_{j=1}^k$ are linearly independent and there exists $\xi \in \mathbb{R}^n$ such that $\nabla h_j(x)^\top \xi = 0$ for all $j \in \{1, \ldots, k\}$ and $\nabla g_i(x)^\top \xi < 0$ for all $i \in I_0(x)$;

- the Extended Mangasarian-Fromovitz Constraint Qualification (EMFCQ) at x if $\{\nabla h_j(x)\}_{j=1}^k$ are linearly independent and there exists $\xi \in \mathbb{R}^n$ such that $\nabla h_j(x)^\top \xi = 0$ for all $j \in \{1, \ldots, k\}$ and $\nabla g_i(x)^\top \xi < 0$ for all $i \in I_0(x) \cup I_+(x)$;

- the Linear Independence Constraint Qualification (LICQ) at x, if $\{\nabla g_i(x)\}_{i \in I_0(x)} \cup \{\nabla h_j(x)\}_{j=1}^k$ are linearly independent.

Note that LICQ implies MFCQ, and EMFCQ implies MFCQ, however CRCQ neither implies nor is implied by MFCQ.

If $x^* \in \mathcal{C}$ is a local minimizer solving (2.2), and any of the above constraint qualification conditions hold at x^*, then there exists $u^* \in \mathbb{R}^m$ and $v^* \in \mathbb{R}^k$ such that the *Karash-Kuhn-Tucker* (KKT) conditions hold,

$$\nabla f(x^*) + \frac{\partial g(x^*)}{\partial x}^\top u^* + \frac{\partial h(x^*)}{\partial x}^\top v^* = 0, \tag{2.4a}$$

$$g(x^*) \leq 0, \tag{2.4b}$$

$$h(x^*) = 0, \tag{2.4c}$$

$$u^* \geq 0, \tag{2.4d}$$

$$(u^*)^\top g(x^*) = 0. \tag{2.4e}$$

The pair (u^*, v^*) are called Lagrange multipliers, and the triple (x^*, u^*, v^*) satisfying (2.4) is referred to as a *KKT triple*. If MFCQ holds at x^*, then the set of all Lagrange multipliers corresponding to x^* is bounded. If LICQ holds at x^*, then the Lagrange multiplier (u^*, v^*) such that (x^*, u^*, v^*) satisfies (2.4) is unique.

2.2.4 Variational Inequalities

Here we review the basic theory of variational inequalities following [FP03]. Let $F : \mathbb{R}^n \to \mathbb{R}^n$ be a map and $\mathcal{C} \subset \mathbb{R}^n$ a set of constraints. A variational inequality refers to the problem of finding $x^* \in \mathcal{C}$ such that

$$(x - x^*)^\top F(x^*) \geq 0, \qquad \forall x \in \mathcal{C}. \tag{2.5}$$

Using the language of variational geometry, the problem (2.5) can be equivalently stated in the form of a *generalized equation*[Rob83],

$$F(x^*) + \mathcal{N}_{\mathcal{C}}(x^*) \ni 0. \tag{2.6}$$

We use $\mathrm{VI}(F, \mathcal{C})$ to refer to either (2.5) or (2.6), and $\mathrm{SOL}(F, \mathcal{C})$ to denote its set of solutions. Variational inequalities provide a framework to study many different analysis and optimization problems, including

- Solving the nonlinear equation $F(x^*) = 0$, which corresponds to $\mathrm{VI}(F, \mathbb{R}^n)$;
- Minimizing the function $f : \mathbb{R}^n \to \mathbb{R}$ subject to the constraint that $x \in \mathcal{C}$, which corresponds to $\mathrm{VI}(\nabla f, \mathcal{C})$;
- Finding saddle points of the function $\ell : \mathbb{R}^n \times \mathbb{R}^m \to \mathbb{R}$ subject to the constraints that $x_1 \in X_1$ and $x_2 \in X_2$, which corresponds to $\mathrm{VI}([\nabla_{x_1}\ell; -\nabla_{x_2}\ell], X_1 \times X_2)$.
- Finding the Nash equilibria of a game with N agents, where the ith agent wants to minimize the cost $J_i(x_i, x_{-i})$ subject to the constraint $x_i \in X_i$, which corresponds to $\mathrm{VI}(F, \mathcal{C})$, where F is the *pseudogradient* operator defined by

  $$F(x) = (\nabla_{x_1} J_1(x), \ldots, \nabla_{x_N} J_N(x))$$

  and $\mathcal{C} = X_1 \times X_2 \times \cdots \times X_N$.

A key concept in the study of variational inequalities is the notion of monotonicity.

We say the map $F : \mathbb{R}^n \to \mathbb{R}^n$ is *monotone* if

$$(x_1 - x_2)^\top (F(x_1) - F(x_2)) \geq 0,$$

for all $x_1, x_2 \in \mathbb{R}^n$, and F is *μ-strongly monotone* if there exists $\mu > 0$ such that

$$(x_1 - x_2)^\top (F(x_1) - F(x_2)) \geq \mu \|x_1 - x_2\|^2,$$

for all $x_1, x_2 \in \mathbb{R}^n$. When F is a gradient map, i.e. $F = \nabla f$ for some function $f : \mathbb{R}^n \to \mathbb{R}$, then monotonicity (resp. μ-strong monotonicity) is equivalent to convexity (resp. μ-strong convexity) of f. When F is monotone and $\mathcal{C}$ is convex, we say $\mathrm{VI}(F, \mathcal{C})$ is a *monotone variational inequality*.

We now provide a characterization of the solution set $\mathrm{SOL}(F, \mathcal{C})$. We assume that $\mathcal{C}$ has the form $\mathcal{C} = \{x \in \mathbb{R}^n \mid g(x) \leq 0,\ h(x) = 0\}$ where $g : \mathbb{R}^n \to \mathbb{R}^m$ and $h : \mathbb{R}^n \to \mathbb{R}^k$ are continuously differentiable. We can formulate necessary conditions for optimality analogous to the KKT conditions for optimization problems (2.4). In particular, if any constraint qualification holds at $x^* \in \mathcal{C}$ and $x^* \in \mathrm{SOL}(F, \mathcal{C})$, then there exists $(u^*, v^*) \in \mathbb{R}^m \times \mathbb{R}^k$ such

that

$$F(x^*) + \sum_{i=1}^{m} u_i^* \nabla g_i(x^*) + \sum_{j=1}^{k} v_j^* \nabla h_j(x^*) = 0 \tag{2.7a}$$

$$g(x^*) \leq 0 \tag{2.7b}$$

$$h(x^*) = 0 \tag{2.7c}$$

$$u^* \geq 0 \tag{2.7d}$$

$$(u^*)^\top g(x) = 0. \tag{2.7e}$$

We refer to (2.7) as the KKT conditions corresponding to $\mathrm{VI}(F, \mathcal{C})$. We denote the set of KKT triples by $X_{\mathrm{KKT}}(F, \mathcal{C})$. For monotone variational inequalities, when $\mathcal{C}$ satisfies any constraint qualification condition at x^*, then the KKT conditions are both necessary and sufficient for $x^* \in \mathrm{SOL}(F, \mathcal{C})$. When F is monotone, $\mathrm{SOL}(F, \mathcal{C})$ is closed and convex. If F is additionally μ-strongly monotone, then the set of solutions is a singleton, provided that a solution exists.

2.2.5 Stability Notions

We recall basic definitions from the theory of nonlinear dynamical systems following [HC08]. Let $\mathcal{G} : \mathbb{R}^n \to \mathbb{R}^n$ be a locally Lipschitz vector field and consider the dynamical system $\dot{x} = \mathcal{G}(x)$. Local Lipschitzness ensures that, for every initial condition $x_0 \in \mathbb{R}^n$, there exists $T > 0$ and a unique trajectory $x : [0, T] \to \mathbb{R}^n$ such that $x(0) = x_0$ and $\dot{x}(t) = \mathcal{G}(x(t))$. If the solution exists for all $t \geq 0$, then it is *forward complete*. In this case, the *flow map* is defined by $\Phi_t : \mathbb{R}^n \to \mathbb{R}^n$ such that $\Phi_t(x) = x(t)$, where $x(t)$ is the unique solution with

$x(0) = x$. The *positive limit set* of $x \in \mathbb{R}^n$ is

$$\omega(x) = \bigcap_{T \geq 0} \overline{\{\Phi_t(x) \mid t > T\}}.$$

A set $\mathcal{S} \subset \mathbb{R}^n$ is *forward invariant* if $x \in \mathcal{S}$ implies that $\Phi_t(x) \in \mathcal{S}$ for all $t \geq 0$. If $\mathcal{S}$ is forward invariant and $x^* \in \mathcal{S}$ is an equilibrium, x^* is *Lyapunov stable relative to* $\mathcal{S}$ if for every open set U containing x^*, there exists an open set $\tilde{U}$ also containing x^* such that for all $x \in \tilde{U} \cap \mathcal{S}$, $\Phi_t(x) \in U \cap \mathcal{S}$ for all $t > 0$. The equilibrium x^* is *asymptotically stable relative to* $\mathcal{S}$ if it is Lyapunov stable relative to $\mathcal{S}$ and there is an open set U containing x^* such that $\Phi_t(x) \to x^*$ as $t \to \infty$ for all $x \in U \cap \mathcal{S}$. We say x^* is *exponentially stable relative to* $\mathcal{S}$ if it is asymptotically stable relative to $\mathcal{S}$ and there exists $\mu > 0$ and an open set U containing x^* such that for all $x \in U \cap \mathcal{S}$, $\|\Phi_t(x) - x^*\| \leq e^{-\mu t} \|x - x^*\|$. Analogous definitions of Lyapunov stability and asymptotically stability can be made for sets, instead of individual points.

Consider a forward invariant set $\mathcal{S}$ and a set of equilibria $\mathcal{S}$ contained in it, $\mathcal{S} \subset \mathcal{S}$. We say $x^* \in \mathcal{S}$ is *semistable relative to* $\mathcal{S}$ if x^* is Lyapunov stable and, for any open set U containing x^*, there is an open set $\tilde{U}$ such that for every $x \in \tilde{U} \cap \mathcal{S}$, the trajectory starting at x converges to a Lyapunov stable equilibrium in $U \cap \mathcal{S}$. Note that if x^* is an isolated equilibrium, then semistability is equivalent to asymptotic stability. For all the concepts introduced here, when the invariant set is unspecified, we mean $\mathcal{S} = \mathbb{R}^n$.

Finally, we discuss Lyapunov based tests for stability of an equilibrium. The first result is a special case of [BB03, Cor. 7.1], and establishes asymptotic stability stability of an isolated equilibrium.

Lemma 2.2.1 (Lyapunov test for relative stability)**.** *Let $\mathcal{S}$ be a forward invariant set of $\dot{x} = \mathcal{G}(x)$ and x^* an isolated equilibrium. Let $U \subset \mathbb{R}^n$ be an open set containing x^* and suppose that $V : U \cap \mathcal{S} \to \mathbb{R}$ is a directionally differentiable function such that*

(i) x^* is the unique minimizer of V on $U \cap \mathcal{S}$.

(ii) $D^+_{\mathcal{G}} V(x) < 0$ for all $x \in U \cap \mathcal{S} \setminus \{x^*\}$.

Then x^* is asymptotically stable relative to $\mathcal{S}$.

2.2.6 Safety-Critical Control

We review here notions from the theory of set invariance for control systems following [Bla99] and discuss methods for synthesizing feedback controllers that ensure it. Consider a control-affine system

$$\begin{aligned} \dot{x} &= \mathcal{F}(x, \mu) \\ &= F_0(x) + \sum_{i=1}^{r} \mu_i F_i(x), \end{aligned} \tag{2.8}$$

with Lipschitz-continuous vector fields $F_i : \mathbb{R}^n \to \mathbb{R}^n$, for $i \in \{0, \ldots, r\}$, and a set $\mathcal{U} \subset \mathbb{R}^m$ of valid control inputs μ. Let $\mathcal{C} \subset \mathbb{R}^n$ be a constraint set of the form $\mathcal{C} = \{x \in \mathbb{R}^n \mid g(x) \leq 0, h(x) = 0\}$, where $g : \mathbb{R}^n \to \mathbb{R}^m$ and $h : \mathbb{R}^n \to \mathbb{R}^k$ are continuously differentiable. We want to restrict the evolution of the system to remain in $\mathcal{C}$. We consider the problem of designing a feedback controller $k : \mathbb{R}^n \to \mathcal{U}$ such that $\mathcal{C}$ is forward invariant and asymptotically stable with respect to the closed-loop dynamics $\dot{x} = \mathcal{F}(x, \kappa(x))$. In applications, $\mathcal{C}$ often corresponds to the set of states for which the system can operate safely. For this reason, we refer to $\mathcal{C}$ as the *safety set*, and call the system *safe* under a controller k if $\mathcal{C}$ is forward

invariant and asymptotically stable. A controller ensuring safety is *safeguarding*. We discuss two optimization-based strategies for synthesizing safeguarding controllers.

A Safeguarding Control via Projection

The first strategy ensures the closed-loop dynamics lie in the tangent cone of the safety set. If MFCQ holds at $x \in \mathcal{C}$, the tangent cone can conveniently be expressed as, cf. [RW98, Theorem 6.31], $T_{\mathcal{C}}(x) = \{\xi \in \mathbb{R}^n \,\big|\, \frac{\partial h(x)}{\partial x}\xi = 0, \frac{\partial g_I(x)}{\partial x}\xi \leq 0\}$. We then define the set-valued map $K_{\text{proj}} : \mathbb{R}^n \rightrightarrows \mathcal{U}$ which characterizes the set of inputs, μ, that ensure the dynamics satisfy $\mathcal{F}(x,\mu) \in T_{\mathcal{C}}(x)$. The set has the form,

$$K_{\text{proj}}(x) = \Bigg\{ \mu \in \mathcal{U} \mid D^+_{F_0} g_i(x) + \sum_{\ell=1}^{r} \mu_\ell D^+_{F_\ell} g_i(x) \leq 0,\ i \in I(x), \\ D^+_{F_0} h_j(x) + \sum_{\ell=1}^{r} \mu_\ell D^+_{F_\ell} h_j(x) = 0,\ j = 1,\dots,k \Bigg\}.$$

Any feedback $k : \mathcal{C} \to \mathcal{U}$ such that $\kappa(x) \in K_{\text{proj}}(x)$ for $x \in \mathcal{C}$ renders $\mathcal{C}$ forward invariant.

Lemma 2.2.2. ***(Projection-based Safeguarding Feedback).*** *Consider the system* (2.8) *with safety set* $\mathcal{C}$ *and suppose that* $K_{proj}(x) \neq \emptyset$ *for all* $x \in \mathcal{C}$*. Then, the feedback controller* $k : \mathcal{C} \to \mathcal{U}$ *is safeguarding if* $\kappa(x) \in K_{proj}(x)$ *for all* $x \in \mathcal{C}$ *and the closed-loop system* $\dot{x} = \mathcal{F}(x, \kappa(x))$ *admits a unique solution for all initial conditions.*

Proof. By hypothesis, the closed-loop system satisfies $\mathcal{F}(x,\kappa(x)) \in T_{\mathcal{C}}(x)$ for all $x \in \mathcal{C}$. It follows that $\mathcal{C}$ is forward-invariant by Nagumo's Theorem [Bla99, Theorem 3.1]. □

To synthesize a safeguarding controller, we propose a strategy where $\kappa(x)$ at each $x \in \mathcal{C}$ is expressed as the solution to a mathematical program. Because $K_{\text{proj}}(x)$ is defined in

terms of affine constraints on the control input μ, we can readily express a feedback satisfying the hypotheses of Lemma 2.2.2 in the form of a mathematical program,

$$\kappa(x) \in \underset{\mu \in K_{\text{proj}}(x)}{\operatorname{argmin}} J(x, \mu), \tag{2.9}$$

for an appropriate choice of cost function $J : \mathcal{C} \times \mathcal{U} \to \mathbb{R}$. In general, care must be taken to ensure that the set K_{proj} is nonempty and that the controller k in (2.9) satisfies appropriate regularity conditions to ensure existence and uniqueness for solutions of the resulting closed-loop dynamics. Even if these properties hold, the approach has several limitations: the controller is ill-defined for initial conditions lying outside the safety set and the closed-loop system in general is nonsmooth.

B Safeguarding Control via Control Barrier Functions

The second strategy for synthesizing safeguarding controllers addresses the limitations of projection-based methods. The approach relies on the notion of a vector control barrier functions, which generalize the usual notion of control barrier functions. Given a set $X \supset \mathcal{C}$ and set of valid control inputs $\mathcal{U} \subset \mathbb{R}^m$, we say the pair $(g, h) : \mathbb{R}^n \times \mathbb{R}^k \to \mathbb{R}^m$ is a (m, k)-*vector control barrier function* (VCBF) for $\mathcal{C}$ on X relative to $\mathcal{U}$ if

(i) The set $\mathcal{C}$ can be expressed as

$$\mathcal{C} = \{x \in X \mid g(x) \leq 0, h(x) = 0\}$$

(ii) There exists $\alpha > 0$ such that the map $K_{\mathrm{cbf},\alpha} : \mathbb{R}^n \rightrightarrows \mathcal{U}$ given by

$$K_{\mathrm{cbf},\alpha}(x) = \Big\{ \mu \in \mathcal{U} \mid D^+_{F_0} g_i(x) + \sum_{\ell=1}^{r} \mu_\ell D^+_{F_\ell} g_i(x) + \alpha g_i(x) \leq 0, \\ D^+_{F_0} h_j(x) + \sum_{\ell=1}^{r} \mu_\ell D^+_{F_\ell} h_j(x) + \alpha h_j(x) = 0, \\ 1 \leq i \leq m,\ 1 \leq j \leq k \Big\},$$

takes nonempty values for all $x \in X$.

In the special case where $m = 1$ and $k = 0$, this definition coincides with the usual notion of control barrier function [ACE+19, Definition 2], where the class $\mathcal{K}$ function is linear, and the Lie derivative has been replaced with the upper-right Dini derivative. The use of vector-valued functions instead of scalar-valued ones allows us to consider a broader class of safe sets.

Similar to the previous strategy, the set $K_{\mathrm{cbf},\alpha}$ characterizes the set of inputs which ensure that the state remains inside the safe set. However unlike the projection-based approach, this assurance is implemented gradually: the parameter α corresponds to how tolerant we are of trajectories approaching the boundary of the safety set, with smaller values of α corresponding to situations where the trajectories beginning in the interior are more aggressively controlled. As $\alpha \to \infty$, the set $K_{\mathrm{cbf},\alpha}$ better corresponds to K_{proj}. We have the following result which is a generalization of [ACE+19, Thm. 2].

Lemma 2.2.3 (VCBF-based Safeguarding Feedback)**.** *Consider the system* (2.8) *with safety set* $\mathcal{C}$ *and suppose* (g, h) *is a vector control barrier function for* $\mathcal{C}$ *on* X *relative to* $\mathcal{U}$*. Then,*

the feedback controller $k : X \to \mathcal{U}$ *is safeguarding if* $\kappa(x) \in K_\alpha(x)$ *for all* $x \in X$ *and the closed-loop system* $\dot{x} = \mathcal{F}(x, \kappa(x))$ *admits a unique solution for all initial conditions.*

To synthesize a safeguarding feedback controller, one can pursue a design using a similar approach to Section 2.2.6.A. Given a cost function $J : X \times \mathcal{U} \to \mathbb{R}$, we let $\kappa(x)$ solve the following mathematical program:

$$\kappa(x) \in \underset{\mu \in K_{\mathrm{cbf},\alpha}(x)}{\operatorname{argmin}} \; J(x, \mu). \tag{2.10}$$

Similar to the case of projection-based safeguarding feedback control, care must be taken to verify the existence and uniqueness of solutions to the closed-loop system, as well as to handle situations where (2.10) does not have unique solutions. If these properties hold, then the control design addresses the challenges of projection-based methods. In particular, we can ensure that a controller of the form (2.10) is well-defined outside the safety set and results in closed-loop system with continuous solutions, under mild conditions which we discuss in the following chapters.

Chapter 3

Control Theoretic Synthesis of Dynamical Systems Solving Constrained Nonlinear Programs

This chapter considers the problem of designing a continuous-time dynamical system that solves a constrained nonlinear optimization problem and makes the feasible set forward invariant and asymptotically stable. The invariance of the feasible set makes the dynamics anytime, when viewed as an algorithm, meaning it returns a feasible solution regardless of when it is terminated. Our approach augments the gradient flow of the objective function with inputs defined by the constraint functions, treats the feasible set as a safe set, and synthesizes a safe feedback controller using techniques from the theory of control barrier functions. The resulting closed-loop system, termed safe gradient flow, can be viewed as a primal-dual flow, where the state corresponds to the primal variables and the inputs

correspond to the dual ones. We provide a detailed suite of conditions based on constraint qualification under which (both isolated and nonisolated) local minimizers are stable with respect to the feasible set and the whole state space. Comparisons with other continuous-time methods for optimization in a simple example illustrate the advantages of the safe gradient flow.

3.1 Problem Formulation

Our goal is to solve an optimization problem of the form

$$\begin{aligned} \underset{x\in\mathbb{R}^n}{\text{minimize}} \quad & f(x) \\ \text{subject to} \quad & g(x) \leq 0 \\ & h(x) = 0, \end{aligned} \tag{3.1}$$

where $f : \mathbb{R}^n \to \mathbb{R}$, $g : \mathbb{R}^n \to \mathbb{R}^m$, and $h : \mathbb{R}^n \to \mathbb{R}^k$ are continuously differentiable, by designing a dynamical system $\dot{x} = \mathcal{G}(x)$ that converges to its solutions. Let the feasible set of (3.1) be denoted by

$$\mathcal{C} = \{x \in \mathbb{R}^n \mid g(x) \leq 0, h(x) = 0\}. \tag{3.2}$$

The dynamics should enjoy the following properties.

(i) trajectories should remain feasible if they start from a feasible point. This can be formalized by asking the feasible set $\mathcal{C}$, defined in (3.2), to be forward invariant;

(ii) trajectories that start from an infeasible point should converge to the set of feasible

points. This can be formalized by requiring that $\mathcal{G}$ is well defined on an open set containing $\mathcal{C}$, and that $\mathcal{C}$ as a set is asymptotically stable with respect to the dynamics.

The requirement (i) ensures that, when viewed as an algorithm, the dynamics is *anytime*, meaning that it is guaranteed to return a feasible solution regardless of when it is terminated. The requirement (ii) ensures in particular that trajectories beginning from infeasible initial conditions approach the feasible set and, if the solutions of the optimization (3.1) belong to the interior of the feasible set, such trajectories enter it in finite time, never to leave it again. The problem is summarized below.

Problem 3.1.1. *Find an open set X containing $\mathcal{C}$ and design a vector field $\mathcal{G} : X \to \mathbb{R}^n$ such that the system $\dot{x} = \mathcal{G}(x)$ satisfies the following properties.*

(i) $\mathcal{G}$ is locally Lipschitz on X;

(ii) $\mathcal{C}$ is forward invariant and asymptotically stable;

(iii) x^* is an equilibrium if and only if $x^* \in X_{\mathrm{KKT}}$;

(iv) x^* is asymptotically stable if x^* is a isolated local minimizer.

3.2 Constrained Nonlinear Programming via Safe Gradient Flow

In this section we introduce our solution to Problem 3.1.1 in the form of a dynamical system called the *safe gradient flow*. We present two interpretations of this system: first

from the perspective of safety critical control, where we augment the standard gradient flow with an input and design a feedback controller using the procedure outlined in Section 2.2.6.B, and second as an approximation of the projected gradient flow. Interestingly, both interpretations are equivalent.

3.2.1 Safe Gradient Flow via Feedback Control

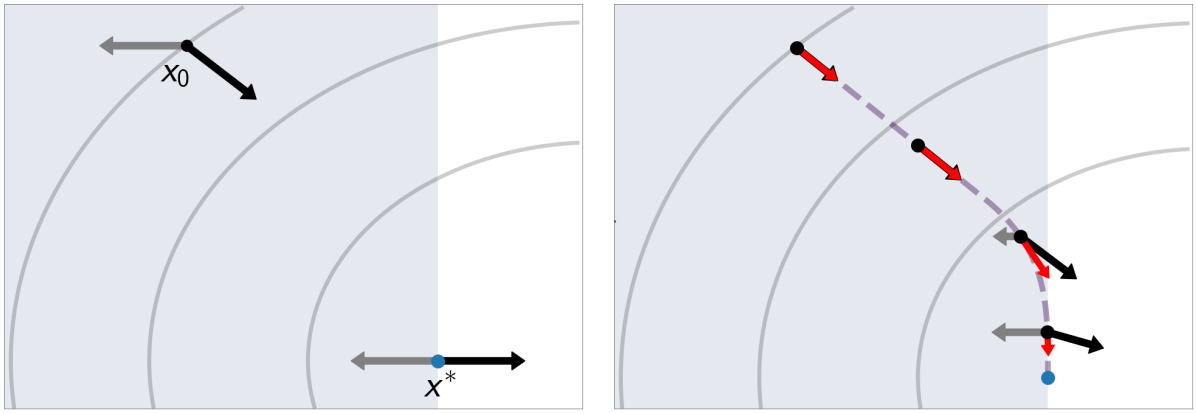

Figure 3.1: Intuition behind the design of the safe gradient flow. Grey lines are the level curves of the objective function and the shaded region is $\mathcal{C}$. In (a), the initial condition is x_0 and the minimizer is x^*, with $-\nabla f(x)$ in black and $-\nabla g(x)$ in gray at both points. In (b), the dashed line is a trajectory of $\dot{x} = -\nabla f(x) - u\nabla g(x)$ starting from x_0. The black vectors are $-\nabla f(x)$, the gray vectors are $-u\nabla g(x)$, and the red vectors are $\dot{x}$. Deep in the interior of $\mathcal{C}$, one has $u \approx 0$, as following the gradient of f does not jeopardize feasibility while minimizing it. As the trajectory approaches the boundary, u increases to keep the trajectory in $\mathcal{C}$.

Consider the control-affine system

$$\dot{x} = -\nabla f(x) - \frac{\partial g(x)}{\partial x}^\top u - \frac{\partial h(x)}{\partial x}^\top v. \tag{3.3}$$

One can interpret this system as the standard gradient flow of f modified by a "control

action" incorporating the gradients of the constraint functions. The intuition is that the drift term takes care of optimizing f toward the minimizer, and this direction can be modified with the input if the trajectory gets close to the boundary of the feasible set, cf. Figure 3.1.

Our idea for the controller design is to only modify the drift when the feasibility of the state is endangered. We accomplish this by looking at the feasible set $\mathcal{C}$ as a safe set and using $\phi = (g, h) : \mathbb{R}^n \to \mathbb{R}^{m+k}$ as an (m, k)-vector control barrier function to synthesize the feedback controller, using the strategy outlined in Chapter 2.2.6.B.

Let $\alpha > 0$ be a design parameter, and define the admissible control set as

$$\begin{aligned} K_{\mathrm{cbf},\alpha}(x) = \Big\{ & (u, v) \in \mathbb{R}^m_{\geq 0} \times \mathbb{R}^k \,\Big| \\ & - \frac{\partial g(x)}{\partial x} \frac{\partial g(x)}{\partial x}^\top u - \frac{\partial g(x)}{\partial x} \frac{\partial h(x)}{\partial x}^\top v \leq \frac{\partial g(x)}{\partial x} \nabla f(x) - \alpha g(x) \\ & - \frac{\partial h(x)}{\partial x} \frac{\partial g(x)}{\partial x}^\top u - \frac{\partial h(x)}{\partial x} \frac{\partial h(x)}{\partial x}^\top v = \frac{\partial h(x)}{\partial x} \nabla f(x) - \alpha h(x) \Big\}. \end{aligned} \tag{3.4}$$

We want to show that ϕ is a valid VCBF for (3.3).

Lemma 3.2.1 (Vector control barrier function for (3.3))**.** *Consider the optimization problem* (3.1)*. If MFCQ holds for all $x \in \mathcal{C}$, then there exists an open set X containing $\mathcal{C}$ such that the function $\phi = (g, h) : \mathbb{R}^n \to \mathbb{R}^{m+k}$ is a valid (m, k)-VCBF for* (3.3) *on X relative to $\mathcal{U} = \mathbb{R}^m_{\geq 0} \times \mathbb{R}^k$.*

Proof. We begin by showing that inequalities parameterizing $K_{\mathrm{cbf},\alpha}(x)$ are strictly feasible

for all $x \in \mathcal{C}$, i.e., for each $x \in \mathcal{C}$, there exists $\epsilon > 0$ and $(u, v) \in \mathbb{R}^m_{\geq 0} \times \mathbb{R}^k$ such that

$$-\frac{\partial g(x)}{\partial x}\frac{\partial g(x)}{\partial x}^\top u - \frac{\partial g(x)}{\partial x}\frac{\partial h(x)}{\partial x}^\top v \leq \frac{\partial g(x)}{\partial x}\nabla f(x) - \alpha g(x) - \epsilon \mathbf{1}_m \tag{3.5a}$$

$$-\frac{\partial h(x)}{\partial x}\frac{\partial g(x)}{\partial x}^\top u - \frac{\partial h(x)}{\partial x}\frac{\partial h(x)}{\partial x}^\top v = \frac{\partial h(x)}{\partial x}\nabla f(x) - \alpha h(x). \tag{3.5b}$$

Let $\tilde{g} = g(x) + \frac{\epsilon}{\alpha}\mathbf{1}_m$. By Farka's Lemma [Roc70], (3.5) is infeasible if and only if there exists a solution (u, v) to

$$-\frac{\partial g(x)}{\partial x}\frac{\partial g(x)}{\partial x}^\top u - \frac{\partial g(x)}{\partial x}\frac{\partial h(x)}{\partial x}^\top v \geq 0 \tag{3.6a}$$

$$-\frac{\partial h(x)}{\partial x}\frac{\partial g(x)}{\partial x}^\top u - \frac{\partial h(x)}{\partial x}\frac{\partial h(x)}{\partial x}^\top v = 0 \tag{3.6b}$$

$$u \geq 0 \tag{3.6c}$$

$$u^\top \left(\frac{\partial g(x)}{\partial x}\nabla f(x) - \alpha\tilde{g}\right) + v^\top \left(\frac{\partial h(x)}{\partial x}\nabla f - \alpha h(x)\right) < 0. \tag{3.6d}$$

Then (3.6a), (3.6b), and (3.6c) imply that

$$\begin{bmatrix} u \\ v \end{bmatrix}^\top \begin{bmatrix} \frac{\partial g(x)}{\partial x}\frac{\partial g(x)}{\partial x}^\top & \frac{\partial g(x)}{\partial x}\frac{\partial h(x)}{\partial x}^\top \\ \frac{\partial h(x)}{\partial x}\frac{\partial g(x)}{\partial x}^\top & \frac{\partial h(x)}{\partial x}\frac{\partial h(x)}{\partial x}^\top \end{bmatrix} \begin{bmatrix} u \\ v \end{bmatrix} \leq 0$$

but, since the matrix is positive semidefinite,

$$(u, v) \in \ker \begin{bmatrix} \frac{\partial g(x)}{\partial x}\frac{\partial g(x)}{\partial x}^\top & \frac{\partial g(x)}{\partial x}\frac{\partial h(x)}{\partial x}^\top \\ \frac{\partial h(x)}{\partial x}\frac{\partial g(x)}{\partial x}^\top & \frac{\partial h(x)}{\partial x}\frac{\partial h(x)}{\partial x}^\top \end{bmatrix} = \ker \begin{bmatrix} \frac{\partial g(x)}{\partial x}^\top & \frac{\partial h(x)}{\partial x}^\top \end{bmatrix}. \tag{3.7}$$

Next, by (3.7) and that $x \in \mathcal{C}$, (3.6d) reduces to

$$-u^\top(\alpha g(x) + \epsilon \mathbf{1}_m) < 0, \tag{3.8}$$

and by a second application of Farka's Lemma, we see that (3.6c), (3.7) and (3.8) are feasible if and only if the following system is infeasible.

$$\frac{\partial g(x)}{\partial x}\xi \leq -\alpha g(x) - \epsilon \mathbf{1}_m \qquad \frac{\partial h(x)}{\partial x}\xi = 0. \tag{3.9a}$$

We claim that a solution to (3.9) can be constructed if MFCQ holds at x. Indeed, by MFCQ, there exists $\tilde{\xi} \in \mathbb{R}^n$ such that $\frac{\partial g_{I_0}}{\partial x}\tilde{\xi} < 0$ and $\frac{\partial h(x)}{\partial x}\tilde{\xi} = 0$, and for ϵ sufficiently small, there exists $\gamma > 0$ such that $\xi = \gamma\tilde{\xi}$ solves (3.9). Thus (3.6) is infeasible, and therefore (3.5) is feasible.

By strict feasibility and the fact that the matrix $\frac{\partial h(x)}{\partial x}\frac{\partial h(x)}{\partial x}^\top$ has full rank, it can be shown by Lemma 3.6.6 that, for all $x \in \mathcal{C}$, the affine inequalities that parameterize $K_{\text{cbf},\alpha}(x)$ are *regular*[1]. Finally, since the affine inequalities parameterizing $K_{\text{cbf},\alpha}$ are continuous, $K_{\text{cbf},\alpha}(y)$ is nonempty for any y sufficiently close to x. Hence there exists an open set X such that $K_{\text{cbf},\alpha}$ takes nonempty values on X. □

[1]Consider a linear system of inequalities of the form $Cz \leq c$, $Dz = d$, and a solution z_0. The system is regular (c.f. [Rob75]) if for C', c', D', d' sufficiently close to C, c, D, d, the perturbed system $C'z \leq c'$, $D'z = d'$ remains feasible, and the distance of z_0 to the solution set of the perturbed system is proportional to the magnitude of the perturbation.

Since ϕ is a VCBF, we can design a feedback of the form (2.10), where the objective function is given by

$$J(x,u,v) = \left\| \frac{\partial g(x)}{\partial x}^\top u + \frac{\partial h(x)}{\partial x}^\top v \right\|^2 .$$

This design has the interpretation of finding a controller which guarantees safety while modifying the drift term in (3.3) as little as possible. The resulting feedback controller is

$$\begin{bmatrix} u(x) \\ v(x) \end{bmatrix} \in \underset{(u,v)\in K_{\mathrm{cbf},\alpha}(x)}{\operatorname{argmin}} \left\{ \left\| \frac{\partial g(x)}{\partial x}^\top u + \frac{\partial h(x)}{\partial x}^\top v \right\|^2 \right\}. \tag{3.10}$$

We refer to the closed-loop system (3.3) under the controller (3.10) as the *safe gradient flow*. In general, the solution to (3.10) might not be unique. Nevertheless, as we show later, the safe gradient flow is well-defined because, the closed-loop behavior of the system is independent of the chosen solution.

Comparing the dynamics (3.3) with the KKT condition (2.4a) suggests that the inputs $(u(x), v(x))$ can be interpreted as approximations of the dual variables of the problem. With this interpretation, the safe gradient flow can be viewed as a primal-dual method. We use this viewpoint later to establish connections between the proposed method and the projected gradient flow.

Remark 3.2.2 (Connection with the Literature)**.** The work [Tan80] considers the problem of designing a dynamical system to solve (3.1) when only equality constraints are present using a differential geometric approach. Here, we show that the safe gradient flow generalizes the solution proposed in [Tan80]. Under the assumption that $h \in C^r$ and LICQ holds, the feasible set $\mathcal{C} = \{x \in \mathbb{R}^n \mid h(x) = 0\}$ is an embedded C^r submanifold of $\mathbb{R}^n$ of codimension

k. The approach in [Tan80] proceeds by identifying a vector field $F : \mathbb{R}^n \to \mathbb{R}^n$ satisfying: (i) $F \in C^r$ and $F(x) \in T_{\mathcal{C}}(x)$ for all $x \in \mathcal{C}$; and (ii) $\dot{h}(x) = -\alpha h(x)$ along the trajectories of $\dot{x} = F(x)$, where $\alpha > 0$ is a design parameter. The proposed vector field satisfying both properties is

$$F(x) = -\Big(I - \frac{\partial h(x)}{\partial x}^{\dagger} \frac{\partial h(x)}{\partial x}\Big)\nabla f(x) - \alpha \frac{\partial h(x)}{\partial x}^{\dagger} h(x). \tag{3.11}$$

To see that this corresponds to the safe gradient flow, note that the admissible control set (3.4) in this case is

$$K_{\mathrm{cbf},\alpha}(x) = \Big\{v \in \mathbb{R}^k \mid -\frac{\partial h(x)}{\partial x}\nabla f(x) - \frac{\partial h(x)}{\partial x}\frac{\partial h(x)}{\partial x}^{\top} v = -\alpha h(x)\Big\}.$$

By the LICQ assumption, $K_{\mathrm{cbf},\alpha}(x)$ is a singleton whose unique element is

$$v(x) = -\Big(\frac{\partial h(x)}{\partial x}\frac{\partial h(x)}{\partial x}^{\top}\Big)^{-1}\Big(\frac{\partial h(x)}{\partial x}\nabla f(x) - \alpha h(x)\Big).$$

Substituting this into (3.3), we obtain the expression (3.11). This provides an alternative interpretation from a control-theoretic perspective of the differential-geometric design in [Tan80], and justifies viewing the safe gradient flow as the natural extension to the case with both inequality and equality constraints. □

Remark 3.2.3 (Inequality Constraints via Quadratic Slack Variables)**.** The work [SS00] pursues a different approach that the one taken here to deal with inequality constraints by reducing them to equality constraints. This is accomplished introducing quadratic slack variables. Formally, for each $i \in \{1, \ldots, m\}$, one replaces the constraint $g_i(x) \leq 0$ with the

equality constraint $g_i(x) = -y_i^2$, and solves the equality-constrained optimization problem in the variables $(x, y) \in \mathbb{R}^{n+m}$ with a flow of the form (3.11). While this method can be expressed in closed form, there are several drawbacks with it. First, this increases the dimensionality of the problem, which can be problematic when there are a large number of inequality constraints. Second, adding quadratic slack variables introduces additional equilibrium points to the resulting flow which do not correspond to KKT points of the original problem. □

3.2.2 Safe Gradient Flow as an Approximation of the Projected Gradient Flow

Here, we introduce an alternative design in terms of a continuous approximation of the projected gradient flow. The latter is a discontinuous dynamical system obtained by projecting the gradient of the objective function onto the tangent cone of the feasible set. Later, we show that this continuous approximation is in fact equivalent to the safe gradient flow.

Let $x \in \mathcal{C}$ and suppose that MFCQ holds at x. Then the tangent cone of $\mathcal{C}$ at x is

$$T_{\mathcal{C}}(x) = \left\{ \xi \in \mathbb{R}^n \,\middle|\, \frac{\partial h(x)}{\partial x}\xi = 0, \frac{\partial g_{I_0}(x)}{\partial x}\xi \leq 0 \right\}.$$

For $x \in \mathcal{C}$, let $\Pi_{T_{\mathcal{C}}(x)}$ be the projection onto $T_{\mathcal{C}}(x)$. In general, the projection is a set-valued map, but the fact that $T_{\mathcal{C}}(x)$ is closed and convex makes the projection onto $T_{\mathcal{C}}(x)$ unique

in this case. The projected gradient flow is

$$\begin{aligned}\dot{x} &= \Pi_{T_{\mathcal{C}}(x)}(-\nabla f(x)) \\ &= \underset{\xi\in\mathbb{R}^n}{\operatorname{argmin}} \quad \frac{1}{2}\left\|\xi + \nabla f(x)\right\|^2 \\ &\qquad \text{subject to} \quad \frac{\partial g_{I_0}(x)}{\partial x}\xi \leq 0, \frac{\partial h(x)}{\partial x}\xi = 0.\end{aligned} \tag{3.12}$$

In general, this system is discontinuous, so one must resort to appropriate notions of solution trajectories and establish their existence, see e.g., [Cor08]. Here, we consider Carathéodory solutions, which are absolutely continuous functions that satisfy (3.12) almost everywhere. When Carathéodory solutions exist in $\mathcal{C}$, then the KKT points of (3.1) are equilibria of (3.12), and isolated local minimizers are asymptotically stable.

Consider the following continuous approximation of (3.12) by letting $\alpha > 0$ and defining $\mathcal{G}_\alpha$ by

$$\begin{aligned}\mathcal{G}_\alpha(x) = \underset{\xi\in\mathbb{R}^n}{\operatorname{argmin}} \quad & \frac{1}{2}\left\|\xi + \nabla f(x)\right\|^2 \\ \text{subject to} \quad & \frac{\partial g(x)}{\partial x}\xi \leq -\alpha g(x) \\ & \frac{\partial h(x)}{\partial x}\xi = -\alpha h(x).\end{aligned} \tag{3.13}$$

Note that (3.13) has a similar form to (3.12), and has a unique solution if one exists. However, as we show later, unlike the projected gradient flow, the vector field $\mathcal{G}_\alpha$ is well defined outside $\mathcal{C}$ and is Lipschitz.

We now show that $\mathcal{G}_\alpha$ approximates the projected gradient flow. Intuitively, this is because for inactive constraints $j \notin I_0(x)$, one has $g_j(x) < 0$ and hence the jth inequality constraint in (3.13), $\nabla g_j(x)^\top \xi \leq -\alpha g_j(x)$, becomes $\nabla g_j(x)^\top \xi \leq \infty$ as $\alpha \to \infty$ and the

constraint is effectively removed, reducing the problem to (3.12). This is formalized next.

Proposition 3.2.4 ($\mathcal{G}_\alpha$ approximates the projected gradient)**.** *Let $x \in \mathcal{C}$ and suppose MFCQ holds. Then*

(i) $\mathcal{G}_\alpha(x) \in T_{\mathcal{C}}(x)$.

(ii) $\lim_{\alpha\to\infty} \mathcal{G}_\alpha(x) = \Pi_{T_{\mathcal{C}}(x)}(-\nabla f(x))$.

Proof. To show (i), note that if $x \in \mathcal{C}$, then $h(x) = 0$ and $g_{I_0}(x) = 0$, so the constraints in (3.13) imply that $\frac{\partial h(x)}{\partial x}\mathcal{G}_\alpha(x) = 0$ and $\frac{\partial g_{I_0}(x)}{\partial x}\mathcal{G}_\alpha(x) \leq 0$, and therefore $\mathcal{G}_\alpha(x) \in T_{\mathcal{C}}(x)$.

Regarding (ii), for fixed $x \in \mathcal{C}$, let $J = I_-(x)$ and consider the following quadratic program

$$\begin{aligned} P_x(\epsilon) = \underset{\xi\in\mathbb{R}^n}{\operatorname{argmin}} \quad & \frac{1}{2}\left\|\xi + \nabla f(x)\right\|^2 \\ \text{subject to} \quad & \frac{\partial g_{I_0}(x)}{\partial x}\xi \leq 0, \frac{\partial h(x)}{\partial x}\xi = 0 \\ & \epsilon\frac{\partial g_J(x)}{\partial x}\xi \leq -g_J(x). \end{aligned} \tag{3.14}$$

When $\epsilon = 0$, the feasible sets of (3.14) and (3.12) are the same. Since the objective functions are also the same, $P_x(0) = \Pi_{T_{\mathcal{C}}(x)}(-\nabla f(x))$. Furthermore, for all $\alpha > 0$, $P_x(\frac{1}{\alpha}) = \mathcal{G}_\alpha(x)$. Finally, since the QP defining P_x has a unique solution, and satisfies the regularity conditions in [BD95, Definition 2.1], P_x is continuous at $\epsilon = 0$ by [BD95, Thm. 2.2]. Hence

$$\lim_{\alpha\to\infty} \mathcal{G}_\alpha(x) = \lim_{\epsilon\to 0^+} P_x(\epsilon) = P_x(0) = \Pi_{T_{\mathcal{C}}(x)}(-\nabla f(x)).$$

□

A consequence of Proposition 3.2.4 is that solutions of $\dot{x} = \mathcal{G}_\alpha(x)$ approximate the solutions of the projected gradient flow, with decreasing error as α increases, cf. Figure 3.2.

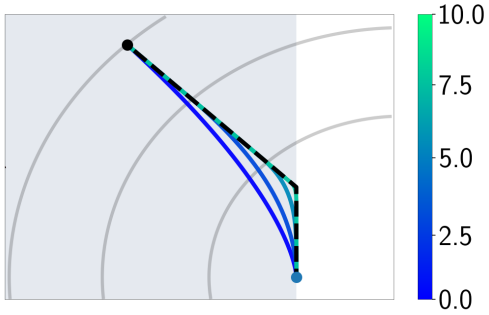

Figure 3.2: Projected gradient flow versus continuous approximation. The solution of the projected gradient flow is in black and solutions of $\dot{x} = \mathcal{G}_\alpha(x)$ for varying values of α are in the colors corresponding to the colorbar. All solutions start from the same initial condition, marked by the black dot.

3.2.3 Equivalence Between the Two Interpretations

Here we establish the equivalence between the two interpretations of the safe gradient flow. Specifically, we show that the control barrier function quadratic program (3.10) can be interpreted as a dual program corresponding to the continuous approximation of the projected gradient flow in (3.13).

Let $L : \mathbb{R}^n \times \mathbb{R}^m_{\geq 0} \times \mathbb{R}^k \times \mathbb{R}^n \to \mathbb{R}$ be

$$L(\xi, u, v; x) = \frac{1}{2} \|\xi + \nabla f(x)\|^2 + u^\top \left(\frac{\partial g(x)}{\partial x} \xi + \alpha g(x) \right) + v^\top \left(\frac{\partial h(x)}{\partial x} \xi + \alpha h(x) \right). \tag{3.15}$$

Then for each $x \in \mathbb{R}^n$, the Lagrangian of (3.13) is $(\xi, u, v) \mapsto L(\xi, u, v; x)$.

For each $x \in \mathbb{R}^n$, the KKT conditions corresponding to the optimization (3.13) are

$$\xi + \nabla f(x) + \frac{\partial g(x)}{\partial x}^\top u + \frac{\partial h(x)}{\partial x}^\top v = 0 \tag{3.16a}$$

$$\frac{\partial g(x)}{\partial x}\xi + \alpha g(x) \leq 0 \tag{3.16b}$$

$$\frac{\partial h(x)}{\partial x}\xi + \alpha h(x) = 0 \tag{3.16c}$$

$$u \geq 0 \tag{3.16d}$$

$$u^\top \left(\frac{\partial g(x)}{\partial x}\xi + \alpha g(x) \right) = 0 \tag{3.16e}$$

Because the (3.13) is strongly convex, the existence of a triple (ξ, u, v) satisfying (3.16) is sufficient for optimality of ξ. Since the optimizer is unique, for any triple (ξ, u, v) satisfying these conditions, $\xi = \mathcal{G}_\alpha(x)$.

Let $\Lambda_\alpha : \mathbb{R}^n \rightrightarrows \mathbb{R}^m_{\geq 0} \times \mathbb{R}^k$ be defined by

$$\Lambda_\alpha(x) = \{(u, v) \in \mathbb{R}^m_{\geq 0} \times \mathbb{R}^k \mid \exists \xi \in \mathbb{R}^n \text{ such that } (\xi, u, v) \text{ solves (3.16)}\}. \tag{3.17}$$

By definition, $\Lambda_\alpha(x)$ is the set of Lagrange multipliers of (3.13) at $x \in \mathbb{R}^n$. When $\Lambda_\alpha(x) \neq \emptyset$, then the conditions (3.16) are also necessary for optimality of (3.13). As we show next, this necessity follows as a consequence of the constraint qualification conditions.

Lemma 3.2.5 (Necessity of optimality conditions)**.** *For $\alpha > 0$, if (3.1) satisfies MFCQ at $x \in \mathcal{C}$ then there is an open set U containing x such that $\Lambda_\alpha(x') \neq \emptyset$ for all $x' \in U$.*

Proof. If MFCQ holds at $x \in \mathcal{C}$, there exists $\xi \in \mathbb{R}^n$ such that $\nabla g_i(x)^\top \xi < 0$ for all $i \in I_0(x)$

and $\nabla h_j(x)^\top \xi = 0$ for all $j \in \{1, \dots, k\}$. Next, for every $j \in I_-(x)$, let $\epsilon_j > 0$ be defined as

$$\epsilon_j \leq \begin{cases} \frac{-\alpha g_j(x)}{\nabla g_j(x)^\top \xi} & \nabla g_j(x)^\top \xi > 0, \\ 1 & \nabla g_j(x)^\top \xi \leq 0. \end{cases}$$

Then taking $0 < \epsilon \leq \min_{j \in I_-(x)}\{\epsilon_j\}$ and $\tilde{\xi} = \epsilon \xi$, satisfies

$$\frac{\partial g(x)}{\partial x}\tilde{\xi} < -\alpha g(x) \qquad \frac{\partial h(x)}{\partial x}\tilde{\xi} = -\alpha h(x). \tag{3.18}$$

The above means that the constraints of (3.13) satisfy Slater's condition [BV09, Ch. 5.2.3] at x, so the affine constraints are *regular* [Rob75, Thm. 2]. This implies that there exists an open set U containing x on which (3.13) is feasible and $\Lambda_\alpha(x') \neq \emptyset$ for all $x' \in U$. □

We use the optimality conditions to show that (3.10) is actually the dual problem corresponding to (3.13) in the appropriate sense.

Proposition 3.2.6 (Equivalence of two constructions of the safe gradient flow)**.** *If* $\Lambda_\alpha(x) \neq \emptyset$*,*

(i) If $(u, v) \in \Lambda_\alpha(x)$*, then* (u, v) *solves* (3.10)*;*

(ii) $\mathcal{G}_\alpha$ *is the closed-loop dynamics corresponding to the implementation of the feedback* (3.10) *over the system* (3.3)*.*

Proof. To show (i), let $(u, v) \in \Lambda_\alpha(x)$. Then there is $\xi \in \mathbb{R}^n$ such that (ξ, u, v) solves (3.16). By (3.16a), $\xi = -\nabla f(x) - \frac{\partial g(x)}{\partial x}^\top u - \frac{\partial h(x)}{\partial x}^\top v$ and substituting ξ into the constraints of (3.13), it follows immediately that $(u, v) \in K_{\text{cbf},\alpha}(x)$, defined in (3.4). We claim that (u, v)

is also optimal for (3.10). To prove this, let (u', v') be a solution of (3.10) and, reasoning by contradiction, suppose

$$\left\| \frac{\partial g(x)}{\partial x}^\top u + \frac{\partial h(x)}{\partial x}^\top v \right\|^2 > \left\| \frac{\partial g(x)}{\partial x}^\top u' + \frac{\partial h(x)}{\partial x}^\top v' \right\|^2.$$

Then, $\xi' = -\nabla f(x) - \frac{\partial g(x)}{\partial x}^\top u' - \frac{\partial h(x)}{\partial x}^\top v'$ satisfies the constraints in (3.13) and $\|\xi' + \nabla f(x)\| < \|\xi + \nabla f(x)\|$, which contradicts the fact that ξ is optimal for (3.13).

To show (ii), suppose that (u, v) solves (3.10), and $\xi = -\nabla f(x) - \frac{\partial g(x)}{\partial x}^\top u - \frac{\partial h(x)}{\partial x}^\top v$. We claim that ξ is optimal for (3.13). Indeed, if $\tilde{\xi}$ is the optimizer of (3.13), since $\Lambda_\alpha(x) \neq \emptyset$, there exists $(\tilde{u}, \tilde{v}) \in \Lambda_\alpha(x)$ such that $(\tilde{\xi}, \tilde{u}, \tilde{v})$ solves (3.16). Note that $(\tilde{u}, \tilde{v})$ is feasible for (3.10), and

$$\|\xi + \nabla f(x)\|^2 = \left\| \frac{\partial g(x)}{\partial x}^\top u + \frac{\partial h(x)}{\partial x}^\top v \right\|^2 \leq \left\| \frac{\partial g(x)}{\partial x}^\top \tilde{u} + \frac{\partial h(x)}{\partial x}^\top \tilde{v} \right\|^2 = \left\| \tilde{\xi} + \nabla f(x) \right\|^2,$$

where the inequality follows by optimality of (u, v). It follows that ξ is optimal, but since the optimizer of (3.13) is unique, $\xi = \mathcal{G}_\alpha(x)$. Hence, $\mathcal{G}_\alpha(x) = -\nabla f(x) - \frac{\partial g(x)}{\partial x}^\top u - \frac{\partial h(x)}{\partial x}^\top v$, which is the closed-loop implementation of (3.10) over (3.3). □

Remark 3.2.7 (Lagrange Multipliers of Continuous Approximation to Projected Gradient)**.** The notion of duality in Proposition 3.2.6 is weaker than the usual notion of Lagrangian duality. While the result ensures that the Lagrange multipliers of (3.13) are solutions to (3.10), the converse is not true in general. This is because if (u, v) solves (3.10), then $(\mathcal{G}_\alpha(x), u, v)$ might not satisfy the complementarity condition (3.16e), in which case $(u, v) \notin \Lambda_\alpha(x)$. An example of this is given by the following constrained problem with objective f and inequality

constraints $g(x) \leq 0$, where

$$f(x) = \|x\|^2 \qquad g(x) = \begin{bmatrix} 0 & 1 \\ 0 & -1 \end{bmatrix} x - \begin{bmatrix} 1 \\ 1 \end{bmatrix}.$$

The constraints satisfy LICQ for all $x \in \mathbb{R}^n$. The solution is $x^* = 0$ and $\Lambda_\alpha(x^*) = \{(0,0)\}$. However, $(1,1)$ is an optimizer of (3.10), even though $(1,1) \notin \Lambda_\alpha(x^*)$. □

Remark 3.2.8 (Lagrangian Dual of Continuous Approximation to Projected Gradient)**.** The safe gradient flow can also be implemented using the Lagrangian dual of (3.13). This is obtained by replacing the feedback controller (3.10) with

$$\begin{bmatrix} u(x) \\ v(x) \end{bmatrix} \in \underset{(u,v)\in\mathbb{R}^m_{\geq 0}\times\mathbb{R}^k}{\operatorname{argmin}} \left\{ \frac{1}{2} \begin{bmatrix} u \\ v \end{bmatrix}^\top \begin{bmatrix} \frac{\partial g(x)}{\partial x}\frac{\partial g(x)}{\partial x}^\top & \frac{\partial g(x)}{\partial x}\frac{\partial h(x)}{\partial x}^\top \\ \frac{\partial h(x)}{\partial x}\frac{\partial g(x)}{\partial x}^\top & \frac{\partial h(x)}{\partial x}\frac{\partial h(x)}{\partial x}^\top \end{bmatrix} \begin{bmatrix} u \\ v \end{bmatrix} + u^\top \left(\frac{\partial g(x)}{\partial x} \nabla f(x) - \alpha g(x) \right) + v^\top \left(\frac{\partial h(x)}{\partial x} \nabla f(x) - \alpha h(x) \right) \right\}$$

and considering its closed-loop implementation over (3.3). Though this controller no longer has the same intuitive interpretation as the CBF-QP (3.10), it has the advantage that its values correspond exactly with $\Lambda_\alpha(x)$. □

Proposition 3.2.6 shows that there are two equivalent interpretations of the safe gradient flow. The first is as the closed-loop system corresponding to (3.3) with the controller (3.10), which maintains forward invariance of the feasible set $\mathcal{C}$ while ensuring the dynamics is as close as possible to the gradient flow of the objective function. The second interpretation is as an approximation of the projection of the gradient flow of the objective function onto the tangent cone of the feasible set. Both interpretations are related by the fact that

the Lagrange multipliers corresponding to the approximate projection are the optimal control inputs solving (3.3). Beyond the interesting theoretical parallelism, this interpretation is instrumental in our ensuing discussion when characterizing the equilibria, regularity, and stability properties of the safe gradient flow.

3.3 Stability Analysis of the Safe Gradient Flow

Here we conduct a thorough analysis of the stability properties of the safe gradient flow and show that it solves Problem 3.1.1. We start by characterizing its equilibria and regularity properties, then focus on establishing the stability properties of local minimizers, and finally characterize the global convergence properties of the flow.

3.3.1 Equilibria, Regularity, and Safety

We rely on the necessary optimality conditions introduced in Section 3.2.3 to characterize the equilibria of $\mathcal{G}_\alpha$.

Proposition 3.3.1 (Equilibria of safe gradient flow correspond to KKT points)**.** *If MFCQ holds at $x^* \in \mathcal{C}$, then*

(i) $\mathcal{G}_\alpha(x^*) = 0$ if and only if $x^* \in X_{\mathrm{KKT}}$;

(ii) If $x^* \in X_{\mathrm{KKT}}$, then $\Lambda_\alpha(x^*)$ is the set of Lagrange multipliers of (3.1) at x^*.

Proof. Suppose that $\mathcal{G}_\alpha(x^*) = 0$. By Lemma 3.2.5, there exists $(u^*, v^*) \in \Lambda_\alpha(x^*)$ such that

$(0, u^*, v^*)$ satisfies the necessary optimality conditions in (3.16), which reduce to

$$\nabla f(x^*) + \frac{\partial g(x^*)}{\partial x}^\top u^* + \frac{\partial h(x^*)}{\partial x}^\top v^* = 0 \tag{3.19a}$$

$$\alpha g(x^*) \leq 0 \tag{3.19b}$$

$$\alpha h(x^*) = 0 \tag{3.19c}$$

$$u^* \geq 0 \tag{3.19d}$$

$$(u^*)^\top (\alpha g(x^*)) = 0 \tag{3.19e}$$

Because $\alpha > 0$, it follows immediately that (3.19) implies that (x^*, u^*, v^*) satisfy (2.4) and $x^* \in X_{\mathrm{KKT}}$.

Conversely, if $x^* \in X_{\mathrm{KKT}}$, then for any (u^*, v^*) such that (x^*, u^*, v^*) solves (2.4), we have that $(0, u^*, v^*)$ solves (3.16), which implies that $\mathcal{G}_\alpha(x^*) = 0$ and $(u^*, v^*) \in \Lambda_\alpha(x^*)$. $\square$

Proposition 3.3.1(i) shows that the safe gradient flow meets Problem 3.1.1(iii). The correspondence in Proposition 3.3.1(ii) between the Lagrange multipliers of (3.13) and the Lagrange multipliers of (3.1) means that the proposed method can be interpreted as a primal-dual method when implemented via (3.13). This is because the state of the system (3.3) corresponds to the primal variable of (3.1), and the inputs to the system (3.3) correspond to the dual variables.

We next establish that $\mathcal{G}_\alpha$ is locally Lipschitz on an open set containing $\mathcal{C}$ when both the CRCQ and MFCQ conditions hold. This ensures the existence and uniqueness of classical solutions to the safe gradient flow.

Proposition 3.3.2 (Lipschitzness of safe gradient flow)**.** *Let $\alpha > 0$ and suppose that* (3.1)

satisfies CRCQ and MFCQ for all $x \in \mathcal{C}$, f, g and h are continuously differentiable, and their derivatives are locally Lipschitz. Then $\mathcal{G}_\alpha$ is well defined and locally Lipschitz on an open set X containing $\mathcal{C}$.

Proof. By the proof of Lemma 3.2.5, if MFCQ holds at $x \in \mathcal{C}$, there is an open neighborhood U_x containing x on which the constraints of (3.13) satisfy Slater's condition. Then, $\mathcal{G}_\alpha$ is the unique solution to (3.13) on U_x. Let $\tilde{g}_i(x, \xi)$ and $\tilde{h}_j(x, \xi)$ be the ith and jth constraints of (3.13) respectively for $i \in \{1, \ldots, m\}$ and $j \in \{1, \ldots, k\}$. Then

$$\tilde{g}_i(x, \xi) = \nabla g_i(x)^\top \xi + \alpha g_i(x)$$

$$\tilde{h}_j(x, \xi) = \nabla h_j(x)^\top \xi + \alpha h_j(x)$$

and therefore $\nabla_\xi \tilde{g}_i(x, \xi) = \nabla g_i(x)$ and $\nabla_\xi \tilde{h}_j(x, \xi) = \nabla h_j(x)$. Thus if CRCQ holds at $x \in \mathcal{C}$, then the constraints of (3.13) also satisfy CRCQ at (x, ξ). It follows by [Liu95, Theorem 3.6] that $\mathcal{G}_\alpha$ is Lipschitz on U_x. The desired result follows by letting $X = \bigcup_{x \in \mathcal{C}} U_x$. □

Proposition 3.3.2 verifies that the safe gradient flow meets Problem 3.1.1(i). Next, we show that under slightly stronger constraint qualification conditions at KKT points, the triple satisfying (3.16) is unique and Lipschitz near them.

Proposition 3.3.3 (Lipschitzness of the solution to (3.16))**.** *Let $x^* \in X_{\mathrm{KKT}}$ and suppose* (3.1) *satisfies LICQ at x^*. Then, there exists an open set U containing x^* and Lipschitz functions $u : U \to \mathbb{R}^m_{\geq 0}$, $v : U \to \mathbb{R}^m$ such that $(\mathcal{G}_\alpha(x), u(x), v(x))$ is the unique solution to* (3.16) *for all $x \in U$.*

Proof. We claim that the variational equation (3.16) is *strongly regular* [Rob80] for all $x^* \in$

X_{KKT}. Strong regularity implies, cf. [Rob80, Cor. 2.1], that there exists an open set U containing x^* and Lipschitz functions $\xi : U \to \mathbb{R}^n$, $u : U \to \mathbb{R}^m_{\geq 0}$, $v : U \to \mathbb{R}^k$ such that $(\xi(x), u(x), v(x))$ is the unique triple solving (3.13). Since the solution (3.13) is unique, if such a triple exists, then $\xi(x) = \mathcal{G}_\alpha(x)$. To prove the claim, we begin by noting that (3.13) satisfies the strong second-order sufficient condition since $\nabla^2_{\xi\xi} L(\xi, u, v; x) = I \succ 0$, where L is the Lagrangian defined in (3.15). Let (x^*, u^*, v^*) be a KKT triple of (3.1). By Proposition 3.3.1, $(0, u^*, v^*)$ satisfies (3.16). Since the ith inequality constraint of (3.13) is $\nabla g_i(x^*)^\top \xi + \alpha g_i(x^*) \leq 0$, when $\xi = 0$ the constraint is active if and only if $g_i(x^*) = 0$. It follows that when $x^* \in X_{\mathrm{KKT}}$, the indices of the active constraints of (3.13) are the same as those of (3.1). Moreover, for all $\xi \in \mathbb{R}^n$,

$$\frac{\partial}{\partial \xi}(\nabla g_i(x^*)^\top \xi + \alpha g_i(x^*)) = \nabla g_i(x^*)^\top,$$
$$\frac{\partial}{\partial \xi}(\nabla h_j(x^*)^\top \xi + \alpha h_j(x^*)) = \nabla h_j(x^*)^\top,$$

so the gradients of the binding (i.e., the active inequality and equality) constraints of (3.13) and (3.1) are also the same. By LICQ, the gradients of the binding constraints are linearly independent, which along with the strong second-order condition implies that (3.16) is strongly regular by [Rob80, Thm. 4.1]. □

The significance of Proposition 3.3.3 is twofold. First, it establishes that, under certain conditions, the Lagrange multipliers of (3.13) are Lipschitz as a function of x, which ensures the existence of a locally Lipschitz continuous feedback solving (3.10). Secondly, the result establishes conditions for uniqueness of the Lagrange multipliers in a neighborhood of

an equilibrium x^*. These facts will play an important role in the stability analysis of local minimizers in the sequel.

We now show in the next result that the safe gradient flow also meets Problem 3.1.1(ii). The result follows by applying Lemma 2.2.3 with $\phi = (g, h)$ as a VCBF and local Lipschitz continuity of the closed-loop dynamics, c.f. Proposition 3.3.2.

Theorem 3.3.4 (Safety of feasible set under safe gradient flow)**.** *Consider the optimization problem* (3.1)*. If MFCQ is satisfied on $\mathcal{C}$, then $\mathcal{C}$ is forward invariant and asymptotically stable under the safe gradient flow.*

Remark 3.3.5 (Advantages of safe gradient flow over projected gradient flow)**.** Unlike the projected gradient flow, the vector field $\mathcal{G}_\alpha$ is locally Lipschitz, so classical solutions to $\dot{x} = \mathcal{G}_\alpha(x)$ exist, and the continuous-time flow can be numerically solved using standard ODE discretization schemes. Secondly, under mild conditions, $\mathcal{G}_\alpha$ is well defined for initial conditions outside $\mathcal{C}$, allowing us to guarantee convergence to a local minimizer starting from infeasible initial conditions. Finally, because both (3.12) and (3.13) are least-squares problems of the same dimension subject to affine constraints, the computational complexity of solving either one is equivalent. □

Remark 3.3.6 (Discretization of safe gradient flow and role of parameter α)**.** When considering discretizations of the safe gradient flow, the parameter α plays an important role. By construction, trajectories of the safe gradient flow beginning at infeasible initial conditions converge to $\mathcal{C}$ at an exponential rate $\alpha > 0$, so larger values of α ensure faster convergence. On the other hand, smaller values of α result in a design that enforces safety more conserva-

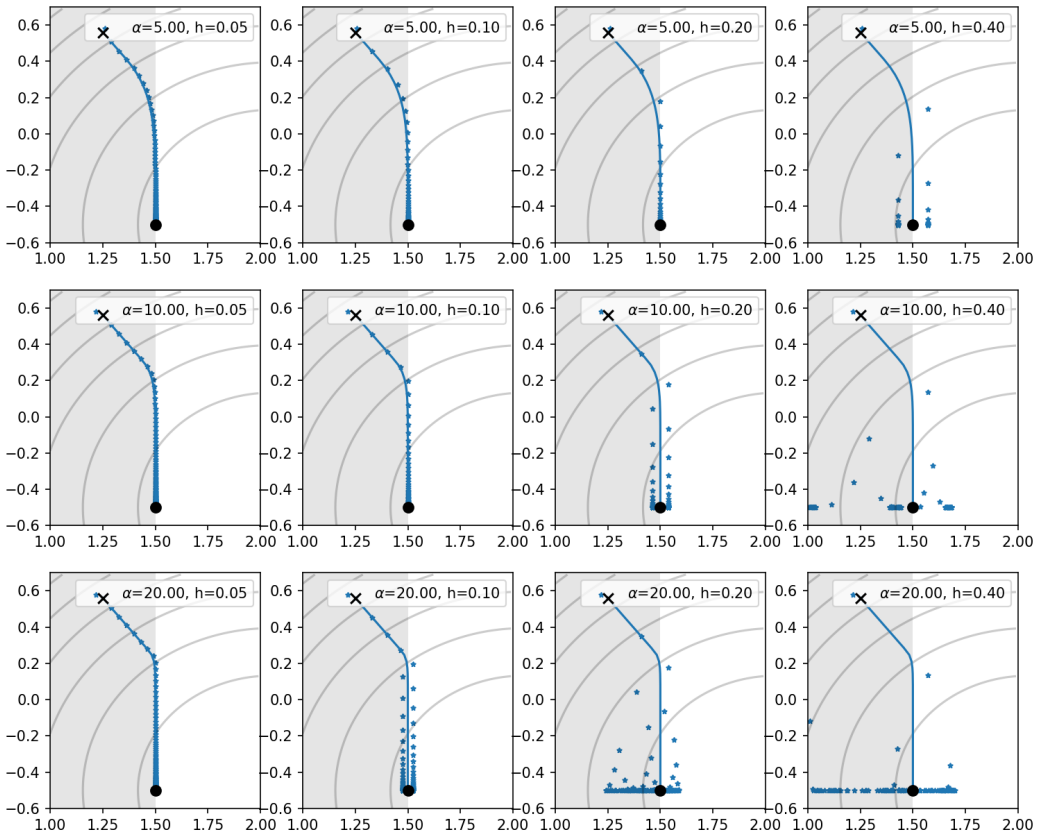

Figure 3.3: Safe gradient flow on an example problem for varying values of the parameter α (increasing from top to bottom) and the discretization stepsize h (increasing from left to right). The gray region is the feasible set and the gray lines are level sets of the objective function. The black dot is the unique optimizer. The blue line is a solution to the safe gradient flow, and the blue dots are iterations of the forward Euler discretization of the safe gradient flow. Larger values of α ensure faster convergence toward the feasible set but reduce the range of admissible stepsizes h to ensure both convergence and safety. This is consistent with the interpretation that smaller α results in a design that enforces safety more conservatively (hence allowing for larger stepsizes).

tively and hence, intuitively, this should allow for larger stepsizes. Our preliminary numerical experiments, with the forward-Euler discretization $x^+ = x + h\mathcal{G}_\alpha(x)$ on an example problem

with a quadratic objective function and affine contraints, confirm these intuitions, showing that larger choices of α reduce the range of allowable stepsizes h that preserve the invariance of the feasible set $\mathcal{C}$ and stability of local minimizers. We depict both the continuous-time trajectories and the discrete-time iterations for varying values of h and α in Figure 3.3. We have noticed that the maximal allowable stepsize h^*_α such that $0 < h < h^*_\alpha$ ensures stability and approximate safety, satisfies $h^*_\alpha \to 0$ as $\alpha \to \infty$. For space reasons, we leave to future work the formal characterization of suitable stepsizes. □

3.3.2 Stability of Isolated Local Minimizers

Here we characterize the stability properties of isolated local minimizers under the safe gradient flow. The following result shows that the safe gradient flow meets Problem 3.1.1(iv).

Theorem 3.3.7 (Stability of isolated local minimizers)**.** *Consider the optimization problem* (3.1)*. Let x^* be a local minimizer and an isolated KKT point, and let U be an open set such that x^* is the only KKT point contained in U. Then,*

(i) If MFCQ holds for all $x \in U \cap \mathcal{C}$, then x^* is asymptotically stable relative to $\mathcal{C}$;

(ii) If EMFCQ holds for all $x \in \bar{U}$, then x^* is asymptotically stable relative to $\mathbb{R}^n$;

(iii) If LICQ, strict complementarity, and the second-order sufficient condition hold at x^*, then x^* is exponentially stable relative to $\mathbb{R}^n$.

We divide the technical discussion leading up to the proof of the result in three parts, corresponding to each statement.

A Stability of Isolated Local Minimizers Relative to $\mathcal{C}$

Here we analyze the stability of local minimizers relative to the feasible set. We start by characterizing the growth of the objective function along solutions of the safe gradient flow.

Lemma 3.3.8 (Growth of objective function along safe gradient flow)**.** *Let $x \in \mathbb{R}^n$ such that $\Lambda_\alpha(x) \neq \emptyset$. Then,*

- *For all $(u, v) \in \Lambda_\alpha(x)$,*

$$D^+_{\mathcal{G}_\alpha} f(x) = -\left\|\mathcal{G}_\alpha(x)\right\|^2 + \alpha u^\top g(x) + \alpha v^\top h(x).$$

- *If $x \in \mathcal{C}$ then,*

$$D^+_{\mathcal{G}_\alpha} f(x) \leq 0,$$

  with equality if and only if $x \in X_{\mathrm{KKT}}$.

Proof. For $x \in X$ (with X given by Proposition 3.3.2) such that $(u, v) \in \Lambda_\alpha(x) \neq \emptyset$, $(\mathcal{G}_\alpha(x), u, v)$ solves (3.16). Next,

$$\begin{aligned} D^+_{\mathcal{G}_\alpha} f(x) &= \mathcal{G}_\alpha(x)^\top \nabla f(x) \\ &\overset{(a)}{=} -\mathcal{G}_\alpha(x)^\top \left(\mathcal{G}_\alpha(x) + \frac{\partial g(x)}{\partial x}^\top u + \frac{\partial h(x)}{\partial x}^\top v\right) \\ &\overset{(b)}{=} -\left\|\mathcal{G}_\alpha(x)\right\|^2 + \alpha u^\top g(x) + \alpha v^\top h(x), \end{aligned}$$

where (a) follows by rearranging (3.16a), and (b) follows from (3.16c) and (3.16e).

To show the second statement, note that if $x \in \mathcal{C}$, then $g(x) \leq 0$ and $h(x) = 0$. Since

$u \geq 0$, it follows $\alpha u^\top g(x) + \alpha v^\top h(x) \leq 0$ and therefore

$$D^+_{\mathcal{G}_\alpha} f(x) \leq - \left\| \mathcal{G}_\alpha(x) \right\|^2 \leq 0.$$

Finally, $D^+_{\mathcal{G}_\alpha} f(x) = 0$ if and only if $\mathcal{G}_\alpha(x) = 0$, which by Proposition 3.3.1, is equivalent to $x \in X_{\mathrm{KKT}}$. □

As a consequence of Lemma 3.3.8, the objective function decreases monotonically along the solutions starting in $\mathcal{C}$. We use this fact to show that isolated local minimizers that are isolated equilibria are asymptotically stable relative to $\mathcal{C}$.

Proof of Theorem 3.3.7(i). By hypothesis and using Lemma 3.2.5, $\Lambda_\alpha(x) \neq \emptyset$ for all $x \in U \cap \mathcal{C}$. Because x^* is the unique strict minimizer of f on $U \cap \mathcal{C}$, and by Lemma 3.3.8, $D^+_{\mathcal{G}_\alpha} f(x) < 0$ for all $x \in U \cap \mathcal{C} \setminus \{x^*\}$, it follows by Lemma 2.2.1 that x^* is asymptotically stable relative to $\mathcal{C}$. □

B Stability of Isolated Local Minimizers Relative to $\mathbb{R}^n$

Here we establish the asymptotic stability of isolated local minima relative to $\mathbb{R}^n$. To do so, we cannot rely any more on the objective function f as a Lyapunov function. This is because outside of $\mathcal{C}$, there may exist points $x \in \mathbb{R}^n \setminus \mathcal{C}$ where $f(x) < f(x^*)$. Therefore, to show stability relative to $\mathbb{R}^n$, we need to identify an alternative function whose unconstrained minimizer is x^*. In fact, the problem of finding a function whose unconstrained minimizers correspond to the local minimizers of a nonlinear program is well studied in the optimization literature [DG89]: such functions are called *exact penalty functions*. Our discussion proceeds

by constructing an exact penalty function that is also a Lyapunov function for the safe gradient flow.

Let $\Omega \subset \mathbb{R}^n$ be a compact set. A function $V : \Omega \times (0, \infty) \to \mathbb{R}$ is a *strong exact penalty function* relative to Ω if there exists $\epsilon^* > 0$ such that for all $0 < \epsilon < \epsilon^*$, $x^* \in \text{int}(\Omega)$ is a local minimizer of $V_\epsilon(x) := V(x, \epsilon)$ if and only if x^* is a local minimizer of (3.1). The following result gives a strong exact penalty function for (3.1) whose upper-right Dini derivative along $\mathcal{G}_\alpha$ is well defined on Ω.

Lemma 3.3.9 (Existence of strong exact penalty function)**.** *Let $\Omega \subset \mathbb{R}^n$ be compact such that $\text{int}(\Omega) \cap \mathcal{C} \neq \emptyset$. Suppose* (3.1) *satisfies EMFCQ at every $x \in \Omega$ and let $V : \Omega \times (0, \infty) \to \mathbb{R}$,*

$$V(x, \epsilon) = f(x) + \frac{1}{\epsilon} \sum_{i=1}^{m} [g_i(x)]_+ + \frac{1}{\epsilon} \sum_{j=1}^{k} |h_j(x)|. \tag{3.20}$$

Then, V is a strong exact penalty function relative to Ω, V is directionally differentiable on Ω, and

$$D^+_{\mathcal{G}_\alpha} V_\epsilon(x) = D^+_{\mathcal{G}_\alpha} f(x) + \frac{1}{\epsilon} \sum_{i \in I_+(x)} D^+_{\mathcal{G}_\alpha} g_i(x) + \frac{1}{\epsilon} \sum_{j=1}^{k} \text{sgn}(h_j(x)) D^+_{\mathcal{G}_\alpha} h_j(x), \tag{3.21}$$

for all $x \in \Omega$.

Proof. The fact that V is a strong exact penalty function relative to Ω readily follows from [DG89, Thm. 4]. From [DG89, Prop. 3], V_ϵ is directionally differentiable on Ω and its

directional derivative in the direction $\xi \in \mathbb{R}^n$ is

$$V_\epsilon'(x;\xi) = \nabla f(x)^\top \xi + \frac{1}{\epsilon} \sum_{i \in I_+(x)} \nabla g_i(x)^\top \xi + \frac{1}{\epsilon} \sum_{i \in I_0(x)} [\nabla g_i(x)^\top \xi]_+ + \frac{1}{\epsilon} \sum_{\substack{j \text{ such that} \\ h_j(x) \neq 0}} \operatorname{sgn}(h_j(x)) \nabla h_j(x)^\top \xi + \frac{1}{\epsilon} \sum_{\substack{j \text{ such that} \\ h_j(x) = 0}} |\nabla h_j(x)^\top \xi|.$$

We examine this expression in the case $V_\epsilon'(x; \mathcal{G}_\alpha(x)) = D^+_{\mathcal{G}_\alpha} V_\epsilon(x)$. For any $1 \leq i \leq m$, the definition of $\mathcal{G}_\alpha$ implies

$$\nabla g_i(x)^\top \mathcal{G}_\alpha(x) = D^+_{\mathcal{G}_\alpha} g_i(x) \leq -\alpha g_i(x).$$

Therefore, if $i \in I_0(x)$, then $[\nabla g_i(x)^\top \mathcal{G}_\alpha(x)]_+ = 0$. Similarly, for any $1 \leq j \leq k$, the definition of $\mathcal{G}_\alpha$ implies that

$$\nabla h_j(x)^\top \mathcal{G}_\alpha(x) = D^+_{\mathcal{G}_\alpha} h_j(x) = -\alpha h_j(x),$$

so if $h_j(x) = 0$, then $|\nabla h_j(x)^\top \mathcal{G}_\alpha(x)| = 0$, and the result follows. □

We now show that V_ϵ is a Lyapunov function for ϵ sufficiently small and use this fact to certify the asymptotic stability of isolated local minimizers.

Proof of Theorem 3.3.7(ii). Assume, without loss of generality, that U is bounded. By Lemma 3.3.9, the function V_ϵ defined in (3.20) is a strong exact penalty relative to $\overline{U}$. By definition, this means that there exists $\epsilon_1 > 0$ such that when $\epsilon < \epsilon_1$, x^* is the only minimizer of V_ϵ in U. Let $x \in U$ and $(u, v) \in \Lambda_\alpha(x)$. Then, using Lemmas 3.3.8 and 3.3.9

and the definition of $\mathcal{G}_\alpha$, we have

$$D^+_{\mathcal{G}_\alpha} V_\epsilon(x) \leq - \|\mathcal{G}_\alpha(x)\|^2 + \alpha u^\top g(x) + \alpha v^\top h(x) - \frac{1}{\epsilon} \sum_{i \in I_+(x)} \alpha g_i(x) - \frac{1}{\epsilon} \sum_{j=1}^{k} \alpha |h_j(x)|.$$

Let $I_{\leq 0} = I_0(x) \cup I_-(x)$. It follows that,

$$\begin{aligned} D^+_{\mathcal{G}_\alpha} V_\epsilon(x) \leq & - \|\mathcal{G}_\alpha(x)\|^2 + \alpha \sum_{i \in I_{\leq 0}} u_i g_i(x) + \\ & \alpha \sum_{i \in I_+(x)} \Big(u_i - \frac{1}{\epsilon}\Big) g_i(x) + \alpha \sum_{j=1}^{k} \Big(|v_j| - \frac{1}{\epsilon}\Big) |h_j(x)|. \end{aligned}$$

Next, by [RW98, Proposition 5.15], Λ_α is locally bounded, so there exists a $B > 0$ such that

$$\sup_{x \in U} \left\{ \sup_{(u,v) \in \Lambda_\alpha(x)} \|(u,v)\|_\infty \right\} < B. \tag{3.22}$$

So if we choose $\epsilon_2 > 0$ such that $\epsilon_2 < \frac{1}{B}$, then for $\epsilon < \epsilon_2$,

$$\sum_{i \in I_+(x)} \Big(u_i - \frac{1}{\epsilon}\Big) g_i(x) + \sum_{j=1}^{k} \Big(|v_j| - \frac{1}{\epsilon}\Big) |h_j(x)| < 0.$$

Finally, since $u \geq 0$, we have $\alpha \sum_{i \in I_{\leq 0}} u_i g_i(x) \leq 0$. Thus,

$$D^+_{\mathcal{G}_\alpha} V_\epsilon(x) \leq - \|\mathcal{G}_\alpha(x)\|^2 < 0,$$

for all $x \in U \setminus \{x^*\}$, whenever $\epsilon < \min\{\epsilon_1, \epsilon_2\}$. Therefore V_ϵ is a Lyapunov function on U and asymptotic stability of x^* relative to $\mathbb{R}^n$ follows by Lemma 2.2.1. □

Remark 3.3.10 (Relationship to merit functions in numerical optimization)**.** In numerical optimization, the ℓ^1 penalty function in (3.20) is often used as a *merit function*, i.e., a function that quantifies how well a single iteration of an optimization algorithm balances the two goals of reducing the value of the objective function and reducing the constraint violation (cf. [NW06, Sec. 15.4]). Typically, the stepsize on each iteration is chosen so that the merit function is nonincreasing. Thus, if the algorithm is viewed as a discrete-time dynamical system, the merit function is a Lyapunov function. The ℓ^1 penalty plays a similar role for the continuous-time system described here. □

C Exponential Stability of Isolated Local Minimizers

We now discuss the exponentially stability of isolated local minimizers. Our first step is to identify conditions under which the safe gradient flow is differentiable. To do so, we introduce the notions of strict complementarity and second-order condition on the optimization problem.

Definition 3.3.11 (Strict complementarity and second-order sufficient conditions)**.** *Let* (x^*, u^*, v^*) *be a KKT triple of* (3.1)*.*

- *The strict complementarity condition holds if* $u_i^* > 0$ *for all* $i \in I_0(x^*)$*;*
- *The second-order sufficient condition holds if* $z^\top Q z > 0$ *for all* $z \in \ker \frac{\partial g_{I_0}(x^*)}{\partial x} \cap \ker \frac{\partial h(x^*)}{\partial x}$*, where*

$$Q = \nabla^2 f(x^*) + \sum_{i=1}^{m} u_i^* \nabla^2 g_i(x^*) + \sum_{j=1}^{k} v_i^* \nabla^2 h_j(x^*). \tag{3.23}$$

When LICQ hold and strict complementarity hold for (3.1), these properties together can be used to establish the differentiability of the KKT triple satisfying (3.16), and one can compute the Jacobian in closed form.

Lemma 3.3.12 (Jacobian of safe gradient flow)**.** *Let $x^* \in X_{\mathrm{KKT}}$ and (u^*, v^*) be the associated Lagrange multipliers. Suppose*

- *LICQ holds at x^*;*
- *(x^*, u^*, v^*) satisfies the strict complementarity condition;*

Then $\mathcal{G}_\alpha$ is differentiable at x^* and

$$\frac{\partial \mathcal{G}_\alpha(x^*)}{\partial x} = -PQ - \alpha(I - P),$$

where I is the $n \times n$ identity matrix, P is the orthogonal projection matrix onto $\ker \frac{\partial g_{I_0}(x^*)}{\partial x} \cap \ker \frac{\partial h(x^*)}{\partial x}$*, and Q is defined in* (3.23)*.*

Proof. Let $J := I_-(x^*)$ and assume. After possibly reordering the rows of $g(x)$, we have $I_0 = \{1, 2, \ldots, |I_0|\}$ and $J = \{|I_0| + 1, \ldots, m\}$. For convenience of notation we write $G = \frac{\partial g(x^*)}{\partial x}$, $G_I = \frac{\partial g_{I_0}(x^*)}{\partial x}$, $G_J = \frac{\partial g_J(x^*)}{\partial x}$ and $H = \frac{\partial h(x^*)}{\partial x}$.

We first show that when LICQ, strict complementarity hold for (3.1), then these properties also hold for the problem (3.13). By the reasoning in Proposition 3.3.3, (3.13) satisfies the strong second-order sufficient condition at x^*, and the ith inequality of constraint of (3.13) is active if and only if $g_i(x^*) = 0$. Since by Proposition 3.3.1, $\mathcal{G}_\alpha(x^*) = 0$, and $\Lambda_\alpha(x^*) = \{(u^*, v^*)\}$, it follows that $u_i^* > 0$ for i such that the ith inequality constraint of (3.13) is active, and therefore the problem satisfies strict complementarity as well.

Therefore, by [Fia76, Theorem 2.3] it follows that $\mathcal{G}_\alpha(x)$, $u(x)$ and $v(x)$ are differentiable at x^*, and the Jacobian, $\mathcal{J} = \frac{\partial}{\partial x}(\mathcal{G}_\alpha(x^*), u(x^*), v(x^*))$, can be computed as

$$\mathcal{J} = \left(\underbrace{\begin{bmatrix} I & H^\top & G^\top \\ -H & 0 & 0 \\ -D_u G & 0 & -\alpha D_g \end{bmatrix}}_{M} \right)^{-1} \underbrace{\begin{bmatrix} -Q \\ \alpha H \\ \alpha D_u G \end{bmatrix}}_{N}, \tag{3.24}$$

where $D_u = \operatorname{diag}(u^*)$ and $D_g = \operatorname{diag}(g(x^*))$. By strict complementarity, $D_u = \operatorname{blkdiag}(\tilde{D}_u, 0)$ and $D_g = \operatorname{blkdiag}(0, \tilde{D}_g)$, where $\tilde{D}_u \succ 0$ and $\tilde{D}_g \prec 0$. We partition matrices M and N in (3.24) to obtain

$$\mathcal{J} = \left[\begin{array}{c|ccc} I & H^\top & G_I^\top & G_J^\top \\ \hline -H & 0 & 0 & 0 \\ -\tilde{D}_u G_I & 0 & 0 & 0 \\ 0 & 0 & 0 & -\alpha \tilde{D}_g \end{array}\right]^{-1} \left[\begin{array}{c} -Q \\ \hline \alpha H \\ \alpha \tilde{D}_u G_I \\ 0 \end{array}\right]. \tag{3.25}$$

Let S be the Schur complement of M when partitioned as above. Then

$$S = \left[\begin{array}{cc|c} HH^\top & HG_I^\top & HG_J^\top \\ \tilde{D}_u G_I H^\top & \tilde{D}_u G_I G_I^\top & \tilde{D}_u G_I G_J^\top \\ \hline 0 & 0 & \alpha \tilde{D}_g \end{array}\right],$$

and the inverse of S is

$$S^{-1} = \begin{bmatrix} \begin{bmatrix} HH^\top & HG_I^\top \\ \tilde{D}_u G_I H^\top & \tilde{D}_u G_I G_I^\top \end{bmatrix}^{-1} & \times \\ 0 & \times \end{bmatrix}$$

where we replace values which will eventually be canceled out by $\times$. Next, we substitute S^{-1} into the formula for the inverse of a 2×2 block matrix given in [LS02, Theorem 2.1] to

compute M^{-1}, and simplify (3.25), which yields

$$\begin{aligned}\frac{\partial \mathcal{G}_\alpha(x^*)}{\partial x} &= -\left(I - \begin{bmatrix} H^\top & G_I^\top & G_J^\top \end{bmatrix} S^{-1} \begin{bmatrix} H \\ \tilde{D}_u G_I \\ 0 \end{bmatrix}\right) Q - \alpha \begin{bmatrix} H^\top & G_I^\top & G_J^\top \end{bmatrix} S^{-1} \begin{bmatrix} H \\ \tilde{D}_u G_I \\ 0 \end{bmatrix} \\ &= -PQ - \alpha(I - P).\end{aligned}$$

where

$$P = I - \begin{bmatrix} H \\ G_I \end{bmatrix}^\top \begin{bmatrix} HH^\top & HG_I^\top \\ \tilde{D}_u G_I H^\top & \tilde{D}_u G_I G_I^\top \end{bmatrix}^{-1} \begin{bmatrix} H \\ \tilde{D}_u G_I \end{bmatrix}.$$

Finally, let $D = \operatorname{blkdiag}(I, \tilde{D}_u)$. It follows that D is invertible and

$$\begin{aligned}P &= I - \begin{bmatrix} H^\top & G_I^\top \end{bmatrix} \left(D \begin{bmatrix} HH^\top & HG_I^\top \\ G_I H^\top & G_I G_I^\top \end{bmatrix}\right)^{-1} D \begin{bmatrix} H \\ G_I \end{bmatrix} \\ &= I - \begin{bmatrix} H^\top & G_I^\top \end{bmatrix} \begin{bmatrix} HH^\top & HG_I^\top \\ G_I H^\top & G_I G_I^\top \end{bmatrix}^{-1} D^{-1} D \begin{bmatrix} H \\ G_I \end{bmatrix} \\ &= I - \begin{bmatrix} H \\ G_I \end{bmatrix}^\dagger \begin{bmatrix} H \\ G_I \end{bmatrix},\end{aligned}$$

so by the properties of the Moore-Penrose inverse, P is the projection onto $\ker \frac{\partial g_I(x^*)}{\partial x} \cap \ker \frac{\partial h(x^*)}{\partial x}$. □

Using the result in Lemma 3.3.12, stability of an isolated local minimizer can be inferred by showing that the eigenvalues of the Jacobian of the safe gradient flow are all strictly negative.

Proof of Theorem 3.3.7(iii). By the second-order sufficient condition, $z^\top PQPz > 0$ for all $z \in \operatorname{im} P \setminus \{0\}$. It follows that $PQPz = 0$ if and only if $z \in \ker P$. Therefore 0 is an eigenvalue of PQP with multiplicity r and PQP has $n-r$ strictly positive eigenvalues, where

$r = \dim \ker P$. Let $z_1, \ldots, z_r$ be the eigenvectors corresponding to the zero eigenvalues, and $z_{r+1}, \ldots, z_n$ be eigenvectors corresponding to the positive eigenvalues, denoted $\lambda_{r+1}, \ldots, \lambda_n$. Then

$$Pz_i = \begin{cases} 0 & i = 1, \ldots, r, \\ \\ z_i & i = r+1, \ldots, n. \end{cases}$$

Let

$$\mu_i = \begin{cases} 0 & i = 1, \ldots, r, \\ \\ \lambda_i - \alpha & i = r+1, \ldots, n. \end{cases}$$

Then, it follows that $(PQP - \alpha P)z_i = \mu_i z_i$ for all $1 \leq i \leq n$. Observe that $PQP - \alpha P = (PQ - \alpha I)P$ has precisely the same eigenvalues as $P(PQ - \alpha I) = PQ - \alpha P$. Therefore, since μ_i is an eigenvalue of $PQ - \alpha P$, it follows that $\mu_i + \alpha$ is an eigenvalue of

$$PQ - \alpha P + \alpha I = PQ + \alpha(I - P) = -\frac{\partial \mathcal{G}_\alpha(x^*)}{\partial x}.$$

Hence the eigenvalues of $\frac{\partial \mathcal{G}_\alpha(x^*)}{\partial x}$ are

$$\{-\alpha, -\alpha, \ldots, -\alpha, -\lambda_{r+1}, \ldots, -\lambda_n\},$$

where $-\alpha$ appears with multiplicity r. Since all the eigenvalues are strictly negative, x^* is exponentially stable. $\square$

3.3.3 Stability of Nonisolated Local Minimizers

We have characterized in Section 3.3.2 the stability under the safe gradient flow of local minimizers that are isolated KKT points. In general, if x^* is strict local minimizer that is not an isolated KKT point (for example, if there are an infinite number of local maximizers arbitrarily close to x^*, cf. [AK06, page 5]), or if x^* is only a local minimizer, then there are no guarantees on Lyapunov stability. However, as we show here, nonisolated minimizers are stable under the safe gradient flow under additional assumptions on the problem data.

When there are no constraints, the safe gradient flow reduces to the classical gradient flow, where conditions for semistability of local minimizers are well known: if the objective function is real-analytic, then all trajectories of the gradient flow have finite arclength, cf. [Loj82], in which case the objective function can be used to construct an arclength-based Lyapunov function satisfying the hypotheses of Lemma 3.6.4 to establish semistability. In this section, we conduct a similar analysis for the constrained case. Our main result is as follows.

Theorem 3.3.13 (Stability of nonisolated local minima)**.** *Consider the optimization problem* (3.1)*, and assume f, g and h are real-analytic. Let $\mathcal{S}$ be a bounded set of local minimizers on which f is constant and equal to f^* such that*

(i) There is an open set U and $\beta > 0$ such that $U \cap X_{\mathrm{KKT}} = \mathcal{S}$ and $f(x) - f^* \geq \beta \mathrm{dist}_{\mathcal{S}}(x)^2$ for all $x \in U \cap \mathcal{C}$;

(ii) LICQ is satisfied at all $x^* \in \mathcal{S}$;

(iii) $T_{\mathcal{S}}(x^*) \cap \mathcal{N}_{\mathcal{S}}^{\mathrm{prox}}(x^*) = \{0\}$ for all $x^* \in \mathcal{S}$.

Then there is $\alpha^* > 0$ such that every $x^* \in \mathcal{S}$ is semistable relative to $\mathbb{R}^n$ under the safe gradient flow $\mathcal{G}_\alpha$, for $\alpha > \alpha^*$.

To prove this result, we first discuss various intermediate results. In particular, the growth condition in Theorem 3.3.13(i) plays a crucial role in the construction of a Lyapunov function to prove the result. Any $x^* \in \mathcal{S}$ satisfying this property is called a *weak sharp minimizer of f relative to $\mathcal{S}$*. Weak sharp minimizers play an important role in sensitivity analysis for nonlinear programs as well as convergence analysis for numerical methods in optimization [BF93, SW99].

We review second-order optimality conditions for weak sharp minimizers. Let $x^* \in X_{\mathrm{KKT}}$, suppose that LICQ holds at x^*, and let (u^*, v^*) be the unique Lagrange multipliers of (3.1) associated to x^*. Define the index set of *strongly active* constraints as

$$I_0^+(x^*) = \{1 \le i \le m \,|\, u_i^* > 0\}.$$

The *critical cone* is

$$\begin{aligned} \Gamma(x^*) = \{d \in \mathbb{R}^n \mid & \nabla h_j(x^*)^\top d = 0, j = 1, \dots k, \\ & \nabla g_i(x^*)^\top d = 0, i \in I_0^+(x^*), \\ & \nabla g_j(x^*)^\top d \le 0, j \in I_0(x^*) \setminus I_0^+(x)\}. \end{aligned} \tag{3.26}$$

Lemma 3.3.14 (Second-order necessary condition for constrained weak sharp minima [SW99, Prop. 3.5])**.** *Consider* (3.1) *and let $\mathcal{S} \subset \mathcal{C}$ be a set on which f is constant. Suppose that $x^* \in \partial\mathcal{S}$ is a weak sharp local minimizer of f relative to $\mathcal{S}$ and LICQ is satisfied at x^*.*

Let u^*, v^* be the Lagrange multipliers and define $\ell(x) = f(x) + (u^*)^\top g(x) + (v^*)^\top h(x)$. Then, there exists $\gamma > 0$ such that, for all $d \in \Gamma(x^*)$,

$$\ell''(x^*; d) \geq \gamma \mathrm{dist}_{T_{\mathcal{S}}(x^*)}(d)^2.$$

Lemma 3.3.15 (Second-order sufficient condition for unconstrained weak sharp minima [SW99, Thm. 2.5])**.** *Consider $W : \mathbb{R}^n \to \mathbb{R}$ and suppose that W is constant on $\mathcal{S}$. Suppose $x^* \in \partial\mathcal{S}$ and $W''(x^*; d) > 0$ for all $d \in \mathcal{N}_{\mathcal{S}}^{\mathrm{prox}}(x^*) \setminus \{0\}$, then x^* is a weak sharp local minimizer of W relative to $\mathcal{S}$.*

We now proceed with the construction of the Lyapunov function. Let $T_{\mathcal{C}}^{(\alpha)} : \mathbb{R}^n \rightrightarrows \mathbb{R}^n$ be the set-valued map where, for each $x \in \mathbb{R}^n$, $T_{\mathcal{C}}^{(\alpha)}(x)$ is the constraint set of (3.13). Let $J_\alpha : \mathbb{R}^n \times \mathbb{R}^n \to \mathbb{R}$ be

$$J_\alpha(x, \xi) = \alpha f(x) + \nabla f(x)^\top \xi + \frac{1}{2} \|\xi\|^2 .$$

Consider the optimization problem

$$\underset{\xi \in T_{\mathcal{C}}^{(\alpha)}(x)}{\text{minimize}} \quad J_\alpha(x, \xi) \tag{3.27}$$

As we show next, the solution to (3.27) is (3.13).

Lemma 3.3.16 (Correspondence between (3.27) and (3.13))**.** *Let $x \in \mathbb{R}^n$. Then the program* (3.13) *has a solution at x if and only if* (3.27) *has a solution, in which case $\mathcal{G}_\alpha(x) = \arg\min_{\xi \in T_{\mathcal{C}}^{(\alpha)}(x)} \{J_\alpha(x, \xi)\}$.*

Proof. Note that the feasible sets of (3.27) and (3.13) coincide. Next, for all $(x, \xi) \in \mathbb{R}^n \times \mathbb{R}^n$

$$J_\alpha(x, \xi) - \frac{1}{2} \|\xi + \nabla f(x)\|^2 = \alpha f(x) - \frac{1}{2} \|\nabla f(x)\|^2 .$$

Since the difference of the objectives in (3.27) and (3.13) does not depend on ξ, both problems have the same optimizer. □

Lemma 3.3.16 shows that (3.27) is another characterization of the safe gradient flow in terms of a parametric quadratic program. Let $W_\alpha : X \to \mathbb{R}$ be the value function

$$\begin{aligned} W_\alpha(x) &= \inf_{\xi \in T_{\mathcal{C}}^{(\alpha)}(x)} \{J_\alpha(x, \xi)\} \\ &= \alpha f(x) + \nabla f(x)^\top \mathcal{G}_\alpha(x) + \frac{1}{2} \|\mathcal{G}_\alpha(x)\|^2 . \end{aligned} \tag{3.28}$$

Our strategy to prove Theorem 3.3.13 consists of showing that W_α is a Lyapunov function satisfying the hypotheses in Lemma 3.6.5 whenever α is sufficiently large. Towards this end, we begin by computing the directional derivative of W_α. Let $Q : X \times \mathbb{R}^m_{\geq 0} \times \mathbb{R}^k \to \mathbb{R}^{n \times n}$ be the matrix-valued function,

$$Q(x, u, v) = \nabla^2 f(x) + \sum_{i=1}^{m} u_i \nabla^2 g_i(x) + \sum_{j=1}^{k} v_j \nabla^2 h_j(x).$$

Since the Lagrange multipliers, $(u(x), v(x))$ are unique in a neighborhood of $\mathcal{S}$, we slightly abuse notation by defining $Q(x) := Q(x, u(x), v(x))$. By Lipschitzness of u and v, Q is continuous on X. The proof of the next result follows from [Jit84, Thm. 2] and [Sha85, Cor. 4.1] and is omitted for brevity.

Lemma 3.3.17 (Differentiability of W_α)**.** *Suppose that $\mathcal{S}$ satisfies the hypotheses in Theorem 3.3.13, and X is an open set containing $\mathcal{S}$ on which $(\mathcal{G}_\alpha(x), u(x), v(x))$ is the unique solution to* (3.16)*. Then*

(i) For all $x \in X$, W_α is differentiable with

$$\nabla W_\alpha(x) = -(\alpha I - Q(x))\mathcal{G}_\alpha(x); \tag{3.29}$$

(ii) For all $x^* \in \mathcal{S}$, W_α is twice directionally differentiable in any direction $d \in \mathbb{R}^n$, where

$$\begin{aligned} W''_\alpha(x^*; d) = \min_{\zeta \in \mathbb{R}^n} \quad & \begin{bmatrix} d \\ \zeta \end{bmatrix}^\top \begin{bmatrix} \alpha Q(x^*) & Q(x^*) \\ Q(x^*) & I \end{bmatrix} \begin{bmatrix} d \\ \zeta \end{bmatrix} \\ \text{s.t.} \quad & \alpha \nabla h_j(x^*)^\top d + \nabla h_j(x^*)^\top \zeta = 0, \ \ \forall j = 1, \ldots, k, \\ & \alpha \nabla g_i(x^*)^\top d + \nabla g_i(x^*)^\top \zeta = 0, \ \ \forall i \in I_0^+(x^*), \\ & \alpha \nabla g_s(x^*)^\top d + \nabla g_s(x^*)^\top \zeta \leq 0, \ \ \forall s \in I_0(x^*) \setminus I_0^+(x^*). \end{aligned} \tag{3.30}$$

Remark 3.3.18 (Dependence of $Q(x)$ on α)**.** In general, for $x \in X$, the value of $Q(x)$ depends on the choice of α, since $u(x)$ and $v(x)$ depend on α. However, if $x^* \in X_{\text{KKT}}$, then $u(x^*), v(x^*)$ correspond to the Lagrange multipliers of (3.1) and $Q(x^*)$ is the Hessian of the Lagrangian of (3.1). In particular, this means that for all $x^* \in X_{\text{KKT}}$, the value of $Q(x^*)$ depends only on the problem data and is independent of α. □

We now proceed with the proof of Theorem 3.3.13.

Proof of Theorem 3.3.13. Let $\alpha^* = \sup_{x^* \in \mathcal{S}}\{\rho(Q(x^*))\}$. For $\alpha > \alpha^*$, we have $\alpha I - Q(x^*) \succ 0$ for all $x^* \in \mathcal{S}$. Assume without loss of generality that $\alpha I - Q(x) \succ 0$ for all $x \in U$ (if not, since Q is continuous, we can always find an open subset of U containing $\mathcal{S}$ for which these

property holds). We claim that W_α satisfies each of the conditions (i)-(iii) in Lemma 3.6.5 with $\mathcal{K} = \mathbb{R}^n$.

We begin by showing condition (iii). If $x^* \in U$ is a local minimizer of W_α, then $\nabla W_\alpha(x^*) = (\alpha I - Q(x^*))\mathcal{G}_\alpha(x^*) = 0$. Since $\alpha I - Q(x^*) \succ 0$, from (3.29) we deduce $\mathcal{G}_\alpha(x^*) = 0$, so $x^* \in X_{\text{KKT}}$ and therefore $x^* \in U \cap X_{\text{KKT}} = \mathcal{S}$.

Conversely, suppose that $x^* \in \mathcal{S}$. Note that, by Proposition 3.3.1, $W_\alpha(x) = \alpha f(x)$ for all $x \in \mathcal{S}$. Therefore, if $x^* \in \text{int}(\mathcal{S})$, it follows that x^* is a local minimizer of W_α. On the other hand, suppose that $x^* \in \partial\mathcal{S}$. For $d \in \mathbb{R}^n$, let ζ_d be the unique optimizer of (3.30). Then

$$W''_\alpha(x^*; d) = \alpha d^\top Q(x^*)d + 2\zeta_d^\top Q(x^*)d + \|\zeta_d\|^2 . \tag{3.31}$$

From the constraints in (3.30), $\zeta_d + \alpha d \in \Gamma(x^*)$. Because $x^* \in \partial\mathcal{S}$ is a weak sharp minimizer of f relative to $\mathcal{S}$, by Lemma 3.3.14, there exists $\gamma > 0$ such that for all $d \in \mathbb{R}^n$,

$$\ell''(x^*; \zeta_d + \alpha d) = (\zeta_d + \alpha d)^\top \nabla^2 \ell(x^*)(\zeta_d + \alpha d) \geq \gamma \text{dist}_{T_{\mathcal{S}}(x^*)}(\zeta_d + \alpha d)^2 \tag{3.32}$$

Since $\nabla^2 \ell(x^*) = Q(x^*)$, we combine (3.31) and (3.32) to get

$$\alpha W''_\alpha(x^*; d) \geq \zeta_d^\top (\alpha I - Q(x^*))\zeta_d + \gamma \text{dist}_{T_{\mathcal{S}}(x^*)}(\zeta_d + \alpha d)^2.$$

Because $\alpha I - Q(x^*) \succ 0$, if $W''_\alpha(x^*; d) = 0$, then $\zeta_d = 0$ and $d \in T_S(x^*)$. But $T_{\mathcal{S}}(x^*) \cap \mathcal{N}_{\mathcal{S}}^{\text{prox}}(x^*) = \{0\}$, which means $W''_\alpha(x^*; d) > 0$ for all $d \in \mathcal{N}_{\mathcal{S}}^{\text{prox}}(x^*) \backslash \{0\}$, so by Lemma 3.3.15, x^* is a weak sharp local minimizer of W_α.

Next we verify condition (ii) in Lemma 3.6.5. For all $x \in U$,

$$D^+_{\mathcal{G}_\alpha} W_\alpha(x) = \nabla W_\alpha(x)^\top \mathcal{G}_\alpha(x) = -\mathcal{G}_\alpha(x)^\top (\alpha I - Q(x)) \mathcal{G}_\alpha(x).$$

Without loss of generality, we can assume that U is bounded. Then, we can choose $c_1, c_2 > 0$ so that

$$c_1 < \inf_{x \in U} \{\lambda_{\min}(\alpha I - Q(x))\}$$

$$c_2 > \sup_{x \in U} \{\lambda_{\max}(\alpha I - Q(x))\}.$$

It follows that $D^+_{\mathcal{G}_\alpha} W_\alpha(x) \leq -c_1 \left\|\mathcal{G}_\alpha(x)\right\|^2$ for all $x \in U$, but since $\left\|\nabla W_\alpha(x)\right\| \leq c_2 \left\|\mathcal{G}_\alpha(x)\right\|$, we have for all $x \in U$,

$$D^+_{\mathcal{G}_\alpha} W_\alpha(x) \leq -\frac{c_1}{c_2} \left\|\nabla W_\alpha(x)\right\| \left\|\mathcal{G}_\alpha(x)\right\|.$$

Finally, we claim that $W_\alpha|_U$ is a globally subanalytic function, and therefore condition (i) holds by [Kur98, Thm. 1] and the fact that the class of globally subanalytic sets is an o-minimal structure (cf. [Kur98, Definition 1]). To prove the claim, first note that, since f is real-analytic, J_α is real-analytic, and therefore subanalytic [BM88, Definition 3.1]. Since U is bounded, and the restriction of any subanalytic function to a bounded open set is globally subanalytic [VdDM96], it follows that $J_\alpha|_U$ is globally subanalytic. Finally, since $T^{(\alpha)}_{\mathcal{C}}|_U : U \rightrightarrows \mathbb{R}^n$ is a globally subanalytic set valued map, and

$$W_\alpha|_U(x) = \inf_{\xi \in T^{(\alpha)}_{\mathcal{C}}|_U(x)} \{J_\alpha|_U(x, \xi)\},$$

it follows by application of Lemma 3.6.2 that $W_\alpha|_U$ is globally subanalytic. The statement

follows by applying Lemma 3.6.5 with $\mathcal{K} = \mathbb{R}^n$. □

3.3.4 Global Convergence

Finally, we turn to the characterization of the global convergence properties of the safe gradient flow. We show that when the problem data are real-analytic and the feasible set is bounded, every trajectory converges to a KKT point.

Theorem 3.3.19 (Global convergence properties)**.** *Consider the optimization problem* (3.1)*, and assume $\mathcal{C}$ is bounded, f, g, and h are real-analytic functions, and LICQ holds everywhere on $\mathcal{C}$. Let X be an open set containing $\mathcal{C}$ on which the safe gradient flow is well defined. Then there is $\alpha^* > 0$ such that for $\alpha > \alpha^*$, every trajectory of the safe gradient flow starting in X converges to some KKT point.*

To prove Theorem 3.3.19, we use the next result characterizing the positive limit set of solutions of the safe gradient flow.

Lemma 3.3.20 (Convergence to connected component)**.** *Consider the optimization problem* (3.1)*, and assume $\mathcal{C}$ is bounded, f, g, and h are real-analytic functions, and MFCQ holds everywhere on $\mathcal{C}$. Let X be an open set containing $\mathcal{C}$ on which the safe gradient flow is well defined. Then for all $x \in X$, $\omega(x)$ is contained in a unique connected component of X_{KKT}.*

Proof. By Theorem 3.3.4, $\mathcal{C}$ is asymptotically stable and forward invariant on X, and by Lemma 3.3.8, $D^+_{\mathcal{G}_\alpha} f(x) \leq 0$ for all $x \in \mathcal{C}$. Using the terminology from [AE10], f is a *height function* of the pair $(\mathcal{C}, \mathcal{G}_\alpha)$.

Because f, g, and h are real-analytic and $\mathcal{C}$ is bounded, $\mathcal{C}$ is a globally subanalytic set. Let $\hat{f} = f + \delta_{\mathcal{C}}$. Then $\hat{f}$ is a globally subanalytic function, $\hat{f}$ is continuous on $\mathrm{dom}(\hat{f}) = \mathcal{C}$, and X_{KKT} is precisely the set of critical points of $\hat{f}$. By the Morse-Sard Theorem for subanalytic functions [BDL06, Thm. 14], X_{KKT} has at most a countable number of connected components, and $\hat{f}$ is constant on each connected component. Since $f(x) = \hat{f}(x)$ for all $x \in \mathcal{C}$, f is also constant on each connected component of X_{KKT}, meaning that the connected components of X_{KKT} are *contained in* f (cf. [AE10, Definition 5]).

Hence, we can apply [AE10, Thm. 6], and conclude that for all $x \in X$, the positive limit set $\omega(x)$ is nonempty and contained in a unique connected component of E, where

$$E = \{x \in \mathcal{C} \mid D^+_{\mathcal{G}_\alpha} f(x) = 0\}.$$

However, by Lemma 3.3.8, $E = X_{\mathrm{KKT}}$, concluding the result. □

We are ready to prove Theorem 3.3.19.

Proof of Theorem 3.3.19. By Lemma 3.3.20, for $x \in X$, there is a connected component $\mathcal{S} \subset X_{\mathrm{KKT}}$ such that $\omega(x) \subset \mathcal{S}$. Since LICQ holds on $\mathcal{S}$, by Proposition 3.3.3 there is an open set U containing $\mathcal{S}$ and Lipschitz functions $(u, v) : U \to \mathbb{R}^m_{\geq 0} \times \mathbb{R}^k$ such that $U \cap X_{\mathrm{KKT}} = \mathcal{S}$ and $(\mathcal{G}_\alpha(x), u(x), v(x))$ is the unique solution to (3.16) on U.

Let W_α be given by (3.28). By Lemma 3.3.17, W_α is differentiable on U, and using the same reasoning as in the proof of Theorem 3.3.13, W_α is a globally subanalytic function, and satisfies the Kurdyka-Łojasiewicz inequality. Furthermore, if $\alpha > \alpha^* = \sup_{x^* \in \mathcal{S}} \{\rho(Q(x^*))\}$, then there is some $c > 0$ such that $D^+_{\mathcal{G}_\alpha} W_\alpha(y) \leq -c \|\nabla W_\alpha(y)\| \, \|\mathcal{G}_\alpha(y)\|$ for all $y \in U$.

Thus, we can apply Lemma 3.6.5 with $\mathcal{K} = \mathbb{R}^n$ to conclude that every trajectory starting in U that remains in U for all time converges to a point in $\mathcal{S}$. However, since $\omega(x) \subset \mathcal{S}$, there exists a $T > 0$ such that $\Phi_T(x) \in U$, and for all $t > 0$, $\Phi_t(\Phi_T(x)) = \Phi_{T+t}(x) \in U$. Thus, there exists $x^* \in \mathcal{S}$ such that $\Phi_{T+t}(x) \to x^*$ as $t \to \infty$, and therefore the trajectory starting at x converges to x^*. □

Remark 3.3.21 (Lower bounds on the parameter α to ensure global convergence)**.** Note that the proof of Theorem 3.3.19 yields the expression $\alpha^* = \sup_{x^* \in \mathcal{S}}\{\rho(Q(x^*))\}$ for the lower bound on α that guarantees global convergence. In general, computing this expression requires knowledge of the primal and dual optimizers of the original problem. However, reasonable assumptions on f, g, and h allow us to obtain upper bounds of α^*. For instance, if $\mathcal{C}$ is polyhedral and ∇f is ℓ_f-Lipschitz on $\mathcal{C}$, it follows that $\|\nabla^2 f(x)\| \leq \ell_f$, and $\nabla^2 g_i(x) = 0$ and $\nabla^2 h_j(x) = 0$ for all $i = 1, \dots m$ and $j = 1, \dots k$. Therefore, $\alpha^* \leq \ell_f$, and ℓ_f can be used instead as a lower bound on α to ensure global convergence. □

3.4 Comparison With Other Optimization Methods

Here we compare the safe gradient flow with other continuous-time flows to solve optimization problems. We consider the problem of minimizing $f(x) = 0.25\|x\|^2 - 0.5x_1 + 0.25x_2$ subject to $x_2 \geq 0$ and $x_1 \leq x_2$ (see also [HBHD21, Figure 8] for a comparison of additional methods). Figure 3.4 shows the outcome of the comparison on the same example problem taken from [HBHD21]. The methods compared are the projected gradient flow, the logarithmic barrier method (see e.g. [FGW02, Sec. 3]), the ℓ^2-penalty gradient flow (see

e.g. [FM90, Ch. 4]), the projected saddle-point dynamics (see e.g., [CMLC18]), the globally projected dynamics (see e.g., [XW00]), and the safe gradient flow.

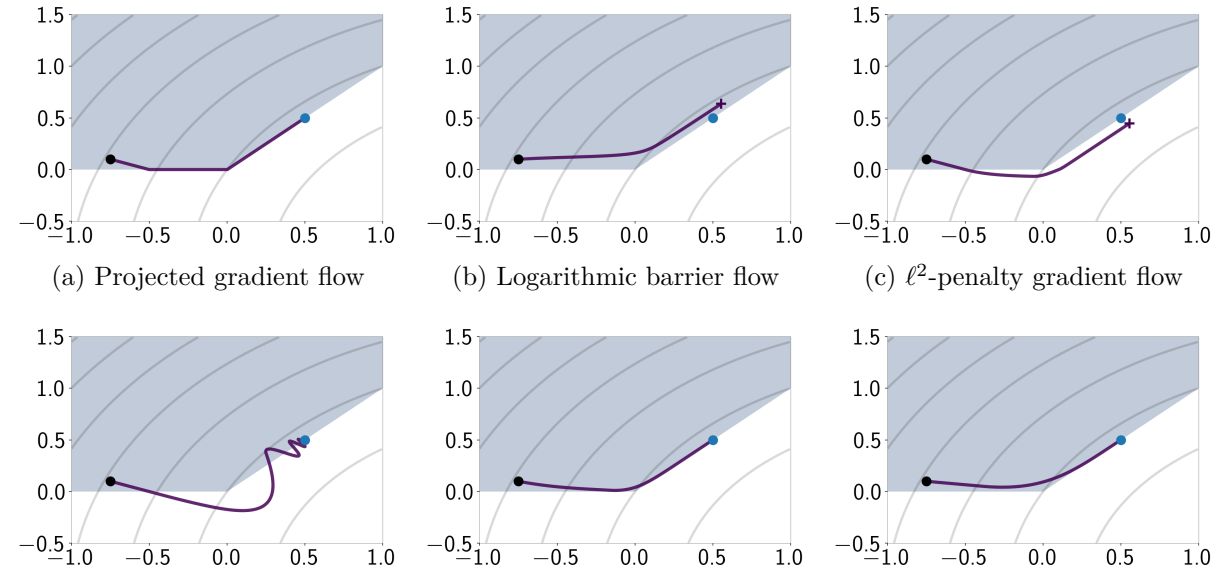

(a) Projected gradient flow (b) Logarithmic barrier flow (c) ℓ^2-penalty gradient flow

(d) Projected saddle-point dynamics (e) Globally projected dynamics (f) Safe gradient flow

Figure 3.4: Comparison of safe gradient flow with other continuous-time optimization algorithms. The blue-shaded region is the feasible set and the grey curves are level sets of the objective function. The initial condition is denoted by the purple dot, and the global minimizer is denoted by a blue dot. (a) The trajectory converges to the global minimizer, and the trajectory remains inside the feasible set for all time but it is nonsmooth. (b) The trajectory is smooth and remains inside the feasible set but does not converge to the global minimizer. However, by choosing μ small enough, the trajectory can be made to converge arbitrarily close to the minimizer. (c) The trajectory is smooth, but does not remain inside the feasible set or converge to the global minimizer. However, by choosing ϵ small enough, the trajectory can be made to converge arbitrarily close to the minimizer. (d) Initialized with $u(0) = 0$, the trajectory does not remain inside the feasible set, but it converges to the global minimum. (e) The trajectory is smooth, converges to the global minimizer, and remains inside the feasible set. However, this method may not be well-defined for nonconvex problems (f) The trajectory is smooth, converges to the global minimizer, and remains inside the feasible set. Of the methods implemented here and in [HBHD21, Figure 8], the safe gradient flow is the only nonconvex method that satisfies all of these properties.

Under the logarithmic barrier method, the feasible set is forward invariant and the minimizer of the logarithmic barrier penalty $f_{\text{barrier}}(x;\mu) = f(x) - \mu \sum_{i=1}^{m} \log(-g_i(x))$, with

$\mu > 0$, does not correspond to the minimizer of (3.1). Under the unconstrained minimizer of the ℓ^2-penalty, $f_{\text{penalty}}(x;\epsilon) = f(x) + \frac{\epsilon}{2}\sum_{i=1}^{m}[g_i(x)]_+^2$, with $\epsilon > 0$, does not correspond to the minimizer of (3.1), and the feasible set is not forward invariant under the gradient flow of f_{penalty}. Under the projected saddle-point dynamics, the feasible set is not forward invariant, but each trajectory converges to x^*. Under the globally projected dynamics, the feasible set is forward invariant, trajectories converge to x^*, and trajectories are smooth. However, unlike the safe gradient flow, the globally projected dynamics may be undefined when the constraints are not convex.

3.5 Conclusions

We have introduced the safe gradient flow, a continuous-time dynamical system to solve constrained optimization problems that makes the feasible set forward invariant. The system can be derived either as a continuous approximation of the projected gradient flow or by augmenting the gradient flow of the objective function with inputs, then using a control barrier function-based QP to ensure safety of the feasible set. The equilibria are exactly the critical points of the optimization problem, and the steady-state inputs at the equilibria correspond to the dual optimizers of the program. We have conducted a thorough stability analysis of the dynamics, identified conditions under which isolated local minimizers are asymptotically stable and nonisolated local minimizers are semistable. Future work will explore the flow's robustness properties, and leverage convexity to obtain stronger global convergence guarantees. Further, we hope to explore issues related to the practical implementation of the safe gradient flow, including interconnections of the optimizing dynamics

with a physical system, , develop discretizations of the dynamics and study their relationship with discrete-time iterative methods for nonlinear programming, and extend the framework to Newton-like flows for nonlinear programs which incorporate higher-order information.

3.6 Chapter Appendix

3.6.1 The Kurdyka-Łojasiewicz Inequality

Here we discuss the Kurdyka-Łojasiewicz inequality, which plays a critical role in the stability analysis of the systems considered in this chapter. The original formulation of the Łojasiewicz inequality[Loj82] states that for a real-analytic function $V : \mathbb{R}^n \to \mathbb{R}$ and a critical point $x^* \in V^{-1}(0)$, there exists $\rho > 0$, $\theta \in [0, 1)$, and $c > 0$ with

$$|V(x)|^\theta < c \left\| \nabla V(x) \right\|,$$

for all x in a bounded neighborhood of x^* such that $|V(x)| \leq \rho$. This inequality is used to establish that trajectories of gradient flows of real-analytic functions have finite arclength and converge pointwise to the set of equilibria.

In many applications, the assumption of real analyticity is too strong. For example, the value function of a parametric nonlinear program generally does not satisfy this assumption, even when all the problem data is real-analytic. However, generalizations of the Łojasiewicz inequality have since been shown [Kur98, BDL07] to hold for much broader classes of functions, which can be characterized using the notion of o-minimal structures,

which we define next.

Definition 3.6.1 (o-minimal structures)**.** *For each $n \in \mathbb{N}$, let $\mathcal{O}_n$ be a collection of subsets of $\mathbb{R}^n$. We call $\{\mathcal{O}_n\}_{n\in\mathbb{N}}$ an o-minimal structure if the following properties hold.*

(i) $\mathcal{O}_n$ is closed under complements, finite unions and finite intersections.

(ii) If $A \in \mathcal{O}_{n_1}$ and $B \in \mathcal{O}_{n_2}$ then $A \times B \in \mathcal{O}_{n_1+n_2}$.

(iii) Let $\pi : \mathbb{R}^{n+1} \to \mathbb{R}^n$ be the projection map onto the first n components. If $A \in \mathcal{O}_{n+1}$, then $\pi(A) \in \mathcal{O}_n$.

(iv) Let $g_1, \ldots, g_m$ and $h_1, \ldots, h_k$ be polynomial functions on $\mathbb{R}^n$ with rational coefficients. Then $\{x \in \mathbb{R}^n \mid g_i(x) < 0, h_j(x) = 0, 1 \leq i \leq m, 1 \leq j \leq k\} \in \mathcal{O}_n$

(v) $\mathcal{O}_1$ is precisely the collection of all finite unions of intervals in $\mathbb{R}$.

Examples of o-minimal structures include the class of semi-algebraic sets and the class of globally subanalytic sets. We refer the reader to [VdDM96] for a detailed overview of these concepts. The notion of o-minimality plays a crucial role in optimization theory, since the remarkable geometric properties of definable functions allows nonlinear programs involving them to be studied using powerful tools from real algebraic geometry and variational analysis, cf. [Iof09].

Let $\{\mathcal{O}_n\}_{n\in\mathbb{N}}$ be an o-minimal structure. A set $X \subset \mathbb{R}^n$ such that $X \in \mathcal{O}_n$ is said to be *definable with respect to* $\{\mathcal{O}_n\}_{n\in\mathbb{N}}$. When the particular o-minimal structure is obvious from context, then we simply call X *definable*. Given a definable set X and $f : X \to \mathbb{R}^m$ and $\mathcal{F} : X \rightrightarrows \mathbb{R}^m$, we say that f (resp. $\mathcal{F}$) is *definable* if $\text{graph}(f) \in \mathcal{O}_{n+m}$ (resp. $\text{graph}(\mathcal{F}) \in$

$\mathcal{O}_{n+m}$). The image and preimage of a definable set with respect to a definable function is also definable, and the class of definable functions is closed with respect to composition and linear combinations. Furthermore, as we show below, the value function of a parametric nonlinear program is definable when the problem data is definable.

Lemma 3.6.2 (Definability of value functions)**.** *Let $X \subset \mathbb{R}^n$, $J : X \times \mathbb{R}^m \to \mathbb{R}$ and $\mathcal{F} : X \rightrightarrows \mathbb{R}^m$ be definable. Let $V : X \to \overline{\mathbb{R}}$ be given by $V(x) = \inf_{\xi \in \mathcal{F}(x)}\{J(x,\xi)\}$, and suppose that* $\mathrm{dom}(V) = X$*. Then V is also definable.*

Finally, functions definable on o-minimal structures satisfy a generalization of the Łojasiewicz inequality [Kur98].

Lemma 3.6.3 (Kurdyka-Łojasiewicz inequality for definable functions)**.** *Let $X \subset \mathbb{R}^n$ be a bounded, open, definable set, and $V : X \to \mathbb{R}$ a definable, differentiable function, and $V^* = \inf_{y \in X} V(y)$. Then there exists $c > 0$, $\rho > 0$, and a strictly increasing, definable, differentiable function $\psi : [0, \infty) \to \mathbb{R}$ such that*

$$\psi'(V(x) - V^*) \, \|\nabla V(x)\| \geq c$$

for all $x \in U$ where $V(x) - V^* \in (0, \rho)$.

3.6.2 Lyapunov Tests for Stability

Here we present Lyapunov based tests for attractivity and stability of a nonisolated equilibria. Each of the tests we discuss exploit the fact that pointwise convergence follows

as a consequence of the trajectories of the system having finite arclength. We begin with the "arclength"-based Lyapunov test from [BB10, Thm. 4.3 and Theorem 5.2].

Lemma 3.6.4 (Arclength-based Lyapunov test)**.** *Let $\mathcal{K}$ be a forward invariant set of $\dot{x} = F(x)$. Let $\mathcal{S} \subset \mathcal{K}$ be a set of equilibria and $U \subset \mathbb{R}^n$ an open set containing $\mathcal{S}$ where $U \cap F^{-1}(\{0\}) = \mathcal{S}$. Let $V : U \cap \mathcal{K} \to \mathbb{R}$ be a continuous function. Consider the following conditions.*

(i) There exists a $c > 0$ such that for all $x \in U \cap \mathcal{K}$,

$$D_F^+ V(x) \leq -c \left\| F(x) \right\|. \tag{3.33}$$

(ii) x^* is a minimizer of V if and only if $x^* \in \mathcal{S}$.

If (i) holds then every bounded trajectory that starts in $U \cap \mathcal{K}$ and remains in $U \cap \mathcal{K}$ for all time has finite arclength and converges to a point in $\mathcal{S}$. If (i) and (ii) hold then, in addition, every $x^* \in \mathcal{S}$ is semistable relative to $\mathcal{K}$.

In the case where the Lyapunov function V is definable with respect to an o-minimal structure, we show that the condition in (3.33) for the arclength-based Lyapunov test can be replaced with $D_F^+ V(x) \leq -c \left\| F(x) \right\| \left\| \nabla V(x) \right\|$. This is referred to as the "angle-condition" and has been exploited [AMA05, Lag07] to show convergence of descent methods to solve non-linear programming problems. The name arises from the fact that the inequality implies that the angle between $F(x)$ and $\nabla V(x)$ remains bounded in a neighborhood of the equilibrium. In the next result, we show that the angle condition, together with the Kurdyka-Łojasiewicz inequality, implies that all trajectories of the system have finite arclength.

Lemma 3.6.5 (Angle-condition-based Lyapunov test)**.** *Let $\mathcal{K}$ be a forward invariant set of $\dot{x} = F(x)$. Let $\mathcal{S} \subset \mathcal{K}$ be a bounded set of equilibria and $U \subset \mathbb{R}^n$ a bounded open set containing $\mathcal{S}$ where $U \cap F^{-1}(\{0\}) = \mathcal{S}$. Let $V : U \cap \mathcal{K} \to \mathbb{R}$ be a differentiable function. Consider the following conditions.*

(i) V is constant and equal to V^* on $\mathcal{S}$ and definable with respect to some o-minimal structure;

(ii) There is $c_2 > 0$ such that for all $x \in U \cap \mathcal{K}$,

$$D_F^+ V(x) \leq -c_2 \|\nabla V(x)\| \|F(x)\|.$$

(iii) x^* is a minimizer of V if and only if $x^* \in \mathcal{S}$.

If (i) and (ii) hold then every trajectory that starts in $U \cap \mathcal{K}$ and remains in $U \cap \mathcal{K}$ for all time has finite arclength and converges to a point in $\mathcal{S}$. If (i)-(iii) hold then, in addition, every $x^* \in \mathcal{S}$ is semistable relative to $\mathcal{K}$.

Proof. Suppose (i) holds. By Lemma 3.6.3, there exists $c_1 > 0$ and a strictly increasing, definable, differentiable function $\psi : [0, \infty) \to \mathbb{R}$ such that $\psi'(|V(x) - V^*|) \|\nabla V(x)\| \geq c_1$ for all $x \in (U \cap \mathcal{K}) \setminus \mathcal{S}$. Assume without loss of generality that $\psi(0) = 0$, and define $\tilde{V} : U \cap \mathcal{K} \to \mathbb{R}$ by

$$\tilde{V}(x) = \begin{cases} \psi(V(x) - V^*) & V(x) > V^* \\ 0 & V(x) = V^* \\ -\psi(V^* - V(x)) & V(x) < V^*. \end{cases}$$

Then for all $x \in U$ with $V(x) > V^*$, we have

$$\begin{aligned} D_F^{\pm}\tilde{V}(x) &= \psi'(V(x) - V^*) D_F^{\pm} V(x) \\ &\leq -c_2 \psi'(V(x) - V^*) \|\nabla V(x)\| \|F(x)\| \\ &\leq -c_1 c_2 \|F(x)\| . \end{aligned}$$

A similar argument can be used to show that the above inequality also holds when $V(x) \leq V^*$. Since ψ is increasing, $x^* \in U \cap \mathcal{K}$ is a local minimizer of $\tilde{V}$ if and only if x^* is a local minimizer of V. Hence, the result follows by applying Lemma 3.6.4 with the Lyapunov function $\tilde{V}$.

□

3.6.3 Regularity of Systems of Linear Inequalities

The proof of Lemma 3.2.1, requires the following technical result which gives conditions for which a linear system of inequalities is regular.

Lemma 3.6.6. *Consider a linear inequality system in the variables $(u, v) \in \mathbb{R}^m \times \mathbb{R}^k$ with the form*

$$G_1 u + G_2 v \leq c \tag{3.34a}$$

$$H_1 u + H_2 v = h \tag{3.34b}$$

$$u \geq 0 \tag{3.34c}$$

where $c \in \mathbb{R}^{n_c}$, $d \in \mathbb{R}^{n_d}$, $G_1 \in \mathbb{R}^{n_c \times m}$, $G_2 \in \mathbb{R}^{n_c \times k}$, $H_1 \in \mathbb{R}^{n_d \times m}$, $H_2 \in \mathbb{R}^{n_d \times k}$. The system (3.34) is regular if H_2 is full rank and there exists (u_0, v_0) such that $G_1 u_0 + G_2 v_0 < c$,

$H_1 u_0 + H_2 v_0 = h$, $u_0 \geq 0$.

Proof. By [Rob75, Theorem 2], the system (3.34) is regular if and only if:

(i) There exists (u_0, v_0) such that $G_1 u_0 + G_2 v_0 < c$, $H_1 u_0 + H_2 v_0 = d$, $u_0 \geq 0$.

(ii) The following system is regular:

$$H_1 u + H_2 v = d \tag{3.35a}$$

$$u \geq 0. \tag{3.35b}$$

We claim that (3.35) is regular whenever H_2 has full rank. Indeed, by a second application of [Rob75, Theorem 2], (3.35) is regular if and only if

(i) There exists u_1, v_1 such that $u_1 > 0$ and $H_1 u_1 + H_2 v_1 = d$

(ii) $[H_1 \;\; H_2]$ has full rank.

Because H_2 has full rank, (i) holds since for any $u_1 > 0$, we can always find some v_1 such that $H_2 v_1 = h - H_1 u_1$ and (ii) holds since if H_2 is full rank, range($[H_1 \;\; H_2]$) = range(H_2). □

Acknowledgements

This chapter, in part, is a reprint of the material [AC24] where it appears as "Control-Barrier-Function-Based Design of Gradient Flows for Constrained Nonlinear Programming" by Ahmed Allibhoy and Jorge Cortés in IEEE Transactions on Automatic Control. The dissertation author is the primary investigator and author of this paper.

Chapter 4

Control Theoretic Synthesis of Dynamical Systems Solving Monotone Variational Inequalities

In this chapter, we extend the framework we developed in Chapter 3 to synthesize anytime algorithms, in the form of continuous-time dynamical systems, to solve monotone variational inequalities. We introduce three algorithms that solve this problem: the projected monotone flow, the safe monotone flow, and the recursive safe monotone flow. The first two systems admit dual interpretations: either as projected dynamical systems or as dynamical systems controlled with a feedback controller synthesized using techniques from safety-critical control. The third flow bypasses the need to solve quadratic programs along the trajectories by incorporating a dynamics whose equilibria precisely correspond to such solutions, and interconnecting the dynamical systems on different time scales. We perform a thorough

analysis of the dynamical properties of all three systems. For the safe monotone flow, we show that equilibria correspond exactly with critical points of the original problem, and the constraint set is forward invariant and asymptotically stable. The additional assumption of convexity and monotonicity allows us to derive global stability guarantees, as well as establish the system is contracting when the constraint set is polyhedral. For the recursive safe monotone flow, we use tools from singular perturbation theory for contracting systems to show KKT points are locally exponentially stable and globally attracting, and obtain practical safety guarantees. We illustrate the performance of the flows on a two-player game example and also demonstrate the versatility for interconnection and regulation of dynamical processes of the safe monotone flow in an example of a receding horizon linear quadratic dynamic game.

4.1 Problem Formulation

Consider a variational inequality

$$(x - x^*)^\top F(x^*) \geq 0, \qquad \forall x \in \mathcal{C}. \tag{4.1}$$

which we denote by $\mathrm{VI}(F, \mathcal{C})$, where $F : \mathbb{R}^n \to \mathbb{R}^n$ is continuously differentiable and $\mathcal{C}$ is a convex set of the form

$$\mathcal{C} = \{x \in \mathbb{R}^n \mid g(x) \leq 0,\ h(x) = Hx - c_h = 0\}, \tag{4.2}$$

where $g : \mathbb{R}^n \to \mathbb{R}^m$ is continuously differentiable. Our goal is to synthesize a dynamical system that solves the variational inequality. We formalize this next.

Problem 4.1.1. ***(Anytime solver of variational inequality).*** *Design a dynamical system, $\dot{x} = \mathcal{G}(x)$, which is well defined on a set X containing $\mathcal{C}$ such that*

(i) Trajectories of the system converge to $\mathrm{SOL}(F, \mathcal{C})$*;*

(ii) $\mathcal{C}$ is forward invariant;

(iii) Trajectories of the system with initial condition outside $\mathcal{C}$ converge to $\mathcal{C}$.

Item (i) ensures that the dynamical system can be viewed as an algorithm which solves (4.1): solutions can be obtained by simulating system trajectories and taking the limit as $t \to \infty$ of $x(t)$. Item (ii) ensures that this algorithm is *anytime*, meaning that even if terminated early, it is guaranteed to return a feasible solution provided the initial condition is feasible. Item (iii) accounts for infeasible initial conditions, and ensures asymptotic safety. Both the expression of the algorithm in the form of a continuous-time dynamical system and the anytime property are particularly useful for real-time applications, where the algorithm might be interconnected with other physical processes – e.g., when the algorithm output is used to regulate a physical plant and constraints of the optimization problem ensure the safe operation of the plant.

In the following, we introduce three dynamics to solve Problem 4.1.1, synthesized using the techniques outlined in Section 2.2.6. The first is the *projected monotone flow*, which is already well-known, but we reinterpret it here through the lens of control theory.

The next two are the *safe monotone flow* and the *recursive safe monotone flow*. Both dynamics are entirely novel.

4.2 Projected Monotone Flow

In this section, we discuss our first solution to Problem 4.1.1, in the form of the *projected monotone flow*. We show that the system can be implemented in two equivalent ways: either as a control system with a feedback controller designed using the strategy outlined in Section 2.2.6.A, or as a projected dynamical system. In fact, this system admits many other equivalent descriptions, for example in terms of monotone differential inclusions, or complementarity systems [BDLA06, HSW00, AC84], and its properties have been extensively studied [NZ96]. However, we focus here on the control-based and projection-based forms. In the following sections we describe in detail the derivation of each implementation, show they are equivalent, and discuss the properties of the resulting flow regarding safety and stability.

4.2.1 Control-Based Implementation

Our design strategy originates from the observation that, when F is monotone, the system $\dot{x} = -F(x)$ finds solutions to the unconstrained variational inequality $\mathrm{VI}(F, \mathbb{R}^n)$. However, trajectories flowing along this dynamics might leave the constraint set $\mathcal{C}$. This

leads us to consider the control-affine system:

$$\begin{aligned}\dot{x} &= \mathcal{F}(x,u,v)\\ &= -F(x) - \sum_{i=1}^{m} u_i \nabla g_i(x) - \sum_{j=1}^{k} v_j \nabla h_j(x).\end{aligned} \tag{4.3}$$

Here, we have augmented the system with inputs from the admissible set $\mathcal{U} = \mathbb{R}^m_{\geq 0} \times \mathbb{R}^k$ to modify the flow of the original drift $-F$ to account for the constraints in a way that ensures that the solutions to (4.3) stay inside of or approach $\mathcal{C}$. The idea is that if the constraint $g_i(x) \leq 0$ is in danger of being violated, the corresponding input u_i can be increased to ensure trajectories continue to satisfy it. Likewise, the input v_j can be increased or decreased to ensure the corresponding constraint $h_j(x) = 0$ is satisfied along trajectories.

Our design proceeds by thinking of $\mathcal{C}$ as a safety set for the system and using the approach outlined in Section 2.2.6.A to synthesize a safeguarding feedback controller $(u, v) = \kappa(x)$. Assuming that MFCQ holds for all $x \in \mathcal{C}$, $K_{\text{proj}} : \mathbb{R}^n \rightrightarrows \mathbb{R}^m_{\geq 0} \times \mathbb{R}^k$ takes the form

$$\begin{aligned}K_{\text{proj}}(x) = \Big\{(u,v) \in \mathbb{R}^m_{\geq 0} \times \mathbb{R}^k \;\Big|\; &-\frac{\partial g_I}{\partial x} F(x) - \frac{\partial g_I}{\partial x}\frac{\partial g}{\partial x}^{\top} u - \frac{\partial g_I}{\partial x}\frac{\partial h}{\partial x}^{\top} v \leq 0,\\ &-\frac{\partial h}{\partial x} F(x) - \frac{\partial h}{\partial x}\frac{\partial g}{\partial x}^{\top} u - \frac{\partial h}{\partial x}\frac{\partial h}{\partial x}^{\top} v = 0\Big\}.\end{aligned}$$

The following result states that the set of admissible controls is nonempty. We omit its proof for space reasons, but note that it readily follows from Farka's Lemma [Roc70].

Lemma 4.2.1. ***(Projection onto Tangent Cone is Feasible).*** *If $x \in \mathcal{C}$ and MFCQ holds at x, then $K_{proj}(x) \neq \emptyset$.*

We then use the feedback controller

$$\kappa(x) \in \underset{(u,v)\in K_{\text{proj}}(x)}{\operatorname{argmin}} J(x,u,v), \tag{4.4}$$

where we set the objective function to be

$$J(x,u,v) = \frac{1}{2}\Big\| \sum_{i=1}^{m} u_i \nabla g_i(x) + \sum_{j=1}^{k} v_j \nabla h_j(x) \Big\|^2. \tag{4.5}$$

This function measures the magnitude of the "modification" of the drift term in (4.3). Thus, the QP-based controller (4.4) has the interpretation, at each x, of finding the control input such that the closed-loop system dynamics are as close as possible to $-F(x)$, while still being in $T_{\mathcal{C}}(x)$. In general, the program given by (4.4) does not have unique solutions. Despite this, we show below that the closed-loop dynamics of (4.3) is well defined regardless of which solution to (2.9) is chosen. We refer to it as the *projected monotone flow* and denote it by $\mathcal{P}$.

4.2.2 Projection-Based Implementation

The second implementation of the projected monotone flow consists of projecting $-F(x)$ onto the tangent cone of the constraint set. In general, the tangent cone does not have a representation that allows us to compute the projection easily. However, when the appropriate constraint qualification condition holds, the tangent cone admits a convenient parameterization which allows for the projection to be implemented as a quadratic program. Let $x \in \mathcal{C}$ and suppose that MFCQ holds at x. It follows that the tangent cone can be

parameterized as

$$T_{\mathcal{C}}(x) = \left\{ \xi \in \mathbb{R}^n \;\middle|\; \frac{\partial h(x)}{\partial x}\xi = 0, \frac{\partial g_{I_0}(x)}{\partial x}\xi \leq 0 \right\}. \tag{4.6}$$

The projection-based implementation of the projected monotone flow takes then the following form:

$$\begin{aligned} \dot{x} &= \Pi_{T_{\mathcal{C}}(x)}(-F(x)) \\ &= \underset{\xi \in \mathbb{R}^n}{\operatorname{argmin}} \quad \frac{1}{2}\left\|\xi + F(x)\right\|^2 \\ &\qquad \text{subject to} \quad \frac{\partial g_{I_0}(x)}{\partial x}\xi \leq 0, \frac{\partial h(x)}{\partial x}\xi = 0. \end{aligned} \tag{4.7}$$

The projection onto the tangent ensures by Nagumo's Theorem [Bla99, Theorem 3.1] that $\mathcal{C}$ is forward invariant.

4.2.3 Properties of Projected Monotone Flow

Here, we lay out the properties of the projected monotone flow. We begin by establishing the equivalence between the control- and projection-based implementations. We then discuss existence and uniqueness of solutions, and finally the stability and safety properties of the dynamics.

A Equivalence of Control-Based and Projection-Based Implementations

Equivalence follows directly from the properties of the tangent cone, as we show next.

Proposition 4.2.2. ***(Equivalence of Control-Based and Projected-Based Implementations).*** *Assume MFCQ holds at $x \in \mathcal{C}$ and let (u, v) be any solution to* (4.4) *(note*

that $\mathcal{P}(x) = \mathcal{F}(x, u, v)$*). Then,* $\mathcal{P}(x) = \Pi_{T_{\mathcal{C}}(x)}(-F(x))$.

Proof. Let (u, v) be any solution to (4.4) and $\xi = \Pi_{T_{\mathcal{C}}(x)}(-F(x))$. Then $\mathcal{F}(x, u, v) \in T_{\mathcal{C}}(x)$, so it follows immediately by optimality of ξ that

$$\|\xi + F(x)\|^2 \leq \|\mathcal{F}(x, u, v) + F(x)\|^2 .$$

Next, because ξ is given by a projection, there exists $w \in N_{\mathcal{C}}(x)$ such that $\xi + F(x) + w = 0$, see e.g., [BDLA06, Corollary 2]. If MFCQ holds at $x \in \mathcal{C}$, by [RW98, Theorem 6.14], there exists $(\bar{u}, \bar{v})$ such that w can be written as

$$w = \sum_{i=1}^{m} \bar{u}_i \nabla g_i(x) + \sum_{j=1}^{k} \bar{v}_j \nabla h_j(x), \qquad \bar{u} \geq 0, \quad \bar{u}^\top g(x) = 0.$$

Combining this expression with the fact that $\xi = -F(x) - w \in T_{\mathcal{C}}(x)$ and using the parameterization of the tangent cone in (4.6), we deduce that $(\bar{u}, \bar{v}) \in K_{\text{proj}}(x)$. By optimality of (u, v),

$$\begin{aligned}
\|\xi + F(x)\|^2 &= \Big\| \sum_{i=1}^{m} \bar{u}_i \nabla g_i(x) + \sum_{j=1}^{k} \bar{v}_j \nabla h_j(x) \Big\|^2 \\
&\geq \Big\| \sum_{i=1}^{m} u_i \nabla g_i(x) + \sum_{j=1}^{k} v_j \nabla h_j(x) \Big\|^2 \\
&= \|\mathcal{F}(x, u, v) + F(x)\|^2 .
\end{aligned}$$

But since the projection onto the tangent cone must be unique, we conclude $\xi = \mathcal{F}(x, u, v)$.

□

The value of Proposition 4.2.2 stems from showing that safety-critical control can be used to systematically design algorithms that solve variational inequalities. Though the control strategy pursued in Section 4.2.1 results in a known flow, this sets up the basis for employing other design strategies from safety-critical control to yield novel methods, as we will show later.

B Existence and Uniqueness of Solutions

The projected monotone flow is discontinuous, and hence one must consider notions of solutions beyond the classical ones, see e.g., [Cor08]. Here, we consider Carathéodory solutions, which are absolutely continuous functions that satisfy (4.7) almost everywhere. The existence and uniqueness of solutions for all initial conditions follows readily from [AC84, Chapter 3.2, Theorem 1(i)].

C Safety and Stability of Projected Monotone Flow

We now show that the projected monotone flow is safe, meaning that the constraint set $\mathcal{C}$ is forward invariant, and the solution set $\mathrm{SOL}(F, \mathcal{C})$ is stable. Forward invariance of $\mathcal{C}$ follows directly from Nagumo's Theorem. The equilibria of the projected monotone flow correspond to solutions to $\mathrm{VI}(F, \mathcal{C})$. Finally, stability of a solution x^* can be certified using the Lyapunov function $V(x) = \frac{1}{2}\|x - x^*\|^2$, as a consequence of [AC84, Chapter 3.2, Theorem 1(ii)]. These properties are summarized in the following result.

Theorem 4.2.3. ***(Safe and Stability Properties of Projected Monotone Flow).*** *Let $\mathcal{C}$ be convex and suppose MFCQ holds everywhere on $\mathcal{C}$. The following hold for the*

projected monotone flow:

(i) $\mathcal{C}$ *is forward invariant;*

(ii) x^* *is an equilibrium of the projected monotone flow if and only if* $x^* \in \mathrm{SOL}(F, \mathcal{C})$*;*

(iii) If $x^* \in \mathrm{SOL}(F, \mathcal{C})$ *and* F *is monotone, then* x^* *is globally Lyapunov stable relative to* $\mathcal{C}$*;*

(iv) If F *is* μ*-strongly monotone, then the projected monotone flow is contracting at rate* μ*. In particular, the unique solution* $x^* \in \mathrm{SOL}(F, \mathcal{C})$ *is globally exponentially stable relative to* $\mathcal{C}$*.*

4.3 Safe Monotone Flow

In this section, we discuss a second solution to Problem 4.1.1, which results in an entirely novel flow, termed *safe monotone flow*. Similar to the projected monotone flow, this system admits two equivalent implementations: either as a control-system with a safeguarding feedback controller or as a projected dynamical system.

4.3.1 Control-Based Implementation

We start with the control system (4.3) with the admissible control set $\mathcal{U} = \mathbb{R}^m_{\geq 0} \times \mathbb{R}^k$, viewing $\mathcal{C}$ as a safety set, and design a safeguarding controller. We synthesize this controller using the function (g, h) as a VCBF, following the approach outlined in Section 2.2.6.B.

Letting $\alpha > 0$ be a parameter, the set of control inputs ensuring safety is given by

$$K_{\mathrm{cbf},\alpha}(x) = \Big\{(u,v) \in \mathbb{R}^m_{\geq 0} \times \mathbb{R}^k \;\Big|\; -\frac{\partial g}{\partial x}F(x) - \frac{\partial g}{\partial x}\frac{\partial g}{\partial x}^\top u - \frac{\partial g}{\partial x}\frac{\partial h}{\partial x}^\top v \leq -\alpha g(x) \\ -\frac{\partial h}{\partial x}F(x) - \frac{\partial h}{\partial x}\frac{\partial g}{\partial x}^\top u - \frac{\partial h}{\partial x}\frac{\partial h}{\partial x}^\top v = -\alpha h(x)\Big\}.$$

The next result shows that this set is nonempty on an open set containing the constraint set.

Lemma 4.3.1. ***(Vector Control Barrier Function for*** (4.3)***).*** *Assume MFCQ holds for all $x \in \mathcal{C}$. Then there exists an open set $X \supset \mathcal{C}$ on which $\phi = (g,h)$ is a vector-control barrier function of* (4.3) *for $\mathcal{C}$, on X, relative to $\mathbb{R}^m_{\geq 0} \times \mathbb{R}^k$.*

The proof of this result is identical to [AC24, Lemma 4.1] and we omit it for brevity. By Lemma 4.3.1, the feedback controller $(u,v) = \kappa(x)$ where

$$\kappa(x) \in \underset{(u,v)\in K_{\mathrm{cbf},\alpha}(x)}{\operatorname{argmin}} J(x,u,v), \tag{4.8}$$

and J is given by (4.5), is well defined on X. This controller has the same interpretation as before: determining the control input belonging to $K_{\mathrm{cbf},\alpha}(x)$ such that the closed-loop system dynamics are as close as possible to $-F(x)$. Similar to the case with projection-based methods, the problem (2.10) does not necessarily have unique solutions. However, we show below that the closed-loop system is well-defined regardless of which solution is chosen. We refer to it as the *safe monotone flow with safety parameter* α, denoted $\mathcal{G}_\alpha$.

4.3.2 Projection-Based Implementation

Here we describe the implementation of the safe monotone flow as a projected dynamical system. Similar to the projected monotone flow, the projected system is obtained by projecting $-F(x)$ onto a set-valued map. However, because the projection onto the tangent cone is in general discontinuous as a function of the state, we replace the tangent cone with the *α-restricted tangent set*, denoted $T_{\mathcal{C}}^{(\alpha)}$, defined as

$$T_{\mathcal{C}}^{(\alpha)}(x) = \Big\{\xi \in \mathbb{R}^n \;\Big|\; \frac{\partial g(x)}{\partial x}\xi \leq -\alpha g(x),\; \frac{\partial h(x)}{\partial x}\xi = -\alpha h(x)\Big\}. \tag{4.9}$$

Figure 4.1 illustrates this definition. This set can be interpreted as an approximation of the usual tangent cone, but differs in several key ways. First, the restricted tangent set is not a cone, meaning that vectors in $T_{\mathcal{C}}^{(\alpha)}(x)$ cannot be scaled arbitrarily: in certain direction, the magnitude of vectors in $T_{\mathcal{C}}^{(\alpha)}(x)$ is restricted. An important property of $T_{\mathcal{C}}^{(\alpha)}(x)$ is that, even though the tangent cone is undefined for $x \notin \mathcal{C}$, this is not the case for the restricted tangent set. In fact, it can be shown that $T_{\mathcal{C}}^{(\alpha)}$ takes nonempty values on an open set containing $\mathcal{C}$. This property allows for the safe monotone flow to be well-defined for infeasible initial conditions. The next result summarizes properties of the α-restricted tangent set.

Proposition 4.3.2. ***(Properties of α-Restricted Tangent Set).*** *Assume MFCQ holds for all $x \in \mathcal{C}$. The set-valued map $T_{\mathcal{C}}^{(\alpha)} : \mathbb{R}^n \rightrightarrows \mathbb{R}^n$ satisfies:*

(i) $T_{\mathcal{C}}^{(\alpha)}(x)$ is convex for all $x \in \mathbb{R}^n$;

(ii) For any fixed $x \in \mathcal{C}$, the set $T_{\mathcal{C}}^{(\alpha)}(x)$ satisfies MFCQ at all $\xi \in T_{\mathcal{C}}^{(\alpha)}(x)$.

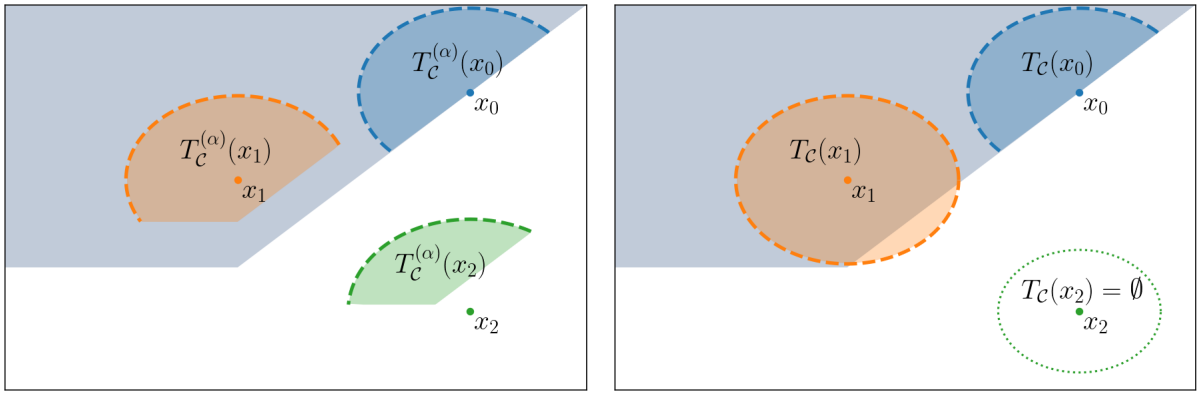

(a) (b)

Figure 4.1: Illustration of the notion of tangent cone, and α-restricted tangent set. The gray-shaded region represents the set $\mathcal{C}$. The colored regions depict either type of set, which consists of vectors centered various points x_i. The dashed border indicates directions in which the magnitude of vectors in the set are unbounded. (a) The α-restricted tangent set. Note that the set is well-defined at $x_2 \notin \mathcal{C}$, however because the region does not overlap with the point x_2, the set $T_{\mathcal{C}}^{(\alpha)}(x_2)$ does not contain any zero vectors, and all vectors point strictly toward the feasible set. (b) The tangent cone. Note that the tangent cone is not well defined at points outside $\mathcal{C}$.

(iii) There exists an open set X containing $\mathcal{C}$ such that $T_{\mathcal{C}}^{(\alpha)}(x) \neq \emptyset$ for all $x \in X$;

(iv) If $x \in \mathcal{C}$, then $T_{\mathcal{C}}^{(\alpha)} \subset T_{\mathcal{C}}(x)$.

Proof. We first observe that (i) follows from the fact that the constraints characterizing $T_C^{(\alpha)}(x)$ are affine in the variable ξ. We prove (ii) using the same strategy as [AC24, Lemma 4.5], which we sketch here. If MFCQ holds at $x \in \mathcal{C}$, then the inequalities defining (4.9) satisfy Slater's condition [BV09, Chapter 5.2.3] at x and therefore MFCQ holds for all $\xi \in T_{\mathcal{C}}^{(\alpha)}(x)$. To show (iii), we note that Slater's condition implies that the affine constraints parameterizing $T_{\mathcal{C}}^{(\alpha)}(x)$ are *regular* [Rob75, Theorem 2], meaning that the system remains feasible with respect to perturbations. Since $T_{\mathcal{C}}^{(\alpha)}(x)$ is nonempty for all $x \in \mathcal{C}$, it follows that there exists an open set X containing $\mathcal{C}$ such that $T_{\mathcal{C}}^{(\alpha)}(x)$ is nonempty for all $x \in X$. Finally, (iv) follows from the definition of the tangent cone. □

Using the α-restricted tangent set, we can define the projected dynamical system

$$\begin{aligned}\dot{x} &= \Pi_{T_{\mathcal{C}}^{(\alpha)}(x)}(-F(x)) \\ &= \underset{\xi\in\mathbb{R}^n}{\operatorname{argmin}} \quad \frac{1}{2}\left\|\xi + F(x)\right\|^2 \\ &\qquad \text{subject to} \quad \frac{\partial g(x)}{\partial x}\xi \leq -\alpha g(x) \\ &\qquad\qquad\qquad \frac{\partial h(x)}{\partial x}\xi = -\alpha h(x).\end{aligned} \tag{4.10}$$

Similar to the projected monotone flow, the projection operation ensures that the trajectories of the system remain in the safety set. However, as we show next, the advantages of projecting onto the restricted tangent cone is that the system is well defined for infeasible initial conditions, and trajectories of the system are smooth.

4.3.3 Properties of Safe Monotone Flow

We now discuss the properties of the safe monotone flow. We begin by establishing the equivalence of the control-based and projection-based implementations. Next, we discuss its stability and safety properties.

A Equivalence of Control-Based and Projection-Based Implementations

We establish here that the control-based and projection-based implementations of the safe monotone flow are equivalent. The next result states that the closed-loop dynamics resulting from the implementation of (2.10) over (4.3) is equivalent to the projection onto $T_{\mathcal{C}}^{(\alpha)}(x)$. The structure of the proof mirrors that of Proposition 4.2.2.

Proposition 4.3.3. ***(Equivalence of Control-Based and Projection-Based Implementations).*** *Assume MFCQ holds for everywhere on $\mathcal{C}$ and let $X \subset \mathbb{R}^n$ be an open set containing $\mathcal{C}$ on which $K_{cbf,\alpha}$ takes nonempty values. Let (u, v) be any solution to (4.8) at $x \in X$ (note that $\mathcal{G}_\alpha(x) = \mathcal{F}(x, u, v)$). Then, $\mathcal{G}_\alpha(x) = \Pi_{T_{\mathcal{C}}^{(\alpha)}(x)}(-F(x))$.*

Proof. Let (u, v) be any solution to (4.8) and $\xi = \Pi_{T_{\mathcal{C}}^{(\alpha)}(x)}(-F(x))$. Then $\mathcal{F}(x, u, v) \in T_{\mathcal{C}}^{(\alpha)}(x)$, so it follows immediately by optimality of ξ that $\|\xi + F(x)\|^2 \leq \|\mathcal{F}(x, u, v) + F(x)\|^2$. Next, because ξ is given by a projection, there exists $w \in N_T(\xi)$, where $T = T_{\mathcal{C}}^{(\alpha)}(x)$ such that $\xi + F(x) + w = 0$, see e.g., [BDLA06, Corollary 2], and where

$$w = \sum_{i=1}^{m} \bar{u}_i \nabla g_i(x) + \sum_{j=1}^{k} \bar{v}_j \nabla h_j(x), \quad \bar{u} \geq 0, \qquad \bar{u}^\top (\nabla g(x)^\top + \alpha g(x)) = 0.$$

Combining this expression with the fact that $\xi = -F(x) - w \in T_{\mathcal{C}}^{(\alpha)}(x)$ and using the definition of the α-restricted tangent cone, we deduce that $(\bar{u}, \bar{v}) \in K_{\text{cbf},\alpha}(x)$. By optimality of (u, v), we have

$$\begin{aligned} \|\xi + F(x)\|^2 &= \Big\| \sum_{i=1}^{m} \bar{u}_i \nabla g_i(x) + \sum_{j=1}^{k} \bar{v}_j \nabla h_j(x) \Big\|^2 \\ &\geq \Big\| \sum_{i=1}^{m} u_i \nabla g_i(x) + \sum_{j=1}^{k} v_j \nabla h_j(x) \Big\|^2 \\ &= \|\mathcal{F}(x, u, v) + F(x)\|^2 . \end{aligned}$$

But since the projection onto the α-restricted tangent cone must be unique, we conclude $\xi = \mathcal{F}(x, u, v)$. □

B Existence and Uniqueness of Solutions

We now discuss conditions for the existence and uniqueness of solutions of the safe monotone flow.

Proposition 4.3.4. ***(Existence and Uniqueness of Solutions to Safe Monotone Flow).*** *Assume MFCQ and the constant-rank condition hold on $\mathcal{C}$ for all $x \in \mathcal{C}$ and let X be the open set containing $\mathcal{C}$ in Proposition 4.3.2(iii). Then*

(i) For all $x_0 \in \mathcal{C}$, there exists a unique solution $x : \mathbb{R}_{\geq 0} \to \mathbb{R}^n$ to the safe monotone flow with $x(0) = x_0$.

(ii) For all $x_0 \in X$, there exists a unique solution $x : [0, t_f] \to \mathbb{R}^n$ such that $x(0) = x_0$. Furthermore, the solution can be extended so that either $t_f = \infty$ or $x(t) \to \partial X$ as $t \to t_f$.

Proof. We first note that the program (4.10) satisfies the General Strong Second-Order Sufficient Condition (cf. [Liu95]) and Slater's condition at $x \in X$. Because the objective function and constraints of (4.10) are twice continuously differentiable, we can apply [Liu95, Theorem 3.6] to conclude that $\mathcal{G}_\alpha$ is locally Lipschitz at x. Therefore, $\mathcal{G}_\alpha$ is also lower semicontinuous and by [AC84, Chapter 2, Theorem 1] there exists for all $x_0 \in X$ a solution $x : [0, t_f] \to \mathbb{R}^n$ for some $t_f > 0$ with $x(0) = x_0$. Furthermore, either $t_f = \infty$ or $x(t) \to \partial X$ as $t \to t_f$. Uniqueness of solutions holds by local Lipschitznes and (ii) follows.

To show (i), we note that $\mathcal{G}_\alpha(x) \in T_{\mathcal{C}}(x)$, and by [Bla99, Theorem 3.1], for any solution with $x(0) \in \mathcal{C}$, we have that $x(t) \in \mathcal{C}$ for all $t \geq 0$ on the interval on which the solution

exists. Since $\mathcal{C} \subset \text{int}(X)$, solutions beginning in $\mathcal{C}$ cannot approach ∂X, and exist for all time. $\square$

C Safety of Safe Monotone Flow

Here we establish the safety properties of the safe monotone flow. We begin by characterizing optimality conditions for the closed-loop dynamics.

Lemma 4.3.5. ***(Optimality Conditions for Closed-loop Dynamics).*** *For $x \in \mathbb{R}^n$, consider the equations*

$$\xi + F(x) + \frac{\partial g(x)}{\partial x}^\top u + \frac{\partial h(x)}{\partial x}^\top v = 0, \tag{4.11a}$$

$$\frac{\partial g(x)}{\partial x}\xi + \alpha g(x) \leq 0, \tag{4.11b}$$

$$\frac{\partial h(x)}{\partial x}\xi + \alpha h(x) = 0, \tag{4.11c}$$

$$u \geq 0, \tag{4.11d}$$

$$u^\top \Big(\frac{\partial g(x)}{\partial x}\xi + \alpha g(x) \Big) = 0, \tag{4.11e}$$

in (ξ, u, v). Let $\Lambda_\alpha : \mathbb{R}^n \rightrightarrows \mathbb{R}^m_{\geq 0} \times \mathbb{R}^k$ be

$$\Lambda_\alpha(x) = \{(u, v) \mid \exists \xi \text{ such that } (\xi, u, v) \text{ solves } (4.11)\}.$$

Assume MFCQ holds everywhere on $\mathcal{C}$. Then, there exists an open set $X \supset \mathcal{C}$ such that, if $x \in X$, then $\Lambda_\alpha(x) \neq \emptyset$. If (ξ, u, v) solves (4.11), then $\mathcal{G}_\alpha(x) = \xi$ and (u, v) solves (4.8).

Proof. Let $\tilde{F}(x, \xi) = F(x) + \xi$. Then

$$\xi = \Pi_{T_{\mathcal{C}}^{(\alpha)}(x)}(-F(x))$$

is a solution to the monotone variational inequality $\text{VI}(\tilde{F}(x, \cdot), T_{\mathcal{C}}^{(\alpha)}(x))$, parameterized by x. Since MFCQ holds at all $\xi \in T_{\mathcal{C}}^{(\alpha)}(x)$ by Proposition 4.3.2(iii), we can use the KKT conditions to characterize $\mathcal{G}_\alpha(x)$, which correspond to (4.11). Further, by Proposition 4.3.2(iv), solutions to (4.11) exist on an open set X containing $\mathcal{C}$. Since $\tilde{F}$ is strongly monotone with respect to ξ, the solution to $\text{VI}(\tilde{F}(x, \cdot), T_{\mathcal{C}}^{(\alpha)}(x))$ is unique, proving the result. □

We rely on the optimality conditions in Lemma 4.3.5 to establish the following result characterizing the equilibria and safety properties of the safe monotone flow.

Theorem 4.3.6. ***(Equilibria and Safety of Safe Monotone Flow).*** *Let $\alpha > 0$, $\mathcal{C}$ be convex, and suppose MFCQ and the constant rank condition holds everywhere on $\mathcal{C}$. The following hold for the safe monotone flow:*

(i) $\mathcal{C}$ is forward invariant and asymptotically stable on X;

(ii) x^* is an equilibrium if and only if $x^* \in \text{SOL}(F, \mathcal{C})$;

Proof. To show (i), note that by Proposition 4.3.3, for all $x \in X$ there exists $(u(x), v(x)) \in K_{\text{cbf},\alpha}(x)$ such that $\mathcal{G}_\alpha(x) = \mathcal{F}(x, u(x), v(x))$. Given the existence and uniqueness of solutions of the closed-loop system, cf. Propositions 4.3.4, the result follows from Lemma 2.2.3 since $\phi(x) = (g(x), h(x))$ is a VCBF. Statement (ii) follows from the observation that, if $\mathcal{G}_\alpha(x^*) = 0$, by Lemma 4.3.5, there exists (u^*, v^*) such that $(0, u^*, v^*)$ solves (4.11), which holds if and

only if (x^*, u^*, v^*) solves (2.7). $\square$

D Stability of Safe Monotone Flow

Here we characterize the stability properties of the safe monotone flow. We begin by establishing conditions for stability relative to $\mathcal{C}$.

Theorem 4.3.7. ***(Stability of Safe Monotone Flow Relative to $\mathcal{C}$).*** *Assume MFCQ holds everywhere on $\mathcal{C}$. Then*

(i) If $x^* \in \mathrm{SOL}(F, \mathcal{C})$ and F is monotone, then x^* is globally Lyapunov stable relative to $\mathcal{C}$;

(ii) If $x^* \in \mathrm{SOL}(F, \mathcal{C})$ and F is μ-strongly monotone, then x^* is globally asymptotically stable relative to $\mathcal{C}$.

Before proving Theorem 4.3.7, we provide several intermediate results. Our strategy relies on fixing $x^* \in \mathrm{SOL}(F, \mathcal{C})$ and considering the candidate Lyapunov function

$$V(x) = \underbrace{\frac{1}{2}\|x - x^*\|^2}_{\tilde{V}(x)} - \frac{1}{\alpha^2} \underbrace{\inf_{\xi \in T_{\mathcal{C}}^{(\alpha)}(x)} \left\{ \xi^\top F(x) + \frac{1}{2}\|\xi\|^2 \right\}}_{W(x)}. \tag{4.12}$$

We first compute bounds on the Dini derivative of $\tilde{V}$ along $\mathcal{G}_\alpha$.

Lemma 4.3.8. ***(Dini Derivative of $\tilde{V}$).*** *Assume MFCQ holds everywhere on $\mathcal{C}$. For $x^* \in \mathrm{SOL}(F, \mathcal{C})$, let (u^*, v^*) be Lagrange multipliers corresponding to x^*. For $x \in X$ and*

$(u, v) \in \Lambda_\alpha(x)$, *then*

$$D^+_{\mathcal{G}_\alpha} \tilde{V}(x) \leq -\mu \left\| x - x^* \right\|^2 - (u - u^*)^\top (g(x) - g(x^*)) - (v - v^*)^\top h(x),$$

if F is μ-strongly monotone (inequality holds with $\mu = 0$ if F is monotone instead).

Proof. Note that

$$D^+_{\mathcal{G}_\alpha} \tilde{V}(x) = -(x - x^*)^\top F(x) - \sum_{i=1}^{m} u_i (x - x^*)^\top \nabla g_i(x) - \sum_{j=1}^{k} v_j (x - x^*)^\top \nabla h_j(x).$$

By μ-strong monotonicity of F, $-(x - x^*)^\top F(x) \leq -\mu \left\| x - x^* \right\|^2 - (x - x^*)^\top F(x^*)$ (the inequality holds with $\mu = 0$ if F is monotone). Next, we rearrange (2.7a) and use that g_i is convex for all $i = 1, \ldots, m$ and h_j is affine for all $j = 1, \ldots, m$ to obtain

$$\begin{aligned} -(x - x^*)^\top F(x^*) &= \sum_{i=1}^{m} u_i^* (x - x^*)^\top \nabla g_i(x^*) + \sum_{j=1}^{k} v_j^* (x - x^*)^\top \nabla h_j(x^*) \\ &\leq \sum_{i=1}^{m} u_i^* (g_i(x) - g_i(x^*)) + \sum_{j=1}^{k} v_j^* (h_j(x) - h_j(x^*)) \\ &= (u^*)^\top (g(x) - g(x^*)) + (v^*)^\top h(x). \end{aligned}$$

where the last equality follows from the fact that $h(x^*) = 0$. By a similar line of reasoning,

we have

$$
\begin{aligned}
-\sum_{i=1}^{m} u_i(x-x^*)^\top \nabla g_i(x) - \sum_{j=1}^{k} v_j(x-x^*)^\top \nabla h_j(x) & \\
&\leq -\sum_{i=1}^{m} u_i(g_i(x)-g_i(x^*)) - \sum_{j=1}^{k} v_j(h_j(x)-h_j(x^*)) \\
&= -u^\top(g(x)-g(x^*)) - v^\top h(x).
\end{aligned}
$$

The result follows by summing the two expressions. □

We now move on to characterizing properties of W.

Lemma 4.3.9. ***(Properties of W).*** *Assume MFCQ holds everywhere on $\mathcal{C}$. Define the matrix-valued function $Q : X \times \mathbb{R}^m_{\geq 0} \to \mathbb{R}^{n\times n}$ by*

$$
Q(x,u) = \frac{1}{2}\Big(\frac{\partial F(x)}{\partial x} + \frac{\partial F(x)}{\partial x}^\top\Big) + \sum_{i=1}^{m} u_i \nabla^2 g_i(x).
$$

Then, for all $x \in X$ and $(u,v) \in \Lambda_\alpha(x)$,

$$
W(x) = -\frac{1}{2}\left\|\mathcal{G}_\alpha(x)\right\|^2 + \alpha u^\top g(x) + \alpha v^\top h(x) \tag{4.13}
$$

and

$$
D^+_{\mathcal{G}_\alpha} W(x) \geq \mathcal{G}_\alpha(x)^\top Q(x,u)\mathcal{G}_\alpha(x) - \alpha^2 u^\top g(x) - \alpha^2 v^\top h(x). \tag{4.14}
$$

Proof. We first show that the solution to the optimization problem in the definition of W is $\xi = \mathcal{G}_\alpha(x)$. Note that the constraints in the definition of W in (4.12) and (4.10) are identical. Let $J(x,\xi)$ denote the objective function in the definition of W. Then $J(x,\xi) -$

$\frac{1}{2}\|\xi + F(x)\|^2 = -\frac{1}{2}\|F(x)\|^2$. Because the difference between the objective functions of (4.10) and the definition of W is independent of ξ, the two optimization problems have the same solution. The claim now follows because the solution to (4.10) is $\mathcal{G}_\alpha(x)$.

Next we show that W can be expressed in closed form as (4.13). Because the optimizer is $\xi = \mathcal{G}_\alpha(x)$, we have

$$W(x) = \mathcal{G}_\alpha(x)^\top F(x) + \frac{1}{2}\|\mathcal{G}_\alpha(x)\|^2. \tag{4.15}$$

Note that $(\mathcal{G}_\alpha(x), u, v)$ satisfies the optimality conditions (4.11) for all $(u, v) \in \Lambda_\alpha(x)$. Therefore we can rearrange (4.11a) to obtain $F(x) = -\mathcal{G}_\alpha(x) - \frac{\partial g(x)}{\partial x}^\top u - \frac{\partial h(x)}{\partial x}^\top v$. Next

$$\begin{aligned}\mathcal{G}_\alpha(x)^\top F(x) &= -\|\mathcal{G}_\alpha(x)\|^2 - u^\top \frac{\partial g(x)}{\partial x}\mathcal{G}_\alpha(x) - v^\top \frac{\partial h(x)}{\partial x}\mathcal{G}_\alpha(x) \\ &= -\|\mathcal{G}_\alpha(x)\|^2 + \alpha u^\top g(x) + \alpha v^\top h(x),\end{aligned}$$

where the second equality follows by rearranging (4.11c) and (4.11e). Then, (4.13) follows by substituting the previous expression into (4.15).

Finally we show (4.14). Let $L(x; \xi, u, v)$ be the Lagrangian of the parametric optimization problem in the definition of W in (4.12). Then

$$\begin{aligned}L(x; \xi, u, v) = \xi^\top F(x) + \frac{1}{2}\|\xi\|^2 \\ + \sum_{i=1}^m u_i(\nabla g_i(x)^\top \xi + \alpha g_i(x)) + \sum_{i=1}^k v_i(\nabla h_i(x)^\top \xi + \alpha h_i(x)).\end{aligned} \tag{4.16}$$

Next by [BLM16, Theorem 4.2], it follows that

$$D^+_{\mathcal{G}_\alpha} W(x) = \sup_{(u,v)\in\Lambda_\alpha(x)} \left\{\nabla_x L(x; \mathcal{G}_\alpha(x), u, v)^\top \mathcal{G}_\alpha(x)\right\} \geq \nabla_x L(x; \mathcal{G}_\alpha(x), u, v)^\top \mathcal{G}_\alpha(x).$$

By direct computation, we can verify that

$$\nabla_x L(x;\xi,u,v) = Q(x,u)\xi + \alpha\frac{\partial g(x)}{\partial x}^\top u + \alpha\frac{\partial h(x)}{\partial x}^\top v$$

Therefore

$$\begin{aligned}\nabla_x L(x;\mathcal{G}_\alpha(x),u,v)^\top\mathcal{G}_\alpha(x) &= \mathcal{G}_\alpha(x)^\top Q(x,u)\mathcal{G}_\alpha(x) + \alpha u^\top\frac{\partial g(x)}{\partial x}\mathcal{G}_\alpha(x) + \alpha v^\top\frac{\partial h(x)}{\partial x}\mathcal{G}_\alpha(x)\\ &= \mathcal{G}_\alpha(x)^\top Q(x,u)\mathcal{G}_\alpha(x) - \alpha^2 u^\top g(x) - \alpha^2 v^\top h(x),\end{aligned}$$

where once again, the last equality above follows by rearranging (4.11c) and (4.11e).

□

We are now ready to prove Theorem 4.3.7.

Proof of Theorem 4.3.7. Let $x^* \in \mathrm{SOL}(F,\mathcal{C})$ and suppose the hypotheses of (i) hold. Consider the function $V : X \to \mathbb{R}$ defined by (4.12). We show that V is a (strict) Lyapunov function when F is (μ-strongly) monotone. Let $x \in \mathcal{C}$ and $(u,v) \in \Lambda_\alpha(x)$. Then, using (4.11d), $\alpha u^\top g(x) + v^\top h(x) \le 0$, so by examining the expression in (4.13) we see that $W(x) \le 0$ for all $x \in \mathcal{C}$ with equality if and only if $x \in \mathrm{SOL}(F,\mathcal{C})$. Thus V is positive definite with respect to x^*. Next, $D^+_{\mathcal{G}_\alpha}V(x) = D^+_{\mathcal{G}_\alpha}\tilde{V}(x) - \frac{1}{\alpha^2}D^+_{\mathcal{G}_\alpha}W(x)$, and by Lemmas 4.3.8 and 4.3.9,

$$\begin{aligned}D^+_{\mathcal{G}_\alpha}V(x) &\le -\frac{1}{\alpha^2}\mathcal{G}_\alpha(x)Q(x,u)\mathcal{G}_\alpha(x) + u^\top g(x) + v^\top h(x)\\ &\quad - (u-u^*)^\top(g(x)-g(x^*))(v-v^*)^\top(h(x)-h(x^*))\\ &= -\frac{1}{\alpha^2}\mathcal{G}_\alpha(x)Q(x,u)\mathcal{G}_\alpha(x) + (u^*)^\top g(x) + (v^*)^\top h(x) + u^\top g(x^*) + v^\top h(x^*).\end{aligned}$$

Since $u \geq 0$ and $x^* \in \mathcal{C}$, we have $g(x^*) \leq 0$ and $h(x^*) = 0$, and therefore $u^\top g(x^*) + v^\top h(x^*) \leq 0$. Similarly, since $u^* \geq 0$, and $x \in \mathcal{C}$, we have $g(x) \leq 0$ and $h(x) = 0$, and therefore $(u^*)^\top g(x) + (v^*)^\top h(x) \leq 0$. Finally, since F is monotone and g is convex, it follows that $Q(x, u)$ is positive semi-definite, and therefore $D^+_{\mathcal{G}_\alpha} V(x) \leq 0$. To show (ii), we can use the same reasoning above to show that $D^+_{\mathcal{G}_\alpha} V(x) \leq -\mu \|x - x^*\|^2$. □

Next, we discuss stability with respect to the entire state space, which ensures the safe monotone flow can be used to solve $\mathrm{VI}(F, \mathcal{C})$ even for infeasible initial conditions.

Theorem 4.3.10. ***(Stability of Safe Monotone Flow with Respect to*** $\mathbb{R}^n$***).*** *Assume MFCQ and the constant-rank condition holds on* $\mathcal{C}$*. Then*

(i) If $x^* \in \mathrm{SOL}(F, \mathcal{C})$ *and* F *is monotone, then* x^* *is globally Lyapunov stable;*

(ii) If $x^* \in \mathrm{SOL}(F, \mathcal{C})$ *and* F *is* μ*-strongly monotone, then* x^* *is globally asymptotically stable.*

To prove Theorem 4.3.10, we can no longer rely on the Lyapunov function V defined in (4.12) because it is no longer positive definite and may take negative values for $x \notin \mathcal{C}$. Instead, we consider the new candidate Lyapunov function

$$V_\epsilon(x) = \tilde{V}(x) + \Big[-\frac{1}{\alpha^2} W(x) \Big]_+ + \delta_\epsilon(x) \tag{4.17}$$

where $\epsilon > 0$ and δ_ϵ is the penalty function given by

$$\delta_\epsilon(x) = \frac{1}{\epsilon} \sum_{i=1}^{m} [g_i(x)]_+ + \frac{1}{\epsilon} \sum_{j=1}^{k} |h_j(x)|.$$

Before proceeding to the proof of Theorem 4.3.10, we provide a bound for the Dini derivative of δ_ϵ along $\mathcal{G}_\alpha$.

Lemma 4.3.11. ***(Dini Derivative of*** δ_ϵ***).*** *For all $x \in X$ and $\xi \in \mathbb{R}^n$, δ_ϵ is directionally differentiable along ξ at x. In particular,*

$$D^+_{\mathcal{G}_\alpha}\delta_\epsilon(x) \leq -\frac{\alpha}{\epsilon}\sum_{i\in I_+(x)} g_i(x) - \frac{\alpha}{\epsilon}\sum_{j\in I_h(x)} |h_j(x)|, \tag{4.18}$$

where $I_h(x) = \{j \in [1,k] \mid h_j(x) \neq 0\}$.

Proof. Note that δ_ϵ corresponds to the ℓ^1 penalty function for the set $\mathcal{C}$. By [DG89, Proposition 3], the directional derivative of δ_ϵ is

$$\begin{aligned}\delta'_\epsilon(x;\xi) =& \frac{1}{\epsilon}\sum_{i\in I_+(x)} \nabla g_i(x)^\top \xi + \frac{1}{\epsilon}\sum_{i\in I_0(x)} [\nabla g_i(x)^\top \xi]_+ + \\ & \frac{1}{\epsilon}\sum_{j\in I_h(x)} \operatorname{sgn}(h_j(x))\nabla h_j(x)^\top \xi + \frac{1}{\epsilon}\sum_{j\notin I_h(x)} |\nabla h_j(x)^\top \xi|.\end{aligned}$$

Note $D^+_{\mathcal{G}_\alpha}\delta_\epsilon(x) = \delta'_\epsilon(x;\mathcal{G}_\alpha(x))$. Expression (4.18) follows by noting that $\nabla g_i(x)^\top \mathcal{G}_\alpha(x) \leq -\alpha g_i(x)$ and $\nabla h_j(x)^\top \mathcal{G}_\alpha(x) = -\alpha h_j(x)$. □

We are now ready to prove Theorem 4.3.10.

Proof of Theorem 4.3.10. We begin by showing (i). Let $x^* \in \mathrm{SOL}(F,\mathcal{C})$. Note that, from the optimality conditions (4.11), $\Lambda_\alpha(x^*)$ corresponds to the set of Lagrange multipliers of the solution x^* to $\mathrm{VI}(F,\mathcal{C})$. Because MFCQ holds at x^*, it follows that $\Lambda_\alpha(x^*)$ is bounded.

Thus, it is possible to choose $\epsilon > 0$ small enough so that

$$\frac{\alpha}{\epsilon} > \sup_{(u^*,v^*)\in\Lambda_\alpha(x^*)} \left\{ \|(u^*, v^*)\|_\infty \right\}. \tag{4.19}$$

Next, it follows immediately from the definition (4.17) that V_ϵ is positive definite with respect to x^*. We now compute $D^+_{\mathcal{G}_\alpha} V_\epsilon(x)$ and show that it is negative semidefinite. Let $x \in X$. We consider three cases: $W(x) < 0$, $W(x) > 0$, and $W(x) = 0$. In the case where $W(x) < 0$,

$$D^+_{\mathcal{G}_\alpha} V_\epsilon = D^+_{\mathcal{G}_\alpha} \tilde{V}(x) - \frac{1}{\alpha^2} D^+_{\mathcal{G}_\alpha} W(x) + D^+_{\mathcal{G}_\alpha} \delta_\epsilon(x).$$

Combining the bounds in Lemmas 4.3.8, 4.3.9, and 4.3.11,

$$\begin{aligned} D^+_{\mathcal{G}_\alpha} V_\epsilon(x) \leq & -\frac{1}{\alpha^2} \mathcal{G}_\alpha(x) Q(x,u) \mathcal{G}_\alpha(x) \\ & + \sum_{i\in I_+(x)} \left(u^* - \frac{\alpha}{\epsilon} \right) g_i(x) + \sum_{j\in I_h(x)} \left(v^* - \frac{\alpha}{\epsilon} \right) |h_j(x)|. \end{aligned} \tag{4.20}$$

Since ϵ satisfies (4.19), it follows that $D^+_{\mathcal{G}_\alpha} V_\epsilon(x) \leq 0$.

For the case where $W(x) > 0$, we rearrange (4.13) to write

$$u^\top g(x) + v^\top h(x) = \frac{1}{\alpha} W(x) + \frac{1}{2\alpha} \|\mathcal{G}(x)\|^2 > \frac{1}{2\alpha} \|\mathcal{G}(x)\|^2 .$$

Then, we have

$$
\begin{aligned}
D^+_{\mathcal{G}_\alpha} V_\epsilon(x) &= D^+_{\mathcal{G}_\alpha} \tilde{V}(x) + D^+_{\mathcal{G}_\alpha} \delta_\epsilon(x) \\
&\leq -(u-u^*)^\top g(x) - (v-v^*)^\top h(x) - \frac{\alpha}{\epsilon} \sum_{i \in I_+(x)} g_i(x) - \frac{\alpha}{\epsilon} \sum_{j \in I_h(x)} |h_j(x)| \\
&\leq -\frac{1}{2\alpha} \left\| \mathcal{G}_\alpha(x) \right\|^2 + \sum_{i \in I_+(x)} \left(u^* - \frac{\alpha}{\epsilon} \right) g_i(x) + \sum_{j \in I_h(x)} \left(v^* - \frac{\alpha}{\epsilon} \right) |h_j(x)|,
\end{aligned} \tag{4.21}
$$

and $D^+_{\mathcal{G}_\alpha} V_\epsilon(x) \leq 0$. In the case where $W(x) = 0$,

$$
D^+_{\mathcal{G}_\alpha} V_\epsilon(x) = D^+_{\mathcal{G}_\alpha} \tilde{V}(x) + \frac{1}{\alpha^2} [-D^+_{\mathcal{G}_\alpha} W(x)]_+ + D^+_{\mathcal{G}_\alpha} \delta_\epsilon(x),
$$

which leads us to two subcases: (a) $D^+_{\mathcal{G}_\alpha} W(x) < 0$ and (b) $D^+_{\mathcal{G}_\alpha} W(x) \geq 0$. In subcase (a), $D^+_{\mathcal{G}_\alpha} V_\epsilon(x)$ satisfies the bound in (4.20) and, therefore, $D^+_{\mathcal{G}_\alpha} V_\epsilon(x) \leq 0$. In subcase (b),

$$
u^\top g(x) + v^\top h(x) = \frac{1}{2\alpha} \left\| \mathcal{G}_\alpha(x) \right\|^2
$$

and, therefore, $D^+_{\mathcal{G}_\alpha} V_\epsilon(x)$ satisfies the bound in (4.21), so $D^+_{\mathcal{G}_\alpha} V_\epsilon(x) \leq 0$.

Finally, for (ii), we can use the same arguments above to show in each case $D^+_{\mathcal{G}_\alpha} V_\epsilon(x) \leq -\mu \left\| x - x^* \right\|^2$. □

We conclude this section by discussing the contraction properties of the safe monotone flow. Contraction refers to the property that any two trajectories of the system approach each other exponentially (cf. [DJB22, Bul23] for a precise definition), and implies exponential stability of an equilibrium. We show that, for sufficiently large α, the safe monotone flow system is contracting provided F is globally Lipschitz and the constraint set $\mathcal{C}$ is polyhedral.

Our analysis relies relies on the following result.

Lemma 4.3.12. ***([Yen95, Lemma 2.1]).*** *Consider the following quadratic program*

$$\min_{(u,v)\in\mathbb{R}^m_{\geq 0}\times\mathbb{R}^k} \frac{1}{2}\left\|\begin{bmatrix}u\\v\end{bmatrix}\right\|^2_{\tilde{Q}} + c^\top \begin{bmatrix}u\\v\end{bmatrix} + p, \tag{4.22}$$

where $\tilde{Q} \succeq 0$. *Then* (u^*, v^*) *solves* (4.22) *if and only if it is a solution to the linear program*

$$\min_{(u,v)\in\mathbb{R}^m_{\geq 0}\times\mathbb{R}^k} \left(\tilde{Q}\begin{bmatrix}u^*\\v^*\end{bmatrix} + c\right)^\top \begin{bmatrix}u\\v\end{bmatrix}. \tag{4.23}$$

We now show that the safe monotone flow is contracting.

Theorem 4.3.13. ***(Contraction and Exponential Stability of Safe Monotone Flow).*** *Let* F *be* μ*-strongly monotone and globally Lipschitz with constant* ℓ_F *and* $\mathcal{C}$ *a polyhedral set defined by* (4.2) *with* $g(x) = Gx - c_g$ *and* $h(x) = Hx - c_h$. *If*

$$\alpha > \frac{\ell_F^2}{4\mu}, \tag{4.24}$$

then the safe monotone flow is contracting with rate $c = \mu - \frac{\ell_F^2}{4\alpha}$. *In particular, the unique solution* $x^* \in \mathrm{SOL}(F, \mathcal{C})$ *is globally exponentially stable.*

Proof. We claim that if the assumptions hold, then

$$(x-y)^\top(\mathcal{G}_\alpha(x) - \mathcal{G}_\alpha(y)) \leq -c\left\|x-y\right\|^2, \tag{4.25}$$

in which case the system is contracting by [DJB22, Theorem 31], and exponential stability

of $x^* \in \mathrm{SOL}(F, \mathcal{C})$ follows as a consequence. To show the claim, from (4.11a), note that

$$\mathcal{G}_\alpha(x) = -F(x) - G^\top u_x - H^\top v_x.$$

for any $(u_x, v_x) \in \Lambda_\alpha(x)$. Let then $x, y \in X$ and $(u_x, v_x) \in \Lambda_\alpha(x)$ and $(u_y, v_y) \in \Lambda_\alpha(y)$. Then, using the strong monotonicity of F,

$$\begin{aligned}(x-y)^\top(\mathcal{G}_\alpha(x) - \mathcal{G}_\alpha(y)) &= -(x-y)^\top(F(x) - F(y)) \\ &\quad + (x-y)^\top(\mathcal{G}_\alpha(x) + F(x) - \mathcal{G}_\alpha(y) - F(y)) \\ &\leq -\mu \|x-y\|^2 - (x-y)^\top \begin{bmatrix} G^\top & H^\top \end{bmatrix} \begin{bmatrix} u_x - u_y \\ v_x - v_y \end{bmatrix} \\ &= -\mu \|x-y\|^2 - \begin{bmatrix} u_x - u_y \\ v_x - v_y \end{bmatrix}^\top \begin{bmatrix} G(x-y) \\ H(x-y) \end{bmatrix}.\end{aligned} \tag{4.26}$$

Next, let $\tilde{J}(x; u, v) = -\inf_{\xi \in \mathbb{R}^n} L(x; \xi, u, v)$, where L is the Lagrangian of (4.10), defined in (4.16), and let

$$\tilde{Q} = \begin{bmatrix} GG^\top & GH^\top \\ HG^\top & HH^\top \end{bmatrix}.$$

For $x \in \mathbb{R}^n$, L is minimized when $\xi = -F(x) - G^\top u - H^\top v$, and therefore

$$\tilde{J}(x; u, v) = \frac{1}{2} \left\| \begin{bmatrix} u \\ v \end{bmatrix} \right\|_{\tilde{Q}}^2 + \begin{bmatrix} GF(x) - \alpha(Gx - c_g) \\ HF(x) - \alpha(Hx - c_h) \end{bmatrix}^\top \begin{bmatrix} u \\ v \end{bmatrix} + \frac{1}{2} \|F(x)\|^2. \tag{4.27}$$

If $(u_x, v_x) \in \Lambda_\alpha(x)$, then (u_x, v_x) is a solution to the program $\min_{(u,v) \in \mathbb{R}^m_{\geq 0} \times \mathbb{R}^k} \tilde{J}(x, u, v)$, which is the Lagrangian dual[1] of (4.10). By Lemma 4.3.12, (u_x, v_x) is also a solution to the linear

[1]By convention, the Lagrangian dual problem is a maximization problem (cf. [BV09, Chapter 5]). However, the minus sign in the definition of $\tilde{J}$ ensures that here it is a minimization. The reason for this sign convention is to make the notation simpler.

program,

$$\min_{(u,v)\in\mathbb{R}^m_{\geq 0}\times\mathbb{R}^k} \left(\tilde{Q}\begin{bmatrix}u_x\\v_x\end{bmatrix} + \begin{bmatrix}GF(x)-\alpha(Gx-c_g)\\HF(x)-\alpha(Hx-c_h)\end{bmatrix}\right)^\top \begin{bmatrix}u\\v\end{bmatrix}.$$

Since (u_y, v_y) is also feasible for the previous linear program, by optimality of (u_x, v_x),

$$-\begin{bmatrix}u_x-u_y\\v_x-v_y\end{bmatrix}^\top \begin{bmatrix}Gx-c_g\\Hx-c_h\end{bmatrix} \leq -\frac{1}{\alpha}\left\|\begin{bmatrix}u_x\\v_x\end{bmatrix}\right\|^2_{\tilde{Q}} + \frac{1}{\alpha}\begin{bmatrix}u_y\\v_y\end{bmatrix}^\top \tilde{Q}\begin{bmatrix}u_x\\v_x\end{bmatrix} - \frac{1}{\alpha}\begin{bmatrix}u_x-u_y\\v_x-v_y\end{bmatrix}^\top \begin{bmatrix}GF(x)\\HF(x)\end{bmatrix}.$$

By a similar line of reasoning,

$$-\begin{bmatrix}u_y-u_x\\v_y-v_x\end{bmatrix}^\top \begin{bmatrix}Gy-c_g\\Hy-c_h\end{bmatrix} \leq -\frac{1}{\alpha}\left\|\begin{bmatrix}u_y\\v_y\end{bmatrix}\right\|^2_{\tilde{Q}} + \frac{1}{\alpha}\begin{bmatrix}u_x\\v_x\end{bmatrix}^\top \tilde{Q}\begin{bmatrix}u_y\\v_y\end{bmatrix} - \frac{1}{\alpha}\begin{bmatrix}u_y-u_x\\v_y-v_x\end{bmatrix}^\top \begin{bmatrix}GF(y)\\HF(y)\end{bmatrix}.$$

Combining the previous two expressions, we obtain

$$\begin{aligned}-\begin{bmatrix}u_x-u_y\\v_x-v_y\end{bmatrix}^\top \begin{bmatrix}G(x-y)\\H(x-y)\end{bmatrix} &\leq -\frac{1}{\alpha}\begin{bmatrix}u_x-u_y\\v_x-v_y\end{bmatrix}^\top \begin{bmatrix}G(F(x)-F(y))\\H(F(x)-F(y))\end{bmatrix} - \frac{1}{\alpha}\left\|\begin{bmatrix}u_x-u_y\\v_x-v_y\end{bmatrix}\right\|^2_{\tilde{Q}}\\ &\leq \frac{\ell_F}{\alpha}\left\|\begin{bmatrix}G\\H\end{bmatrix}^\top \begin{bmatrix}u_x-u_y\\v_x-v_y\end{bmatrix}\right\| \|x-y\| - \frac{1}{\alpha}\left\|\begin{bmatrix}G\\H\end{bmatrix}^\top \begin{bmatrix}u_x-u_y\\v_x-v_y\end{bmatrix}\right\|^2,\end{aligned}$$

where we used $\|(u,v)\|_{\tilde{Q}} = \|M^\top(u,v)\|$, with $M = [G;H]$. For any $\epsilon > 0$, by Young's Inequality [RF10, pp. 140],

$$-\begin{bmatrix}u_x-u_y\\v_x-v_y\end{bmatrix}^\top \begin{bmatrix}G(x-y)\\H(x-y)\end{bmatrix} \leq \frac{\ell_F}{2\epsilon\alpha}\|x-y\|^2 - \left(\frac{1}{\alpha}-\frac{\epsilon\ell_F}{2\alpha}\right)\left\|\begin{bmatrix}G\\H\end{bmatrix}^\top \begin{bmatrix}u_x-u_y\\v_x-v_y\end{bmatrix}\right\|^2.$$

Substituting into (4.26), we obtain

$$(x-y)^\top(\mathcal{G}_\alpha(x)-\mathcal{G}_\alpha(y)) \leq -\left(\mu-\frac{\ell_F}{2\epsilon\alpha}\right)\|x-y\|^2 - \left(\frac{1}{\alpha}-\frac{\epsilon\ell_F}{2\alpha}\right)\left\|\begin{bmatrix}G\\H\end{bmatrix}^\top \begin{bmatrix}u_x-u_y\\v_x-v_y\end{bmatrix}\right\|^2.$$

Therefore, (4.25) holds with $c = \mu - \frac{\ell_F}{2\epsilon\alpha}$ if ϵ satisfies

$$\frac{\ell_F}{2\alpha\mu} \leq \epsilon \leq \frac{2}{\ell_F}.$$

Such ϵ can be chosen if $\alpha > \frac{\ell_F^2}{4\mu}$, which corresponds to the condition (4.24). The optimal estimate of the contraction rate is $c = \mu - \frac{\ell_F^2}{4\alpha}$. □

Remark 4.3.14. ***(Connection with Safe Gradient Flow).*** The safe monotone flow is a generalization of the *safe gradient flow* introduced in [AC24]. The latter was originally studied in the context of nonconvex optimization and, similar to the case of the safe monotone flow, enjoys safety of the feasible set and correspondence between equilibria and critical points. Further, under certain constraint qualifications, the local stability of equilibria relative to the constraint set under the safe gradient flow can be established using the objective function as a Lyapunov function. Because we are working with variational inequalities, F may not correspond to the gradient of a scalar objective function, so the Lyapunov functions used in [AC24] are not directly applicable. The assumption of convexity and monotonicity here allows us to construct novel Lyapunov functions to obtain global stability results. □

4.4 Recursive Safe Monotone Flow

A drawback of the projected and safe monotone flows is that, in order to implement them, one needs to solve either the quadratic programs (4.4) or (4.8) at each time along the trajectory of the system. As a third algorithmic solution to Problem 4.1.1, in this section we introduce the *recursive safe monotone flow* which gets around this limitation

by incorporating a dynamics whose equilibria correspond to the solutions of the quadratic program. We begin by showing how to derive the dynamics for general constraint sets $\mathcal{C}$ by interconnecting two systems on multiple time scales. Next, we use the theory of singular perturbations of contracting flows to obtain stability guarantees in the case where $\mathcal{C}$ is polyhedral, and show that trajectories of the recursive safe monotone flow track those of the safe monotone flow. The latter property enables us to formalize a notion of "practical safety" that the recursive safe monotone flow satisfies.

4.4.1 Construction of the Dynamics

We discuss here the construction of the recursive safe monotone flow. The starting point for our derivation is the control-affine system (4.3). The safe monotone flow consists of this system with a feedback controller specified by the quadratic program (4.8). Rather than solving this program exactly, the approach we take is to replace it with a monotone variational inequality parameterized by the state. For fixed $x \in X$, we can solve solve this inequality, and hence obtain the feedback $\kappa(x)$, using the safe monotone flow corresponding to this problem. Coupling this flow with the control system (4.3) yields the *recursive safe monotone flow*.

In this section we carry out this strategy in mathematically precise terms. We rely on the following result, which provides an alternative characterization of the CBF-QP (4.8).

Lemma 4.4.1. ***(Alternative Characterization of Safe Feedback).*** *For $x \in \mathbb{R}^n$,*

consider the optimization

$$\begin{aligned}\underset{(u,v)\in\mathbb{R}^m_{\geq 0}\times\mathbb{R}^k}{\text{minimize}}\ & \frac{1}{2}\Big\|\sum_{i=1}^m u_i\nabla g_i(x)+\sum_{j=1}^k v_j\nabla h_j(x)\Big\|^2 \\ & + u^\top\Big(\frac{\partial g}{\partial x}F(x)-\alpha g(x)\Big)+v^\top\Big(\frac{\partial h}{\partial x}F(x)-\alpha h(x)\Big).\end{aligned} \tag{4.28}$$

If (u,v) is a solution to (4.28)*, then (u,v) is a solution to* (4.8)*.*

Proof. Note that the constraints of (4.28) satisfy MFCQ for all $(u,v)\in\mathbb{R}^m_{\geq 0}\times\mathbb{R}^k$. Since the objective function in (4.28) is convex in (u,v), one can see that necessary and sufficient conditions for optimality are given by a KKT system that, after some manipulation, takes the form

$$\begin{aligned}-\frac{\partial g}{\partial x}\frac{\partial g}{\partial x}^\top u-\frac{\partial g}{\partial x}\frac{\partial h}{\partial x}^\top v-\frac{\partial g}{\partial x}F(x)-\alpha g(x)&\leq 0\\ -\frac{\partial h}{\partial x}\frac{\partial g}{\partial x}^\top u-\frac{\partial h}{\partial x}\frac{\partial h}{\partial x}^\top v-\frac{\partial h}{\partial x}F(x)-\alpha h(x)&=0\\ u&\geq 0\\ u^\top\Big(-\frac{\partial g}{\partial x}\frac{\partial g}{\partial x}^\top u-\frac{\partial g}{\partial x}\frac{\partial h}{\partial x}^\top v-\frac{\partial g}{\partial x}F(x)-\alpha g(x)\Big)&=0.\end{aligned}$$

It follows immediately that if (u,v) satisfies the above equations, then $(u,v)\in K_{\mathrm{cbf},\alpha}(x)$ given by (4.8). □

The rationale for considering (4.28), rather than working with (4.8) directly, is that the constraints of (4.28) are independent of x, which will be important for reasons we show next. Being a constrained optimization problem, (4.28) can be expressed in terms of a variational inequality (parameterized by $x\in\mathbb{R}^n$). Formally, let $\tilde{F}(x,u,v)$ be given by

$$\tilde{F}(x,u,v)=\begin{bmatrix}-\frac{\partial g}{\partial x}\mathcal{F}(x,u,v)-\alpha g(x)\\ -\frac{\partial h}{\partial x}\mathcal{F}(x,u,v)-\alpha h(x)\end{bmatrix}, \tag{4.29}$$

where $\mathcal{F}$ is given by (4.3) and let $\tilde{\mathcal{C}} = \mathbb{R}^m_{\geq 0} \times \mathbb{R}^k$, which we parameterize as

$$\tilde{\mathcal{C}} = \{(u, v) \in \mathbb{R}^m \times \mathbb{R}^k \mid u \geq 0\}. \tag{4.30}$$

The optimization problem (4.28) corresponds to the variational inequality $\mathrm{VI}(\tilde{F}(x, \cdot, \cdot), \tilde{\mathcal{C}})$.

Our next step is to write down the safe monotone flow with safety parameter $\beta > 0$ corresponding to the variational inequality $\mathrm{VI}(\tilde{F}(x, \cdot), \tilde{\mathcal{C}})$. Note that the β-restricted tangent set (4.9) of $\tilde{\mathcal{C}}$ is

$$T^{(\beta)}_{\tilde{\mathcal{C}}}(u, v) = \Big\{(\xi_u, \xi_v) \in \mathbb{R}^m \times \mathbb{R}^k \mid \xi_u \geq -\beta u\Big\}.$$

The projection onto $T^{(\beta)}_{\tilde{\mathcal{C}}}(u, v)$ has the following closed-form solution

$$\Pi_{T^{(\beta)}_{\tilde{\mathcal{C}}}(u,v)}\left(\begin{bmatrix} a \\ b \end{bmatrix}\right) = \begin{bmatrix} \max\{-\beta u, a\} \\ b \end{bmatrix}.$$

Using this expression and applying Proposition 4.3.3, we write the safe monotone flow corresponding to $\mathrm{VI}(\tilde{F}(x, \cdot), \tilde{\mathcal{C}})$ as

$$\begin{aligned} \dot{u} &= \max\Big\{ -\beta u, \frac{\partial g(x)}{\partial x}\mathcal{F}(x, u, v) + \alpha g(x)\Big\} \\ \dot{v} &= \frac{\partial h(x)}{\partial x}\mathcal{F}(x, u, v) + \alpha h(x). \end{aligned} \tag{4.31}$$

Under certain assumptions, which we formalize in the sequel, for a fixed x, trajectories of (4.31) converge to solutions of the QP (4.8).

This discussion suggests a system solving the original variational inequality $\mathrm{VI}(F, \mathcal{C})$

can be obtained by coupling (4.31) with the dynamics (4.3) as follows:

$$\dot{x} = \mathcal{F}(x, u, v) \tag{4.32a}$$

$$\tau\dot{u} = \max\left\{ -\beta u, \frac{\partial g(x)}{\partial x}\mathcal{F}(x, u, v) + \alpha g(x)\right\} \tag{4.32b}$$

$$\tau\dot{v} = \frac{\partial h(x)}{\partial x}\mathcal{F}(x, u, v) + \alpha h(x). \tag{4.32c}$$

We refer to the system (4.32) as the *recursive safe monotone flow*. The parameter τ characterizes the separation of timescales between the system (4.32a) and (4.32b)-(4.32c). The interpretation of the dynamics is that, when $\tau > 0$ are sufficiently small, (4.32b)-(4.32c) evolve on a much faster timescale and rapidly approach the solution set of (4.8). The system on the slower timescale (4.32a) then approximates the safe monotone flow. We formalize this analysis next.

4.4.2 Stability of Recursive Safe Monotone Flow

To prove stability of the system (4.32), we rely on results from contraction theory [DJB22]. Specifically, we derive conditions on the time-scale separation τ that ensures that (4.32) is contracting and, as a consequence, globally attractive and locally exponentially stable. Throughout the section, we assume the following assumption holds.

Assumption 4.4.2. ***(Strong Monotonicity, Lipschitzness, and Polyhedral Constraints).*** *The following holds:*

(i) F is μ-strongly monotone and ℓ_F-Lipschitz;

(ii) $\mathcal{C}$ is a polyhedral set defined by (4.2) *with $g(x) = Gx - c_g$ and $h(x) = Hx - c_h$, and the matrix*

$$\tilde{Q} = \begin{bmatrix} GG^\top & GH^\top \\ HG^\top & HH^\top \end{bmatrix} \tag{4.33}$$

has full rank.

Next, we show that it is possible to tune the parameters β so the system (4.31) is contracting, uniformly in x.

Lemma 4.4.3. ***(Contractivity of*** (4.31)***).*** *Under Assumption 4.4.2, if*

$$\beta > \frac{1}{4}\frac{\lambda_{\max}(\tilde{Q})}{\lambda_{\min}(\tilde{Q})},$$

then the system (4.31) *is contracting with rate $\bar{c} = \lambda_{\min}(\tilde{Q}) - \frac{\lambda_{\max}(\tilde{Q})}{4\beta}$ uniformly in x.*

Proof. We first observe that $\tilde{F}$ is given by

$$\tilde{F}(x, u, v) = \tilde{Q}\begin{bmatrix} u \\ v \end{bmatrix} - \alpha \begin{bmatrix} Gx - c_g \\ Hx - c_h \end{bmatrix}.$$

By Assumption 4.4.2, $\tilde{Q} \succ 0$ and therefore $\tilde{F}$ is (i) $\lambda_{\min}(\tilde{Q})$-strongly monotone in (u, v) uniformly in x and (ii) $\|\tilde{Q}\|$-Lipschitz in (u, v) uniformly in x. By Theorem 4.3.13, if $\beta > \frac{\|\tilde{Q}\|^2}{4\lambda_{\min}(\tilde{Q})}$, the system (4.31) is uniformly contracting. The result follows by observing that $\|\tilde{Q}\|^2 = \lambda_{\max}(\tilde{Q})$. □

We now characterize the contraction and stability properties of the recursive safe monotone flow.

Theorem 4.4.4. ***(Contractivity of Recursive Safe Monotone Flow).*** *Assume F is μ-strongly monotone and ℓ_F globally Lipschitz, and α satisfies* (4.24)*. Under Assumption 4.4.2 and β chosen as in Lemma 4.4.3, then*

(i) the unique KKT triple, (x^*, u^*, v^*) corresponding to $\mathrm{VI}(F, \mathcal{C})$ is the only equilibrium of (4.32)*.*

Moreover, for all $\epsilon > 0$, there exists $\tau^* > 0$, such that for all $0 < \tau < \tau^*$,

(ii) the system (4.32) *is contracting on the set*

$$\mathcal{Z}_\epsilon = \Big\{(x, u, v) \in X \times \mathbb{R}^m \times \mathbb{R}^k \;\Big|\; \|(u, v) - \kappa(x)\| \leq \epsilon\Big\},$$

and every solution of (4.32) *eventually enters $\mathcal{Z}_\epsilon$ in finite time. In particular, there exists a class $\mathcal{KL}$ function $\beta : \mathbb{R}_{\geq 0} \times \mathbb{R}_{\geq 0} \to \mathbb{R}$ such that for every solution $(x(t), u(t), v(t))$*

$$\Big\|\Big(u(x(t)), v(x(t))\Big) - \kappa(x(t))\Big\| \leq \beta\Big(\Big\|\Big(u(x(0)), v(x(0))\Big) - \kappa(x(0))\Big\|, t\Big);$$

(iii) the unique KKT triple (x^*, u^*, v^*) is locally exponentially stable and globally attracting.

Proof. We begin with (i). By direct examination of (4.32), we see that the equilibria correspond exactly with triples satisfying (2.7). Since the matrix $\tilde{Q}$ has full rank, the gradients of all the constraints are linearly independent, and hence MFCQ holds on $\mathcal{C}$. Since F is μ-strongly monotone, the solution $x^* \in \mathrm{SOL}(F, \mathcal{C})$ is unique and there exists a unique Lagrange multiplier (u^*, v^*) such that (x^*, u^*, v^*) satisfies (2.7).

To show (ii), we verify that all hypotheses in [CBD23, Theorem 4] hold. First, note that the map $x \mapsto \mathcal{F}(x, u, v)$ is ℓ_F-Lipschitz in x uniformly in (u, v), and $\|[G; H]\|$-Lipschitz in (u, v), uniformly in x. Let $\mathcal{H}$ denote the righthand side of (4.31). Because $\mathcal{H}$ is piecewise affine in (u, v) and F globally Lipschitz, there exists constants $\ell_{\mathcal{H},x}$, $\ell_{\mathcal{H},u,v} > 0$, such that $\mathcal{H}$ is $\ell_{\mathcal{H},x}$-Lipschitz in x uniformly in (u, v) and $\ell_{\mathcal{H},u,v}$-Lipschitz in (u, v) uniformly in x. By Lemma 4.4.3, there exists $\bar{c} > 0$ such that (4.31) is $\bar{c}$-contracting, uniformly in x. Finally, we note that the reduced system corresponding to (4.32) is $\dot{x} = \mathcal{G}_\alpha(x)$, which is contracting by Theorem 4.3.13. Thus all the hypotheses of [CBD23, Theorem 4] hold and (ii) follows. Finally (iii) follows from combining (i) and (ii). □

4.4.3 Safety of Recursive Safe Monotone Flow

Here we discuss the safety properties of the recursive safe monotone flow. In general, even if the initial condition belongs to $\mathcal{C}$, i.e., $x(0) \in \mathcal{C}$, it is not guaranteed that solutions of the system (4.32) satisfy $x(t) \in \mathcal{C}$ for $t > 0$. However, under appropriate conditions, we can show that the system is "practically safe", in the sense that $x(t)$ remains in a slightly expanded form of the original constraint set $\mathcal{C}$.

Theorem 4.4.5. ***(Practical Safety of Recursive Safe Monotone Flow).*** *Assume F is μ-strongly monotone and ℓ_F globally Lipschitz, and α satisfies* (4.24)*. Under Assumption 4.4.2 and β chosen as in Lemma 4.4.3, then for all $\epsilon > 0$, there exists $\delta > 0$ and τ^* such that, if $0 < \tau < \tau^*$, any solution to* (4.32) *with*

- $x(0) \in \mathcal{C}$;

- $\|(u(0), v(0)) - \kappa(x(0))\| \leq \delta$;

satisfies $x(t) \in \mathcal{C}_\epsilon = \{x \in \mathbb{R}^n \,|\, g(x) \leq \epsilon, |h(x)| \leq \epsilon\}$ *for all* $t \geq 0$.

To prove Theorem 4.4.5, we rely on the notion of input-to-state safety. Consider the system

$$\dot{x} = \mathcal{G}_\alpha(x) - \sum_{i=1}^{n} e_i(t) \nabla g_i(x) - \sum_{j=1}^{m} d_j(t) \nabla h_j(x). \tag{4.34}$$

This system can be interpreted as the safe monotone flow perturbed by a disturbance determined by $(e(t), d(t))$. The set $\mathcal{C}$ is *input-to-state safe* (ISSf) with respect to (4.34), with gain γ, if there exists a class $\mathcal{K}$ function γ such that, if $\gamma(\|(e, d)\|_\infty) < \epsilon$, then $\mathcal{C}_\epsilon$ is forward invariant under (4.34). This notion of input-to-state safety is a slight generalization of the standard definition, cf. [KA18], to the case where the safe set is parameterized by multiple equality and inequality constraints. We show next that (4.34) is ISSf.

Lemma 4.4.6. ***(Perturbed Safe Monotone Flow is ISSf).*** *Under Assumption 4.4.2, the set* $\mathcal{C}$ *is input-to-state safe with respect to* (4.34) *with gain* $\gamma(r) = \frac{\lambda_{\max}(\tilde{Q})}{\alpha} r$, *where* $\tilde{Q}$ *is defined in* (4.33).

Proof. For $i \in \{1, \ldots, m\}$, under (4.34)

$$\begin{aligned}
\dot{g}_i(x) &= G_i^\top \Big(\mathcal{G}_\alpha(x) - \sum_{i=1}^{n} e_i(t) \nabla g_i(x) - \sum_{j=1}^{m} d_j(t) \nabla h_j(x) \Big) \\
&\leq -\alpha g_i(x) - G_i^\top \Big(\sum_{i=1}^{n} e_i(t) \nabla g_i(x) - \sum_{j=1}^{m} d_j(t) \nabla h_j(x) \Big) \\
&\leq -\alpha g_i(x) + \lambda_{\max}(\tilde{Q}) \, \|(e(t), d(t))\| \,,
\end{aligned}$$

where $G_i^\top$ is the ith row of G. It follows from [KA18, Theorem 1] that the set $\mathcal{C}_{g_i} = \{x \in$

$\mathbb{R}^n \mid G_i^\top x - (c_g)_i \leq 0\}$ is input-to-state safe with gain γ with respect to (4.32).

For $j \in \{1, \ldots, k\}$, under (4.34),

$$\begin{aligned}\dot{h}_j(x) &= H_j^\top \Big(\mathcal{G}_\alpha(x) - \sum_{i=1}^{n} e_i(t)\nabla g_i(x) - \sum_{j=1}^{m} d_j(t)\nabla h_j(x)\Big) \\ &= -\alpha h_j(x) - H_j^\top \Big(\sum_{i=1}^{n} e_i(t)\nabla g_i(x) - \sum_{j=1}^{m} d_j(t)\nabla h_j(x)\Big),\end{aligned}$$

where $H_j^\top$ is the jth row of H. It follows that

$$\dot{h}_j(x) \leq -\alpha h_j(x) + \lambda_{\max}(\tilde{Q}) \left\|(e(t), d(t))\right\|,$$

$$\dot{h}_j(x) \geq -\alpha h_j(x) - \lambda_{\max}(\tilde{Q}) \left\|(e(t), d(t))\right\|.$$

Thus, by [KA18, Theorem 1], the sets $\mathcal{C}_{h_j}^- = \{x \in \mathbb{R}^n \mid H_j^\top x - (c_h)_j \leq 0\}$, and $\mathcal{C}_{h_j}^+ = \{x \in \mathbb{R}^n \mid H_j^\top x - (c_h)_j \geq 0\}$ are also input-to-state safe with gain γ with respect to (4.32). Finally, input-to-state safety of $\mathcal{C}$ follows from the fact that

$$\mathcal{C} = \Big(\bigcap_{i=1}^{m} \mathcal{C}_{g_i}\Big) \cap \Big(\bigcap_{j=1}^{k} (\mathcal{C}_{h_j}^+ \cap \mathcal{C}_{h_j}^-)\Big).$$

□

We are now ready to prove Theorem 4.4.5.

Proof of Theorem 4.4.5. By Lemma 4.4.6, $\mathcal{C}$ is input-to-state safe with respect to (4.34), with gain $\gamma(r) = \frac{\lambda_{\max}(\tilde{Q})}{\alpha} r$. Note that, for any solution $(x(t), u(t), v(t))$ of (4.32), the trajectory $x(t)$ solves (4.34) with

$$\begin{bmatrix} e(t) \\ d(t) \end{bmatrix} = \begin{bmatrix} u(t) \\ v(t) \end{bmatrix} - \kappa(x(t)).$$

Next, by Theorem 4.4.4, for all ϵ, there exists $\tau^* > 0$ such that if $0 < \tau < \tau^*$, then for all $t \geq 0$, $\left\|\Big(e(t), d(t)\Big)\right\| \leq \beta\Big(\left\|\Big(e(0), d(0)\Big)\right\|, t\Big)$ for some class $\mathcal{KL}$ function β. Now, choose $\delta > 0$ such that $\alpha^{-1}\lambda_{\max}(\tilde{Q})\beta(\delta, 0) < \epsilon$ and let $\|(u(0), v(0)) - \kappa(x(0))\| \leq \delta$. Then, for all $t \geq 0$,

$$\gamma\left(\left\|\Big(e(t), d(t)\Big)\right\|\right) \leq \gamma(\beta(\delta, t)) \leq \gamma(\beta(\delta, 0)) < \epsilon.$$

Hence, for $x(0) \in \mathcal{C} \subset \mathcal{C}_\epsilon$, since $\mathcal{C}$ is input-to-state safe with respect to (4.34), we conclude $x(t) \in \mathcal{C}_\epsilon$ for all $t \geq 0$. □

4.5 Numerical Examples

Here we illustrate the behavior of the proposed flows on two example problems. The first example is a variational inequality on $\mathbb{R}^2$ corresponding to a two-player game with quadratic payoff functions where we compare the projected monotone flow. The second example is a constrained linear-quadratic dynamic game where we implement the safe monotone flow in a receding horizon manner to examine its anytime properties.

4.5.1 Nash Equilibria of Two-Player Game

The first numerical example we discuss is a variational inequality on $\mathbb{R}^2$ corresponding to a two-player game, where player $i \in \{1, 2\}$ wants to minimize a cost $J_i(x_1, x_2)$ subject to the constraints that $x_i \in \mathcal{C}_i \subset \mathbb{R}$. We take $\mathcal{C} = \mathcal{C}_1 \times \mathcal{C}_2 \subset \mathbb{R}^2$. We have selected a two-dimensional example that allows us to visualize the constraint set and the trajectories of the proposed flows to better illustrate their differences. The problem of finding the Nash

equilibria of a game of this form is equivalent to the variational inequality $\mathrm{VI}(F, \mathcal{C})$, where F is the *pseudogradient* map, given by $F(x) = (\nabla_{x_1} J_1(x_1, x_2), \nabla_{x_2} J_2(x_1, x_2))$. For $i \in \{1, 2\}$, let $\mathcal{C}_i = \{x \in \mathbb{R} \mid -1 \leq x \leq 1\}$ and J_i be the quadratic function $J_i(x_1, x_2) = \frac{1}{2} x^\top Q_i x + r_i^\top x$, with

$$Q_1 = \begin{bmatrix} 1 & -1 \\ -1 & 1 \end{bmatrix} \in \mathbb{R}^{2\times 2}, \qquad r_1 = \begin{bmatrix} 0 \\ 0 \end{bmatrix} \in \mathbb{R}^2,$$
$$Q_2 = \begin{bmatrix} 1 & 1 \\ 1 & 1 \end{bmatrix} \in \mathbb{R}^{2\times 2}, \qquad r_2 = \begin{bmatrix} 0.5 \\ 0.5 \end{bmatrix} \in \mathbb{R}^2.$$

The pseudogradient map is given by $F(x) = Qx + r$ where

$$Q = \begin{bmatrix} 1 & -1 \\ 1 & 1 \end{bmatrix} \qquad r = \begin{bmatrix} 0 \\ 0.5 \end{bmatrix}$$

Because $\frac{1}{2}(Q + Q^\top) = I \succ 0$, it follows that the F is 1-strongly monotone, and therefore the problem has a unique solution $x^* \in \mathrm{SOL}(F, \mathcal{C})$.

Figure 4.2 shows the results of implementing each of the proposed flows to find the Nash equilibrium. The projected monotone flow, cf. Figure 4.2(a), is only well defined in $\mathcal{C}$. However, the constraint set remains forward invariant and all trajectories converge to the solution x^*. The safe monotone flow with $\alpha = 1.0$, cf. Figure 4.2(b), also keeps the constraint set forward invariant and has all trajectories converge to x^*. In addition, the system is well defined outside of $\mathcal{C}$, and trajectories beginning outside the feasible set converge to it.

In Figure 4.2(c), we consider the recursive safe monotone flow with $\alpha = 1.0$, $\beta = 1.0$ and $\tau = 0.25$, where $u(0) = 0$. The trajectories converge to x^* and closely approximate the trajectories of the safe monotone flow. Note, however, that the set $\mathcal{C}$ is not safe but only practically safe. This is illustrated in the zoomed-in Figure 4.2(d), where it is apparent that

the trajectories do not always remain in $\mathcal{C}$ but remain close to it.

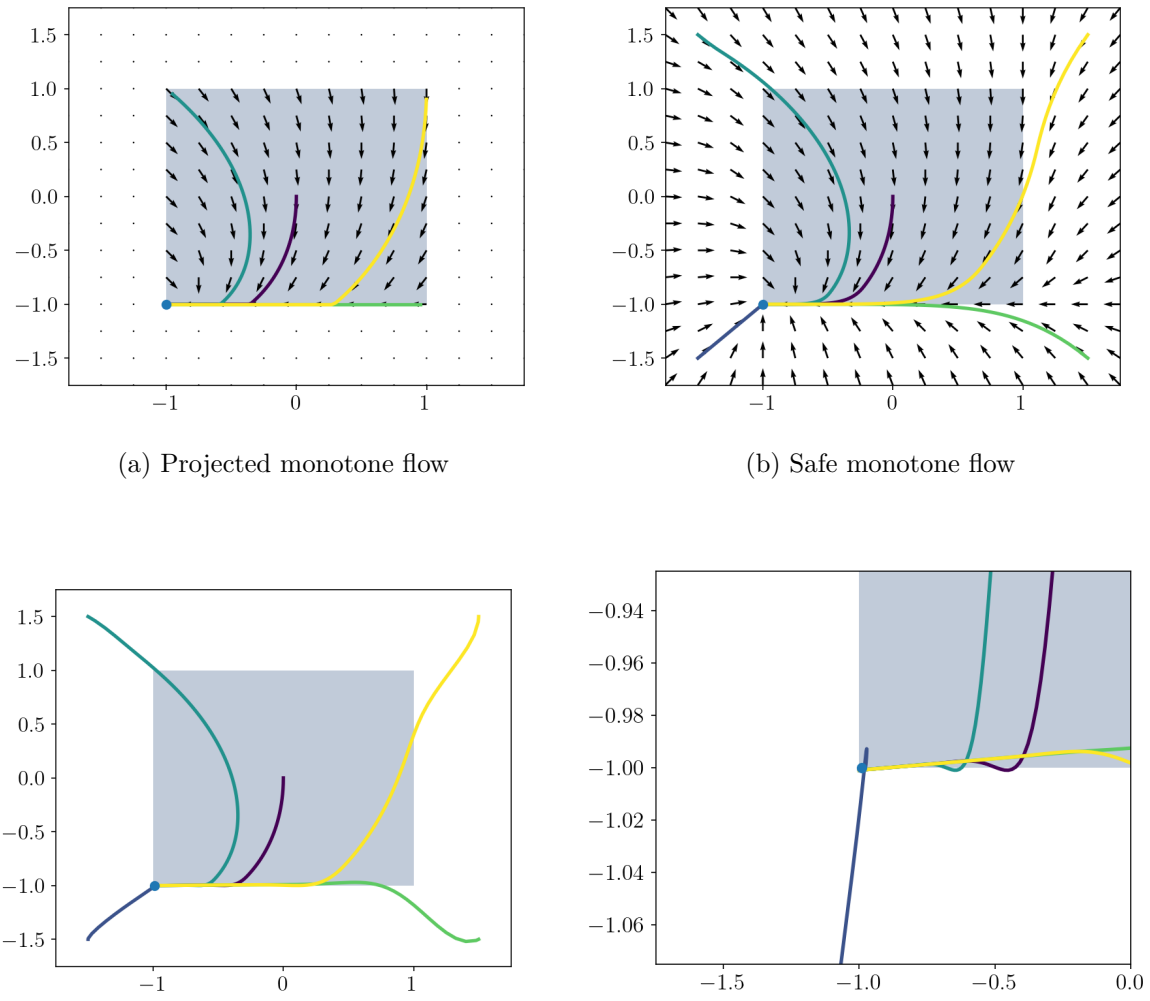

(a) Projected monotone flow

(b) Safe monotone flow

(c) Recursive safe monotone flow

(d) Zoomed-in plot of (c)

Figure 4.2: Implementation of (a) projected monotone flow, (b) safe monotone flow ($\alpha = 1.0$), and (c) recursive safe monotone flow ($\tau = 0.25$) in a two-player game. The shaded region shows the constraint set $\mathcal{C}$ and the colored paths represent trajectories of the corresponding flow starting from various initial condition. (d) shows a zoomed-in portion of the boundary of $\mathcal{C}$ to illustrate the practical safety of the recursive safe monotone flow.

4.5.2 Receding Horizon Linear-Quadratic Dynamic Game

We now discuss a more complex example, where the input to a plant is specified by the solution to a variational inequality parameterized by the state of the plant. To solve it, we interconnect the plant dynamics with the safe monotone flow, and demonstrate that the anytime property of the latter ensures good performance and satisfaction of the constraints even when terminated terminated early. The plant takes the form of a discrete-time linear time-invariant system with two inputs,

$$z(s+1) = Az(s) + B_1 w_1(s) + B_2 w_2(s), \tag{4.35}$$

where $A \in \mathbb{R}^{n_z \times n_z}$ and $B_i \in \mathbb{R}^{n_z \times n_w}$ for $i \in \{1, 2\}$. We consider a linear-quadratic dynamic game (LQDG) between two players, where each player $i \in \{1, 2\}$ can influence the system (4.35) by choosing the corresponding input $w_i \in W_i \subset \mathbb{R}^{n_w}$. We fix a time horizon, $N > 0$, and an initial condition $z(0) = z_0$, and define a cost J as the quadratic payoff function,

$$J(w_1(\cdot), w_2(\cdot)) = \|z(N)\|_{Q_f}^2 + \sum_{s=0}^{N-1} \|z(s)\|_Q^2 + \|w_1(s)\|_{R_1}^2 - \|w_2(s)\|_{R_2}^2 , \tag{4.36}$$

where $Q_f, Q \succeq 0$ and $R_1, R_2 \succ 0$. The goal of player 1 is to minimize the payoff (4.36), whereas the goal of player 2 is to maximize it. This problem can be solved in closed form when the constraints W_i are trivial (cf. [BO99, Chapter 6], [PP10]), but must be solved numerically for nontrivial ones.

We first note the LQDG problem can be written as a variational inequality. Indeed,

let $\bar{z} = (z(1), \ldots, z(N))$ and, for $i \in \{1, 2\}$, let $\bar{w}_i = (w_i(0), \ldots, w_i(N-1))$. Define

$$\mathcal{A} = \begin{bmatrix} A \\ A^2 \\ \vdots \\ A^N \end{bmatrix}, \qquad C_i = \begin{bmatrix} B_i & 0 & \cdots & 0 \\ AB_i & B_i & \cdots & 0 \\ A^2B_i & AB_i & \cdots & 0 \\ \vdots & \vdots & \ddots & \vdots \\ A^{N-1}B_i & A^{N-2}B_i & \cdots & B_i \end{bmatrix}.$$

Next, letting $\bar{Q} = \mathrm{diag}(Q, \ldots, Q, Q_f)$ and $\bar{R}_i = \mathrm{diag}(R_i, \ldots, R_i)$, and using the fact that $\bar{z} = \mathcal{A}z_0 + C_1\bar{w}_1 + C_2\bar{w}_2$, we see that the payoff function (4.36) can be written as,

$$J(\bar{w}_1, \bar{w}_2) = \begin{bmatrix} \bar{w}_1 \\ \bar{w}_2 \end{bmatrix}^\top \begin{bmatrix} C_1^\top \bar{Q} C_1 + \bar{R}_1 & C_1^\top \bar{Q} C_2 \\ C_2^\top \bar{Q} C_1 & C_2^\top \bar{Q} C_2 - \bar{R}_2 \end{bmatrix} \begin{bmatrix} \bar{w}_1 \\ \bar{w}_2 \end{bmatrix} + 2 \begin{bmatrix} C_1^\top \bar{Q} \mathcal{A} z_0 \\ C_2^\top \bar{Q} \mathcal{A} z_0 \end{bmatrix}^\top \begin{bmatrix} \bar{w}_1 \\ \bar{w}_2 \end{bmatrix} + z_0^\top \mathcal{A}^\top \bar{Q} \mathcal{A} z_0.$$

Finally, letting $x = (\bar{w}_1, \bar{w}_2)$, we see that the problem corresponds to the variational inequality $\mathrm{VI}(F(\cdot, z_0), \mathcal{C})$, where

$$F(x, z_0) = \begin{bmatrix} C_1^\top \bar{Q} C_1 + \bar{R}_1 & C_1^\top \bar{Q} C_2 \\ -C_2^\top \bar{Q} C_1 & \bar{R}_2 - C_2^\top \bar{Q} C_2 \end{bmatrix} \begin{bmatrix} \bar{w}_1 \\ \bar{w}_2 \end{bmatrix} + \begin{bmatrix} C_1^\top \bar{Q} \mathcal{A} z_0 \\ -C_2^\top \bar{Q} \mathcal{A} z_0 \end{bmatrix}$$

and the constraint set is

$$\mathcal{C} = \underbrace{W_1 \times W_1 \times \cdots W_1}_{N \text{ times}} \times \underbrace{W_2 \times W_2 \times \cdots \times W_2}_{N \text{ times}}.$$

If the problem data satisfies

$$\begin{bmatrix} C_1^\top \bar{Q} C_1 + \bar{R}_1 & 0 \\ 0 & \bar{R}_2 - C_2^\top \bar{Q} C_2 \end{bmatrix} \succ 0,$$

then F is strongly monotone.

For simulation purposes, we take $n_z = 5$, $n_w = 2$, $B_i = I$, $W_i = \mathbb{R}^2_{\geq 0}$, and A a marginally stable matrix selected randomly. We use the safe monotone flow to solve the variational inequality and implement the solution in a receding horizon manner: given the initial state z_0, we solve for the optimal input sequence $(w_1(\cdot), w_2(\cdot))$ over the entire time horizon, apply the input $(w_1(0), w_2(0))$ to (4.35) to obtain $z(1)$, update the initial condition $z_0 \leftarrow z(1)$ and repeat. When F is strongly monotone, on each iteration the flow converges to the exact solution as $t \to \infty$. However, we also consider here the effect of terminating the solver early at some $t = t_f < \infty$.

Figure 4.3 shows the results of the simulation. In Figure 4.3(a), we plot $\|z(s)\|$ for various values of termination times. We denote the exact solution with $t_f = \infty$. The closed-loop dynamics with the exact solution to the receding horizon LQDG is stabilizing, and as t_f grows larger, the early terminated solution drives the state of the system closer to the origin. In Figure 4.3(b), we plot the first component of $w_1(s)$ in blue and the first component of $w_2(s)$ in red. Regardless of when terminated, the inputs satisfy the input constraints on each iteration due to the safety properties of the safe monotone flow.

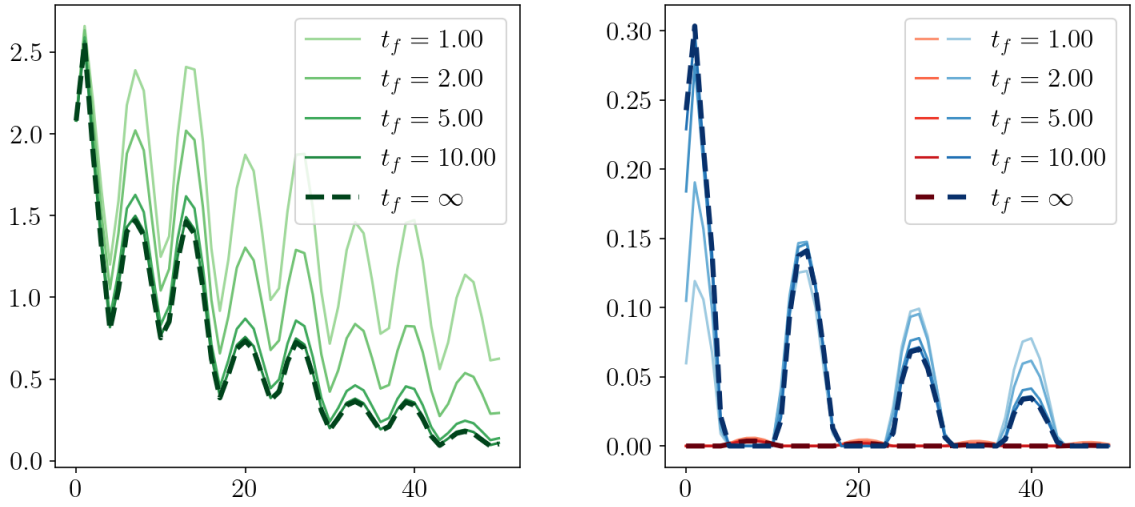

(a) $\|z(s)\|$ on each iteration

(b) First component of $\{w_i(s)\}_{i\in\{1,2\}}$ on each iteration

Figure 4.3: Receding horizon implementation of the safe monotone flow solving a linear quadratic dynamic game for different choices of termination time t_f. The closed-loop implementation of the exact solution corresponds to $t_f = \infty$ (dashed lines). (a) We plot the evolution of $\|z(s)\|$ in green. (b) We plot the evolution of the first component of $w_1(s)$ in blue-green (scale in left y-axis) and the first component of $w_2(x)$ in red-orange (scale in right y-axis).

4.6 Conclusions

We have tackled the design of anytime algorithms to solve variational inequalities as a feedback control problem. Using techniques from safety-critical control, we have synthesized three continuous-time dynamics which find solutions to monotone variational inequalities: the projected monotone flow, already well known in the literature, and the novel safe monotone and recursive safe monotone flows. The equilibria of these flows correspond to solutions of the variational inequality, and so we have embarked in the precise characterization of their asymptotic stability properties. We have established asymptotic stability of equilibria in the case of strong monotonicity, and contractivity and exponential stability in the case of poly-

hedral constraints. We have also shown that the safe monotone flow renders the constraint forward invariant and asymptotically stable. The recursive safe monotone flow offers an alternative implementation that does not necessitate the solution of a quadratic program along the trajectories. This flow results from coupling two systems evolving on different timescales, and we have established local exponential stability and global attractivity of equilibria, as well as practical safety guarantees. We have illustrated in two game scenarios the properties of the proposed flows and, in particular, their amenability for interconnection and regulation of physical processes. Future work will develop methods for distributed network problems and consider applications to feedback optimization arising in applications such as power systems, traffic networks, and communications systems.

Acknowledgements

This chapter, in full, is a reprint of material submitted for publication where it may appear as "Anytime Solvers for Variational Inequalities: the (Recursive) Safe Monotone Flows" by Ahmed Allibhoy and Jorge Cortés in Automatica. The dissertation author is the primary investigator and author of this paper.

Part II

Human Focal Epilepsy as a Network Dynamical Disease

Chapter 5

Dynamical Models of Brain Networks

5.1 Introduction

Epilepsy is a chronic neurological disorder characterized by intermittent episodes of hypersynchronous electrical activity in the brain. These episodes, commonly known as *seizures*, are marked by symptoms such as abnormal sensations, muscle contractions, and loss of consciousness. Approximately 50 million individuals have epilepsy, making the disease one of the most widespread neurological conditions in the world. Despite this, there is no known cure for epilepsy. Current treatment strategies merely aim to reduce the frequency of seizures and manage symptoms when seizures occur. While modern anti-epileptic drugs result in full remission of seizures in most patients, in around 20-40% of cases the condition does not respond to pharmacological intervention [SS06, BBB$^+$12]. Surgical treatment may be indicated for drug-resistant patients, however outcomes are highly variable, with cessation of seizures being achieved 34-84% of the time, depending on the type of epilepsy and the

surgical target [SH08].

The difficulties in treating epilepsy arise from the complexity of the disease. To motivate the models and analysis considered in this section, we highlight two defining features of epilepsy. The first is that epilepsy is a *dynamical disease* [MG77, GM79, dSBK$^+$03]. This refers to the fact that the brain activity (when measured with e.g. EEG) can be characterized with an oscillatory temporal signal that, in epileptic patients, appears normal between seizure episodes but undergoes qualitative changes during seizures. Thus the epileptic brain, if viewed as a dynamical system, exhibits a type of multi-stability, with healthy and seizure-like modes corresponding to different attractors in the state-space. The second is that epilepsy is a *network disorder* [Spe02]. This refers to the fact that the brain is composed of many different components interconnected through a network structure, and while seizures may be localized to certain brain regions, their emergence results from interactions among all elements of the network. These network effects complicate the identification of appropriate targets for surgical resection or neurostimulation, since simply targeting regions with pathological activity might not have the intended effect due to the global nature of these interactions.

Mathematical models that account for both the dynamical and network aspects of the epileptic brain provide a promising route to managing this complexity, and designing effective interventions to mitigate epileptic seizures. In this part of the thesis we show how tools from nonlinear dynamics, non-smooth systems, and network optimization can be used to derive such models and analyze their properties, as well as mathematically formalize the problem of suppressing the spread of seizures and solve it optimally. Here, we review the current

state-of-the-art in modeling brain networks, then we discuss mathematical preliminaries in order to set the stage for our contributions in later chapters.

5.2 Related Work

In this section we discuss prior work in dynamic modeling of the human brain. Though the field is vast and has a rich history, we restrict our attention here to models in the form of ordinary differential equations on networks. For a more comprehensive overview we refer the interested reader to, e.g., [Izh07, DA01, FZB16]. The human brain consists of on the order of 10^{11} neurons and 10^{14} synaptic connections between these neurons. Because of the enormous scale involved, it is not tractable to capture all the neurons and their connections in a single model of the brain. For this reason, network models of the human brain exist on different spatial scales[GCC+21], depending on the phenomenon of interest, or the particular features of the brain one wants to understand (cf. Figure 5.1 for a depiction of different spatial scales of brain modeling). At the smallest scale, each node in the network corresponds to a single neuron, whereas at the largest scale a single node may represent an entire brain region. Here we briefly review network brain models on the entire spectrum of spatial scales.

5.2.1 Microscopic or Single-Neuron Models

We begin by discussing *microscopic* or *single-neuron models* (cf. Figure 5.1(left)), where as the name suggestions, nodes in the network correspond to individual neurons. These systems are typically *mechanistic*, meaning they are derived from the fundamental

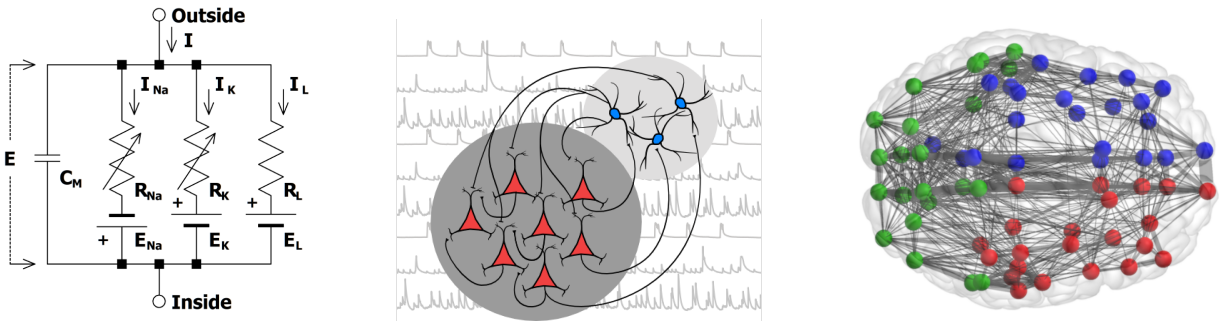

Figure 5.1: Figure showing brain networks at different spatial scales. (Left) Schematic of Hodgkin-Huxley model describing a single-neuron as a nonlinear circuit [HH52] (Center) Depiction of brain network at the mesoscopic scale [SVW+21] (Right) Depiction of brain network at the macroscopic scale [MBBP19].

physical laws, as opposed to *phenomenological* models which describe empirical observations but are not derived from first-principles. The most famous examples are the Hodgkin-Huxley model [HH52], and closely related Fitzhugh-Nagumo model [Fit61, NAY62], which explains the origination and propagation of action potentials in neurons through the diffusion of ions across the cell membrane using the model of a leaky capacitor. While these systems are used to understand the physiology of neuronal networks, recent work [SBS22] focuses on controlling them, both in biomedical applications as well as engineering applications such as neuromorphic computing.

5.2.2 Macroscopic Models

We now discuss *macroscopic models* (cf. Figure 5.1(right)), which exist on the opposite end of the spectrum of spatial scales to single-neuron models. Here, nodes correspond to entire brain regions, and edges represent long-range cortical connections between these regions. At the macroscocpic scale the celebrated *Kuramoto model* (see e.g. [DB14, ADGK+08]

for a review of this system and its properties) is often used. This system can be written as

$$\dot{\theta}_i = \omega_i + \sum_{j=1}^{N} W_{ij} \sin(\theta_j - \theta_i),$$

where $\mathbf{W}$ is the weighted adjacency matrix of the network and θ_i is the state of the ith node. This model is employed when the relevant information about each node can be captured by a single phase variable, for example when one cares about synchronization between oscillatory signals in the brain [BHD10]. Recent work involving Kuramoto models has focused on controlling brain networks using deep-brain stimulation, e.g., through optimal control [MWMM19, WM22] or vibrational control [QBP22b].

5.2.3 Mesoscopic Models

We finally review here *mesoscopic models* (cf. Figure 5.1(center)) which describe phenomena occurring between the single-neuron and macroscopic scales, and will be the main focus of the rest of this thesis. At this scale, the nodes in the network describe large populations of neurons. Unlike single-neuron models, the mesoscopic models we discuss are usually phenomenological, though in special cases it has been shown these models corresponding to mean-field approximations of single-neuron models [WC72]. Here we focus on *rate models*, where the state of the ith node, x_i, models the average firing rate of the ith neural population. Examples of rate models include the Wilson-Cowan model [WC72] and the Jansen-Rit

model [JR95]. Typically these models have the following form

$$\tau\dot{\mathbf{x}} = -\mathbf{x} + f(\mathbf{W}\mathbf{x} + \mathbf{u}), \tag{5.1}$$

where $\mathbf{W}$ is the weighted adjacency matrix of the network, $\mathbf{u}$ represents the vector of exogenous inputs to each node, and f is an activation function. In the case where f is a sigmoidal activation, one recovers the Wilson-Cowan model, however Gaussian functions [MEK+15], Heaviside functions [HE15], and piecewise linear activation functions [NC21a, NC21b] have also been used.

5.3 Mathematical Preliminaries

5.3.1 Notation

We use $\mathbb{R}$, $\mathbb{R}_{\geq 0}$, and $\mathbb{R}_{\leq 0}$ to denote the set of reals, nonnegative reals and non-positive reals, respectively. We use lower case bold letters to denote vectors, and upper case bold letters to denote matrices. The identity matrix is denoted by $\mathbf{I}$. Given a vector $\mathbf{x} \in \mathbb{R}^n$, we use x_i to refer to its ith component, and given a matrix $\mathbf{A} \in \mathbb{R}^{n\times m}$ we use A_{ij} to refer to its (i,j)th component. For $\mathbf{x} \in \mathbb{R}$ and $\mathbf{m} \in \mathbb{R}_{\geq 0}$, $[x]_0^m = \min\{\max\{x, 0\}, m\}$, which is the projection of x onto $[0, m]$. Similarly, when $\mathbf{x} \in \mathbb{R}^n$ and $\mathbf{m} \in \mathbb{R}^n_{\geq 0}$, $[\mathbf{x}]_{\mathbf{0}}^{\mathbf{m}} = [[x_1]_0^{m_1} \dots [x_n]_0^{m_n}]^T$. The open ball in $\mathbb{R}^n$ with radius $\epsilon > 0$ centered at $\mathbf{x} \in \mathbb{R}^n$ is denoted by $B_\epsilon(\mathbf{x}) = \{\mathbf{y} \in \mathbb{R}^n \mid \|\mathbf{y} - \mathbf{x}\| < \epsilon\}$.

5.3.2 Graph Theory

Here we review basic notions from graph theory, which is theoretical framework we employ for modeling networks. A *graph* is a pair $\mathcal{G} = (\mathcal{V}, \mathcal{E})$ consisting of a set of *nodes*, $\mathcal{V} = \{1, 2, \ldots, N\}$, and a set of *edges* $\mathcal{E} \subset \mathcal{V} \times \mathcal{V}$ which describe connections between nodes. We say that the graph is *undirected* if $(i, j) \in \mathcal{E}$ implies that $(j, i) \in \mathcal{E}$, otherwise we refer to the graph as *directed*. The connectivity structure of the graph can be described by the *adjacency matrix*, $\mathbf{A} \in \mathbb{R}^{N \times N}$, defined by

$$A_{ij} = \begin{cases} 1 & (i, j) \in \mathcal{E} \\ 0 & (i, j) \notin \mathcal{E} \end{cases}$$

Note that when the graph is undirected, $\mathbf{A}$ is a symmetric matrix. In certain applications, we want to assign a weight w_{ij} to each edge (i, j), where $w_{ij} = 0$ whenever $(i, j) \notin \mathcal{E}$. In this case we refer to the graph as a *weighted graph*, and describe its structure using a *weighted adjacency matrix* $\mathbf{W} \in \mathbb{R}^{N \times N}$ with $W_{ij} = w_{ij}$.

5.3.3 Linear Threshold Networks

Here we go over the theory of Linear-Threshold Networks (LTNs), which are a specific instance of the rate model (5.1) where the activation function is piecewise linear. Our exposition follows that of [NC21a]. Consider a graph $\mathcal{G} = (\mathcal{V}, \mathcal{E})$ where $\mathcal{V} = \{1, 2, \ldots, N\}$, and $\mathcal{E} \subset \mathcal{V} \times \mathcal{V}$. Let $\mathbf{W}$ be a weighted adjacency matrix of the network. The dynamics of

the LTN are given by

$$\dot{\mathbf{x}} = -\mathbf{x} + [\mathbf{W}\mathbf{x} + \mathbf{u}]_{\mathbf{0}}^{\mathbf{m}}, \tag{5.2}$$

where $\mathbf{m}$ is a vector describing the maximum firing rates of each node. The state-space of the system is $X = [0, m_1] \times [0, m_2] \times \cdots \times [0, m_N]$. Note that by construction, if $\mathbf{x}(0) \in X$ then $\mathbf{x}(t) \in X$ for all $t \geq 0$.

For Neuroscience applications, it is common to assume that the network satisfies the following assumption, commonly known as Dale's Law.

Assumption 5.3.1 (Dale's Law)**.** *For all $j = 1, \ldots, N$, either $W_{ij} > 0$ for all $i = 1, \ldots, N$ or $W_{ij} < 0$ for all $i = 1, \ldots, N$*

Informally, Assumption 5.3.1 states that every node in the network is either *excitatory*, meaning an increase in its activity enhances the firing rates of its neighbors, or *inhibitory*, meaning that an increase in its activity decreases the firing rates of its neighbors. This property is commonly observed in real-world examples of brain networks.

5.3.4 Existence and Stability of Equilibria

We now discuss equilibria in LTNs. We begin by partitioning the state-space of the system (5.2) into 3^N regions parametrized by a switching index $\sigma = (\sigma_1, \ldots, \sigma_N)$, where

$\sigma_i \in \{0, \ell, s\}$. Given a switching index σ, we define the corresponding switching region by

$$\begin{aligned}\Omega_\sigma = \{\mathbf{x} \in X \mid (\mathbf{W}\mathbf{x} + \mathbf{u})_i \leq 0 \text{ if } \sigma_i = 0,\\ (\mathbf{W}\mathbf{x} + \mathbf{u})_i \in [0, m_i] \text{ if } \sigma_i = L,\\ (\mathbf{W}\mathbf{x} + \mathbf{u})_i \geq m_i \text{ if } \sigma_i = S\}.\end{aligned} \tag{5.3}$$

We also define the switching matrices Σ_σ^L and Σ_σ^S by

$$(\Sigma_\sigma^L)_{ii} = \begin{cases} 1 & \text{if } \sigma_i = L \\ 0 & \text{if } \sigma_i \neq L \end{cases} \qquad (\Sigma_\sigma^S)_{ii} = \begin{cases} 1 & \text{if } \sigma_i = S \\ 0 & \text{if } \sigma_i \neq S \end{cases}.$$

Using the switching matrices, the dynamics (5.2) can be equivalently written as

$$\dot{\mathbf{x}} = (-\mathbf{I} + \Sigma_\sigma^L \mathbf{W})\mathbf{x} + \Sigma_\sigma^L \mathbf{u} + \Sigma_\sigma^S \mathbf{m} \qquad \text{if } \mathbf{x} \in \Omega_\sigma \tag{5.4}$$

From the form of the equation (5.4), it is clear that the LTN is a switched affine system with 3^N modes. However, even though the dynamics are affine in each switching region, switched affine systems exhibit much richer behavior than affine systems, include multiple equilibria, limit-cycles and even chaotic trajectories.

Our analysis requires the following assumption.

Assumption 5.3.2. *Assume that*

(i) $\det(\mathbf{W}) \neq 0$

(ii) For all $\sigma \in \{0, \ell, s\}^N$*, we have that* $\det(-\mathbf{I} + \Sigma_\sigma^L \mathbf{W}) \neq 0$.

Note that Assumption 5.3.2 is not restrictive because the set of matrices in $\mathbb{R}^{N\times N}$ which fail this assumption has Lebesgue measure zero, and it is therefore satisfied by almost all matrices $\mathbf{W} \in \mathbb{R}^{N\times N}$. With this assumption, we can rearrange (5.4) to define for each switching region σ, an *equilibrium candidate*,

$$\mathbf{x}^*_\sigma = (-\mathbf{I} + \Sigma^L_\sigma \mathbf{W})^{-1}(\Sigma^L_\sigma \mathbf{u} + \Sigma^S_\sigma \mathbf{m}).$$

Clearly $\mathbf{x}^*_\sigma$ is an equilibrium of (5.2) if and only if $\mathbf{x}^*_\sigma \in \Omega_\sigma$, and the corresponding equilibrium is stable if $-\mathbf{I} + \Sigma^L_\sigma \mathbf{W}$ is a Hurwitz matrix.

5.3.5 Existence of Oscillations

Finally, we discuss sufficient conditions for the existence of oscillatory solutions to (5.2). The notion of oscillation varies in the mathematical neuroscience literature. Here, we use definition of oscillation which appears in [NPC22]. We say that a solution $\mathbf{x}(t)$ is *oscillatory* if (i) its power spectrum contains distinct and pronounced peaks and (ii) $\mathbf{x}(t)$ does not converge to a fixed point as $t \to \infty$. Although this definition is imprecise, it includes both limit cycles and chaotic trajectories, and encompasses the types of oscillatory patterns typically encountered in neuroscience applications [BD04, WGTB14].

Recent work[NC19, NPC22] has characterized the existence of oscillations using an approach inspired by the Poincaré-Bendixson Theorem [Str00, Chapter 7.3]. Informally, this theorem states that periodic solutions to a system exist when the state-space is compact, and does not contain any stable equilibrium points. This condition, which we refer to as

"*Lack of Stable Equilibria*" (LoSE) is both necessary and sufficient for the existence of a limit cycle when $N = 2$. For $N > 2$, the condition is only sufficient for the existence of an oscillation, which is possibly chaotic.

We conclude this chapter with a result which characterizes exactly when stable limit cycles exist in LTNs satisfying Dale's Law, with $N = 2$. We refer the reader to [NPC22] for results for larger networks.

Theorem 5.3.3 (Existence of Stable Limit Cycle in Planar LTNs)**.** *Consider the system* (5.2) *with* $N = 2$ *where*

$$\mathbf{W} = \begin{bmatrix} a & -b \\ c & -d \end{bmatrix} \qquad a, b, c, d \geq 0.$$

The system has a globally stable limit cycle if

$$d + 2 < a, \tag{5.5a}$$

$$(a-1)(d+1) < bc, \tag{5.5b}$$

$$(a-1)m_1 < bm_2, \tag{5.5c}$$

$$0 < u_1 < bm_2 - (a-1)m_1, \tag{5.5d}$$

$$0 < (d+1)u_1 - bu_2 < (bc - (a-1)(d+1))m_1. \tag{5.5e}$$

Chapter 6

Modeling Epileptic Behavior using Excitatory-Inhibitory Pairs

In this chapter, we provide a detailed characterization of the equilibria and bifurcations of two-dimensional linear-threshold models, referred to as excitatory-inhibitory pairs (EI pairs). Using the input to the system as the bifurcation parameter, we characterize the location of the admissible equilibria, show that bifurcations can arise only when equilibria lie on the boundary of well-defined regions of the state space, and prove that (codimension-one) bifurcations can only be of three different types: persistent, non-smooth fold, and Hopf. We show how these bifurcations change the qualitative properties of the system trajectories, and how these behaviors resemble prototypical patterns of EEG activity observed before, during, and after seizure events in the human brain. Our findings suggest that low-dimensional linear threshold models can effectively be used to model, analyze, predict, and ultimately regulate the interactions of neuronal populations in the human brain.

6.1 Problem Formulation

We model the interaction between populations of neurons using Linear-Threshold Networks, An epileptic seizure can be viewed as an abrupt intermittent transition between highly ordered and disordered states [NdS05]. In a dynamical systems' context, this may correspond to a qualitative change in the behavior of the system, which is typically linked to the study of bifurcations. Evidence suggests that, even during highly disruptive events such as seizures, the underlying connectivity structure between neurons does not experience a significant change in its nature, while the inputs to the system may be altered by exogenous and endogenous events. Following this evidence, here we study how changes in the input $\mathbf{u}$ in (5.2) can generate qualitative changes in the behavior of the neurons firing rates.

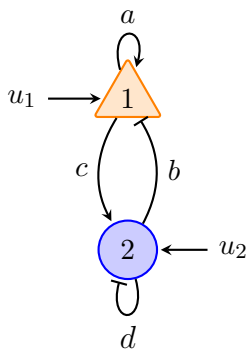

Figure 6.1: Schematic of EI Pair, where node 1 is excitatory and node 2 is inhibitory.

We consider a network of excitatory and inhibitory neurons satisfying Dale's Law (c.f Assumption 5.3.1) with $N = 2$ all-to-all connectivity. We let the state x_1 (resp. x_2) correspond to the lumped activity of the population of excitatory (resp. inhibitory) neurons, which have positive (resp. negative) feedforward contribution to the network. We refer to the system in this special case as an *EI Pair*, and is depcited schematically in Figure 6.1. As

our ensuing analysis reveals, the EI pair case shows much of the complexity of the general case and is rich enough to capture a variety of epileptic behaviors.

In this case, the state space of the system is $X = [0, m_1] \times [0, m_2]$, and the dynamics of the EI pair simplify as follows.

$$\dot{x}_1 = -x_1 + [ax_1 - bx_2 + u_1]_0^{m_1} \tag{6.1a}$$

$$\dot{x}_2 = -x_2 + [cx_1 - dx_2 + u_2]_0^{m_2}. \tag{6.1b}$$

The parameters u_1 and u_2 capture changes in the neurological background activity. In this chapter, we seek to understand how changes in this activity result in seizure like behavior. Since qualitative changes occur due to bifurcations, we wish to identify all possible bifurcations in (6.1) using u_1 as a bifurcation parameter. Additionally, we want to identify conditions on the parameters of the system that ensure the existence of a stable limit cycle, without relying on the "Lack of Stable Equilibria" (LoSE) condition.

6.2 Bifurcations in EI Pairs

In this section we characterize the bifurcations of (6.1) as a function of the external input $\mathbf{u}$. Throughout the rest of this chapter we assume that Assumption 5.3.2 holds. Recall that the LTN can be viewed as a switched affine system with $3^2 = 9$ modes. Let $\dot{\mathbf{x}} = f_\sigma(\mathbf{x}, \mathbf{u})$, where

$$f_\sigma(\mathbf{x}, \mathbf{u}) = (-\mathbf{I} + \Sigma_\sigma^L \mathbf{W})\mathbf{x} + \Sigma_\sigma^S \mathbf{m} + \Sigma_\sigma^L \mathbf{u},$$

denote the dynamics (6.1) in the case $\mathbf{x} \in \Omega_\sigma$, where Ω_σ is the switching region defined in (5.3) and $\sigma \in \{0, \ell, s\}\}^2$. Let $\mathbf{x}^*_\sigma$ denote the equilibrium candidate corresponding to the region Ω_σ.

We focus on codimension-one bifurcations, since they arise more frequently in biological systems than higher-dimensional bifurcations [Izh00]. In particular, we choose u_1 as the bifurcation parameter, and leave u_2 constant. An equivalent analysis can be carried out using u_2 as the bifurcation parameter and keeping u_1 constant. Because u_2 is constant, we abuse notation slightly by writing the equilibrium candidates as a function of u_1 only.

We now characterize the equilibrium candidates in each switching region. To do this, we rely on the following assumption.

Assumption 6.2.1. *The parameters of* (6.1) *satisfy*

$$-m_1 c < u_2 < (1+d)m_2. \tag{6.2}$$

The condition bounding u_2 in (6.2) limits the number of admissible equilibria to five (down from nine). For $u_2 < -m_1 c$, (resp. $u_2 > (1+d)m_2$), we have $x_2 = 0$, (resp. $x_2 = m_2$), for all u_1, which are of little interest and we therefore exclude to keep the problem tractable.

When (6.2) holds, the 5 equilibrium candidates are:

$$\mathbf{x}^*_{00}(u_1) = \mathbf{0}, \tag{6.3a}$$

$$\mathbf{x}^*_{\ell 0}(u_1) = \left(\frac{1}{1-a}u_1, 0\right), \tag{6.3b}$$

$$\mathbf{x}^*_{\ell s}(u_1) = \left(\frac{1}{1-a}u_1 - \frac{bm_2}{1-a}, m_2\right) \tag{6.3c}$$

$$\mathbf{x}^*_{\ell\ell}(u_1) = \left(\frac{(1+d)u_1 - bu_2}{(1+d)(1-a)+bc}, \frac{cu_1 + (1-a)u_2}{(1+d)(1-a)+bc}\right) \tag{6.3d}$$

$$\mathbf{x}^*_{ss}(u_1) = \mathbf{m}. \tag{6.3e}$$

A bifurcation can occur only when $\mathbf{x}^*_\sigma(\mathbf{u})$ is on the boundary of Ω_σ. In this case, the equilibrium candidate $\mathbf{x}^*_\sigma$ overlaps with the equilibrium candidate of another region. Therefore, we call $\mathbf{u}$ a *bifurcation candidate* if there exist $\sigma_1, \sigma_2 \in \{0, \ell, s\}^2$ with $\sigma_1 \neq \sigma_2$ such that $\mathbf{x}^*_{\sigma_1}(\mathbf{u}) = \mathbf{x}^*_{\sigma_2}(\mathbf{u})$. A *boundary equilibrium bifurcation* occurs when $\mathbf{u}$ is a bifurcation candidate and $\mathbf{x}^*_\sigma$ is admissible in both Ω_{σ_1} and Ω_{σ_2}, i.e., when $\mathbf{x}^*_{\sigma_1}(\mathbf{u}) \in \Omega_{\sigma_1}$ and $\mathbf{x}^*_\sigma(\mathbf{u}) \in \Omega_{\sigma_2}$.

Suppose a boundary equilibrium bifurcation occurs at $\mathbf{u}$. Then, $\mathbf{u}$ is

(i) a *Persistent BEB* (P-BEB) if the number of equilibria is constant in a neighborhood of $\mathbf{u}$;

(ii) a *Non-smooth fold BEB* (NSF-BEB) if the number if equilibria is not constant in a neighborhood of $\mathbf{u}$;

(iii) a *Hopf bifurcation*[1] if it is an NSF-BEB such that a limit cycle emerges.

[1]As highlighted in [BBCK08], the definition of Hopf bifurcation does not generalize well to piecewise smooth systems since there is no sense in which eigenvalues cross the imaginary axis at the bifurcation onset. However, with a slight but common abuse of terminology, we refer to a Hopf bifurcation if the only attractor in the system is a limit cycle.

We next state our main theoretical result which characterizes explicitly all possible bifurcation diagrams of (6.1).

Theorem 6.2.2. (Bifurcation diagram) *Let u_1 be the bifurcation parameter of the system* (6.1)*, and suppose Assumption 6.2.1 holds. Then, there exist at most eight bifurcation candidates. Further, there exist four qualitatively different bifurcation diagrams induced by the following inequalities:*

$$a < 1, \tag{6.4a}$$

$$(a-1)(d+1) < bc, \tag{6.4b}$$

$$a < d + 2, \tag{6.4c}$$

In particular, the possible bifurcation diagrams are defined as follows (see Table 6.2 for an illustration):

(A) If (6.4a) *is satisfied, then there exists a unique equilibrium for every* $\mathbf{u}$ *and all bifurcations are P-BEB.*

(B) If inequalities (6.4a) *and* (6.4b) *are not satisfied, then the system has one equilibrium (for small and big values of u_1) or three equilibria. Then, bifurcations involving the $\Omega_{\ell\ell}$ region and only one other region are P-BEB. Otherwise, bifurcations are NSF-BEB.*

(C) If (6.4b)-(6.4c) *are satisfied and* (6.4a) *is not satisfied, then the bifurcation candidates involving either the region Ω_{00} or Ω_{ss} and only one other region are P-BEB. Otherwise, bifurcations are NSF-BEB.*

(D) If (6.4b) *is the only satisfied inequality, then the analysis of BEB is equivalent to that of Case C. However, condition* (6.4c) *makes* $\mathbf{x}^*_{\ell\ell}$ *an unstable fixed point resulting in a Hopf bifurcation at* $\mathbf{u}^{\ell 0}_{00}$ *and at* $\mathbf{u}^{\ell s}_{ss}$.

Proof. Recall that $\mathbf{u}$ is a bifurcation candidate if and only if there exist distinct σ_1 and σ_2 such that $\mathbf{x}^*_{\sigma_1}(\mathbf{u}) = \mathbf{x}^*_{\sigma_2}(\mathbf{u})$. Examining only the x_1 component in equations (6.3a)-(6.3e), we see that these are affine in u_1. Moreover, the affine functions (6.3a) and (6.3e) are parallel and never intersect, so there is no bifurcation candidate when $\sigma_1 = 00$ and $\sigma_2 = ss$. By a similar line of reasoning, we conclude that there is no bifurcation candidate when $\sigma_1 = l0$ and $\sigma_2 = ls$. Hence there are only eight possible bifurcation candidates.

Let Ω_{σ_1} and Ω_{σ_2} be neighboring regions. We claim that there exists

$$h : \Omega_{\sigma_1} \cup \Omega_{\sigma_2} \times \mathbb{R} \to \mathbb{R}$$

such that the dynamics (6.1), on $\Omega_{\sigma_1} \cup \Omega_{\sigma_2}$, become

$$\dot{x} = \begin{cases} f_{\sigma_1}(\mathbf{x}, u_1), & h(\mathbf{x}, u_1) \leq 0, \\ \\ f_{\sigma_2}(\mathbf{x}, u_1), & h(\mathbf{x}, u_1) \geq 0, \end{cases} \tag{6.5}$$

where $h(\mathbf{x}, u_1) = 0$ on $\Omega_{\sigma_1} \cap \Omega_{\sigma_2}$. Let u_{σ_1,σ_2} be the bifurcation candidate, i.e., $\mathbf{x}^*_{\sigma_1}(u_{\sigma_1,\sigma_2}) = \mathbf{x}^*_{\sigma_2}(u_{\sigma_1,\sigma_2}) = \mathbf{x}^*$. Then, a BEB occurs if $h(\mathbf{x}^*, u_{\sigma_1,\sigma_2}) = 0$. Further, a P-BEB occurs if there exists a neighborhood of u_{σ_1,σ_2} such that, for all u_1 in such neighborhood, the following inequality holds:

$$h(\mathbf{x}^*_{\sigma_1}(u_1), u_1) h(\mathbf{x}^*_{\sigma_2}(u_1), u_1) > 0.$$

A NSF-BEB occurs instead when the inequality is not satisfied in any neighborhood of u_{σ_1,σ_2}.

We will now show explicitly how to compute the type of bifurcation when $\sigma_1 = 00$ and $\sigma_2 = \ell 0$. Let $\Omega_1 = \Omega_{00}$ and $\Omega_2 = \Omega_{\ell 0}$. Then, (6.5) becomes

$$\dot{x}_1 = \begin{cases} -x_1, & h(\mathbf{x}, u_1) < 0, \\ (a-1)x_1 - bx_2 + u_1, & h(\mathbf{x}, u_1) > 0, \end{cases}$$

with $h(\mathbf{x}, u_1) = ax_1 - bx_2 + u_1$. From (6.3) we have $(x^*_{00}(u_1))_1 = 0$ and $(x^*_{\ell 0}(u_1))_1 = 1/(1-a)u_1$. Hence, $h(\mathbf{x}^*_{00}(u_1), u_1) = u_1$ and $h(\mathbf{x}^*_{0\ell}(u_1), u_1) = u_1/(1-a)$, which identifies a P-BEB at $u_1 = 0$ if and only if $a < 1$. Thus, in Case A the bifurcation candidate involving regions Ω_{00} and $\Omega_{\ell 0}$ is a P-BEB, while it is a NSF-BEB in cases B, C, and D. An equivalent analysis involving the remaining seven bifurcation candidates can be performed. In the interest of space, the explicit computations are here omitted.

Finally, cases C and D exhibit equivalent conditions for the boundary equilibrium bifurcations. However, when condition (6.4c) is met, the equilibrium in $\Omega_{\ell\ell}$ is unstable (both eigenvalues of the $\mathbf{I} - \mathbf{W}$ are positive), are are also satisfied. This gives rise to a discontinuity-induced Hopf bifurcation, which differentiates case D from case C. □

We plot the possible bifurcation diagram of (6.1) as described in Theorem 6.2.2. To make things easier to visualize, we only show the first coordinate of the equilibrium candidates. The first coordinate of (6.3a), which corresponds to the equilibrium candidate of the region Ω_{00}, is zero for every value of u_1 and is referenced as 00 in Case A of Table 6.2. Similarly, the first coordinate of the equilibrium candidate (6.3d), which corresponds to the

equilibrium candidate of the region $\Omega_{\ell\ell}$, varies linearly as a function of u_1 and is referenced as $\ell\ell$ in Case A of Table 6.2. A bifurcation candidate arises whenever two of these lines intersect. Bifurcation candidates are shown as black dots in Table 6.2. When the equilibrium candidates are admissible, then a BEB occurs, which is shown with a square in Table 6.2. Further, when the number of equilibria remains constant on both sides of a bifurcation, a P-BEB occurs: this can be seen, for instance, in Case A, where all bifurcations are P-BEB (black squares). On the other hand, in Case B, the number of admissible equilibria to the left of the bifurcation occurring at $u_1 = 0$ are three, $\mathbf{x}^*_{00}$, $\mathbf{x}^*_{\ell 0}$ and $\mathbf{x}^*_{ss}$, while there is just one admissible equilibrium, $\mathbf{x}^*_{ss}$, to its right. This is an example of NSF-BEB, which is denoted with white squares.

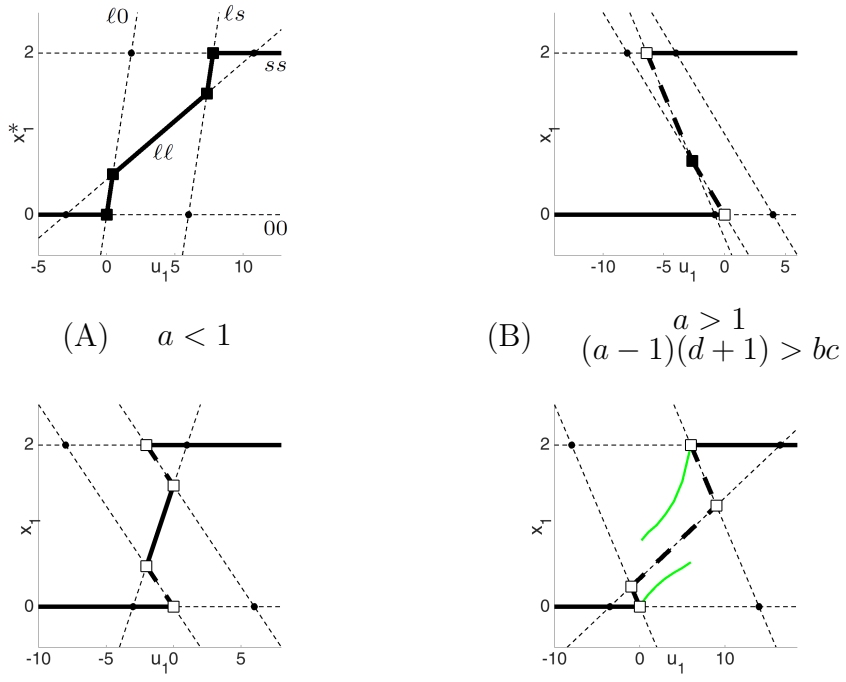

(A) $a < 1$

(B) $a > 1$, $(a-1)(d+1) > bc$

(C) $a > 1$, $(a-1)(d+1) < bc$, $a < d+2$

(D) $a > 1$, $(a-1)(d+1) < bc$, $a > d+2$

Figure 6.2: Different types of bifurcation diagrams as discussed in Theorem 6.2.2. Thin dashed lines show families of virtual equilibria. Thick lines show equilibria: thick solid lines show stable fixed points, while thick dashed lines show unstable fixed points. Black (white) square markers show P-BEB (NSF-BEB), while circles show non-admissible bifurcation candidates. In Case (D) conditions for the existence of a limit cycle (c.f. Theorem 5.3.3 are satisfied and the maximum and minimum values of the limit cycle are shown in green.

6.3 Oscillations in EI Pairs

We now discuss conditions for the presence of oscillations in EI pairs, in the form of a stable limit cycle. Our analysis leads to a refinement of Theorem 5.3.3 whose proof does not rely on the "Lack of Stable Equilibria" condition. We state this result next.

Theorem 6.3.1 (Limit Cycles in EI Pairs)**.** *The system* (6.1) *has a globally stable limit cycle if and only if*

$$d + 2 < a, \tag{6.6a}$$

$$(a-1)(d+1) < bc, \tag{6.6b}$$

$$(a-1)m_1 < bm_2, \tag{6.6c}$$

$$0 < u_1 < bm_2 - (a-1)m_1, \tag{6.6d}$$

$$0 < (d+1)u_1 - bu_2 < [bc - (a-1)(d+1)]m_1. \tag{6.6e}$$

If (6.6) *holds, the system has a unique unstable equilibrium:*

$$\mathbf{x}^* = \frac{1}{bc - (1+d)(a-1)} \begin{bmatrix} (1+d)u_1 - bu_2 \\ cu_1 - (a-1)u_2 \end{bmatrix}. \tag{6.7}$$

Proof. We begin by characterizing the *nullclines* of the system. Consider the x_1 nullcline

set, $X_1^*(\mathbf{u}) = \{\mathbf{x} \in X \mid (f_\sigma(\mathbf{x}, \mathbf{u}))_1 = 0, \text{ if } \mathbf{x} \in \Omega_\sigma\}$. Note that $\mathbf{x} \in X_1^*(\mathbf{u})$ if and only if

$$x_1 = 0, \qquad x_2 \geq \frac{u_1}{b}, \tag{6.8a}$$

$$x_1 \in (0, m_1), \qquad x_2 = \frac{a-1}{b} x_1 + \frac{u_1}{b}, \tag{6.8b}$$

$$x_1 = m_1, \qquad x_2 \leq \frac{a-1}{b} m_1 + \frac{u_1}{b}. \tag{6.8c}$$

Similarly, for the nullcline set $X_2^*(\mathbf{u}) = \{\mathbf{x} \in X \mid (f_\sigma(\mathbf{x}, \mathbf{u}))_2 = 0, \text{ if } \mathbf{x} \in \Omega_\sigma\}$ we have $\mathbf{x} \in X_2^*(\mathbf{u})$ if and only if

$$x_1 \leq -\frac{u_2}{c}, \qquad x_2 = 0, \tag{6.9a}$$

$$x_1 = \frac{d+1}{c} x_2 - \frac{u_2}{c}, \qquad x_2 \in (0, m_2), \tag{6.9b}$$

$$x_1 \geq \frac{d+1}{c} m_2 - \frac{u_2}{c}, \qquad x_2 = m_2. \tag{6.9c}$$

We first show how the conditions in the statement are necessary and sufficient for (6.1) to have a unique fixed point $\mathbf{x}^*$ which, furthermore, is unstable. For $\mathbf{x}^*$ to be the unique equilibrium, the nullclines $X_1^*(\mathbf{u})$ and $X_2^*(\mathbf{u})$ must intersect exactly once. This condition is satisfied when (i) the slope of the nullcline $X_1^*(\mathbf{u})$ in the linear region is less than the ratio m_1/m_2, cf (6.6c); (ii) the slope of the nullcline $X_1^*(\mathbf{u})$ is smaller than that of $X_2^*(\mathbf{u})$ in the same region, cf. (6.6b); (iii) and $0 < \mathbf{x}_1(m_1) < m_2$, cf. (6.6d). Using the equations defining the nullclines, we obtain the coordinates of $\mathbf{x}^*$ in (6.7). Finally, since $\mathbf{x}^*$ needs to belong to the linear region, we have $0 < \mathbf{x}_1^* < m_1$, which reduces to (6.6e). Furthermore, the equilibrium is unstable since the Jacobian at this fixed point is $\mathbf{A} = -\mathbf{I} + \mathbf{W}$ and, by (6.6a)

and (6.6b), $\text{trace}(\mathbf{A})^2 - 4\det(\mathbf{A}) < 0$. Thus, the eigenvalues of $\mathbf{A}$ are conjugate roots with real part $\frac{(-d-1)+(a-1)}{2} > 0$.

Next, let $\mathcal{R} = [0, m_1] \times [0, m_2] \setminus B_\epsilon(\mathbf{x}^*)$ for ϵ small enough so that $B_\epsilon(\mathbf{x}^*) \subset \Omega_{\ell\ell}$. Note that $\mathcal{R}$ is compact by definition, and that $[0, m_1] \times [0, m_2]$ is forward invariant with respect to the dynamics (6.1). Furthermore, since $\mathbf{x}^*$ is the unique fixed point, is in the interior of the region $\Omega_{\ell\ell}$, and both eigenvalues of the Jacobian have a positive real component, we deduce that $\mathcal{R}$ is forward invariant. By the Poincaré-Bendixon Theorem [Sma00, Chapter 7.3], since $\mathcal{R}$ is compact, forward invariant, and contains no fixed points, the system has a stable limit cycle in $\mathcal{R}$, concluding the proof. □

6.4 Reproducing Epileptic Patterns

Here, we show how EI pairs can be used to model epileptic seizures. To obtain EEG-like waveforms from the linear threshold model, we simulate the dynamics in (6.1) by adding noise $\mathbf{w}$ in the linear threshold function:

$$\dot{\mathbf{x}} = -\mathbf{x} + [\mathbf{W}\mathbf{x} + \mathbf{u} + \mathbf{w}]_{\mathbf{0}}^{\mathbf{m}}.$$

The noise $\mathbf{w}$ is obtained by filtering Gaussian white-noise, with variance 1.4, through a filter with 1Hz cut-off frequency.

Although EEG measurements of the epileptic brain can exhibit a variety of behaviors, the EEG response can typically be constructed from a small number of prototypical waveforms [NdS05]. The transition from healthy activity to a seizure is marked by a sudden

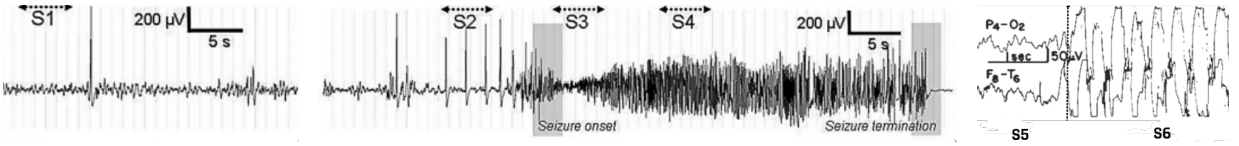

(a) Healthy background activity [Cha96]. (b) Seizure onset and termination [Cha96]. (c) Slow wave [NdS05].

Figure 6.3: EEG recordings showing prototypical epileptic waveforms.

dramatic change in the qualitative nature of the EEG signal. A seizure may contain several further changes before normal neurological activity is restored [Cha96]. For example, the EEG recording of the seizure in Fig. 6.3 can be divided into four segments based on the qualitative nature of the waveform, labeled S1, S2, S3, and S4. The healthy background activity, S1, is characterized by small fluctuations about a steady state. The presence of spikes in S2 indicates the onset of a seizure, with irregular low-frequency oscillations in S3, and quasi-sinusoidal oscillations in S4.

In [TWCF11], the authors introduce a "dictionary" relating prototypical waveforms to attractors of a nonlinear dynamical system. Here, we introduce a similar dictionary to associate prototypical waveforms to features in the phase-plane of the linear threshold model. This dictionary, along with the bifurcation analysis in Section 6.2, can be used to systematically determine conditions on the connectivity matrix W so that the desired waveform can be replicated and the desired transitions can be obtained by varying the input to the excitatory and inhibitory populations.

In Table 6.1, we relate the characteristic waveforms to features in the phase plane, and in Table 6.2 we use the bifurcation analysis from Section 6.2 to show which transitions between these waveforms each system is capable of exhibiting. These two tables can be used

Table 6.1: EEG activity and features in the phase-space [TWCF11].

Waveform Description	Dynamical Behavior	Clinical Setting
Normal background	Stable Fixed Point	Preictal activity
High-frequency Osc	Stable Limit Cycle	Interictal activity
Low-frequency Osc	Multistability	Interictal activity
Spikes	Multistability of $(0,0)$ and another fixed point	Seizure onset

Table 6.2: Relationship between all bifurcations each system exhibits and transition in type of EEG activity as outlined in Table 6.1.

System	Bifurcations	Seizure behavior
A	P-BEB	No change
	P-BEB	
	P-BEB	
	P-BEB	
B	NSF	Normal $\rightarrow$ Spikes
	P-BEB	No change
	NSF	Spikes $\rightarrow$ Normal
C	NSF	Normal $\rightarrow$ Spikes
	NSF	Spikes $\rightarrow$ Normal
D	NSF	Normal $\rightarrow$ Spikes
	Hopf	Spikes $\rightarrow$ High frequency Oscillations
	Hopf	High Frequency Oscillations $\rightarrow$ Slow waves
	NSF	Slow waves $\rightarrow$ Normal

to explain epileptic patterns through the dynamical properties of linear-threshold pairs, to characterize possible seizures each pair can create, and to synthesize a system that can recreate an EEG pattern associated with a seizure event.

As we show next, with the correct values of parameters, the linear threshold model can have solutions sharing qualitative characteristics with EEG waveforms during epileptic seizures.

In Figure 6.4a we replicate the seizure in Figure 6.3b having the characteristic waveforms S1-S4. Figure 6.4b shows the input $u_1 + w_1$ as a function of time. To replicate the normal background activity in S1, we initialize system (D) choosing u_1 so that $(0,0)$ is the unique (stable) fixed point. The system then fluctuates around the equilibrium and there will be minimal activity in both the excitatory and inhibitory populations with sporadic firings caused by the system noise.

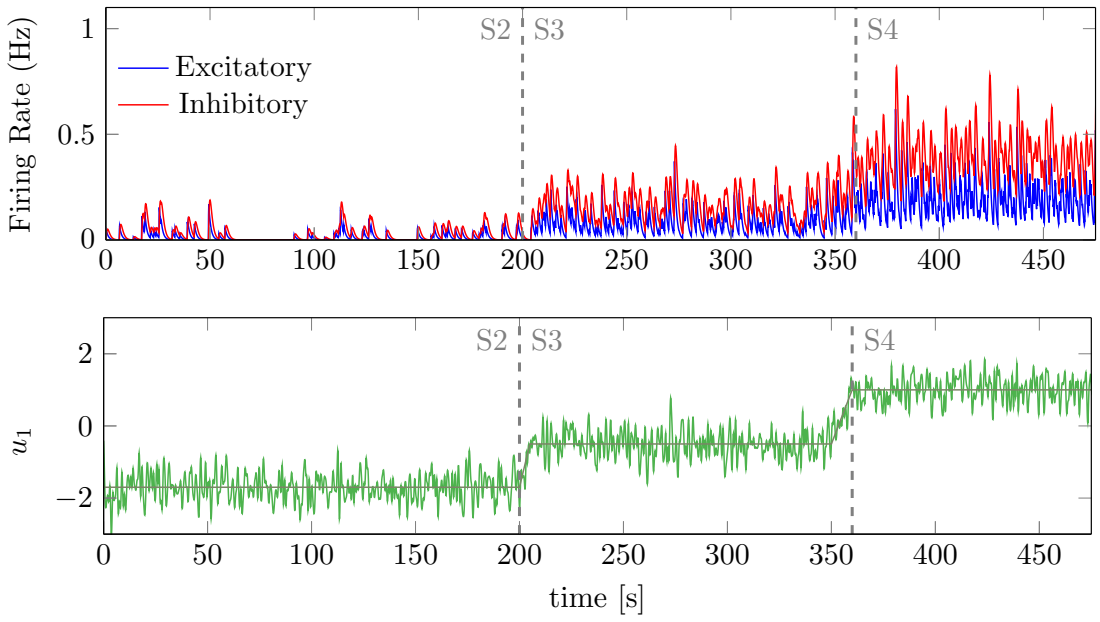

Figure 6.4: Recreating epileptic dynamics using the LTN in Case D. (Top) Simulation of EEG recording. (Bottom) Input $u_1 + w_1$ as a function of time.

To obtain spikes in S2, we increase u_1 so that it is near the first NSF-BEB bifurcation. If $w_1 + u_1 < 0$,then $\mathbf{x}_{00}$ is a stable fixed point. However, when $u_1 + w_1 > 0$, the system has a unique limit cycle and $\mathbf{x}_{00}$ is unstable. In this case, the state $\mathbf{x}$ will initially oscillate until the noise restores the stability of $\mathbf{x}_{00}$, at which point the state will be attracted toward the origin. As u_1 is increased, the stable limit cycle persists even with noise. The state oscillates about $\mathbf{x}_{\ell\ell}$ with small amplitude as in S3. Increasing u_1 further increases both components of $\mathbf{x}_{\ell\ell}$ (c.f. (6.3d)) as well as the amplitude of the oscillations, resulting in behavior similar to S4. We notice that, instead of increasing u_1, a similar behavior can be achieved by decreasing u_2 since it has a negative contribution on the value of $\mathbf{x}^*_{\ell\ell}$ in (6.3d). This is to be expected, since u_2 is the input to the inhibitory population. In fact, a higher input to a population translates in a higher firing rate for the population itself. This, in return, increases oscillations when increasing the input to an excitatory population, or decreases oscillations in the case of an

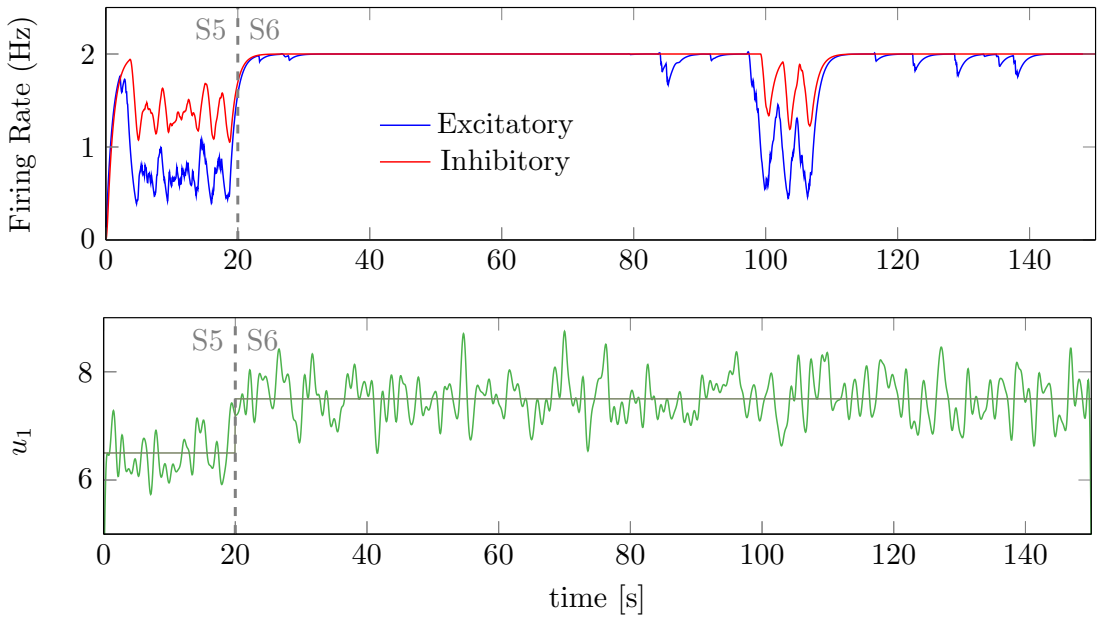

Figure 6.5: Recreating slow waves using Case D. Simulation of EEG recording (top) and input $u_1 + w_1$ as a function of time.

inhibitory population.

An additional behavior typical of epileptic seizures is a slow wave, consisting of a low-frequency high amplitude oscillation with intermittent spikes. Figure 6.3c shows an EEG recording of a seizure initially with high frequency oscillations in S5, then with slow waves with intermittent spikes in S6. To recreate slow waves in the linear threshold model, we initialize system (D) with u_1 near the second NSF-BEB bifurcation. When $w_1 > 0$, $\mathbf{x}_{ss}$ is a stable fixed point and system fluctuates around (m_1, m_2). When $w_1 < 0$, $\mathbf{x}_{ss}$ is unstable and the system has a limit cycle, resulting in a high frequency spiking which is halted once the stability of $\mathbf{x}_{ss}$ is restored. A simulation showing this behavior is in Fig. 6.5a, with the corresponding input in Figure 6.5b.

6.5 Conclusions

We have shown how LTNs can be used to model a variety of prototypical brain waves measured in both healthy and epileptic brains. Focusing on a two-dimensional network, we provide an exhaustive analysis of the equilibria and bifurcations occurring as a function of the input to the system. We also provide a map and numerical evidence to associate these bifurcations to patterns of EEG signals observed before, during, and after seizure events. Directions of future research include a formal analysis of the results suggested in Section 6.4 to relate the behavior of this model with real life EEG data, the study of higher-dimensional linear threshold models, and the design of control algorithms to detect and regulate seizure behaviors.

Acknowledgements

This chapter, in full, is a reprint of the material [CAPC21] where it appears as "Linear-Threshold Dynamics for the Study of Epileptic Events" by Federico Celi, Ahmed Allibhoy, Fabio Pasqualetti, and Jorge Cortés in IEEE Control Systems Letters. The dissertation author is one of the primary investigators and authors of this paper.

Chapter 7

Optimal Network Interventions to Control Localization of Oscillations

Oscillations are a prominent feature of neuronal activity and are associated with a variety of phenomena in brain tissue, both healthy and unhealthy. Characterizing how oscillations spread through regions of the brain is of particular interest when studying countermeasures to pathological brain synchronizations. A recent study [SBB+10] revealed the existence of pathological activity in brains of clinically asymptomatic subjects. In other words, epileptic-like oscillations are observed in the brains of both healthy and non-healthy patients, however only in the latter class do localized oscillations spread throughout different regions of the brain into a symptomatic epileptic event. It is hypothesized in [Spe02, SBB+10] that healthy and non-healthy brains differ with respect to their structural robustness to the spreading of localized oscillations. Modification of the network structure to increase structural robustness is a potential avenue for treatment of neuro-

logical disorders. This modification can be done via electrical stimulation, as is the case with deep brain stimulation[KLA+21, QBP22a], or surgical resection, where connections between certain brain regions are severed in order to prevent the spread of harmful oscillations [RL01]. This motivates the importance of characterizing the spatiotemporal dynamics of oscillations onset and propagation in the context of pathological activity in the brain [KTG+10, SBB+10, TDH+11], as well as developing design principles for modifying the network structure optimally.

The main contribution of this chapter is to characterize conditions for the spreading of oscillations in brain networks and to formulate and solve optimization problems for the design of networks that are robust to oscillation spreading. In particular, we model the excitatory and inhibitory activity of a small brain tissue (micro-domain) using EI pairs, whose structural properties were characterized in Chapter 6. We begin by stating conditions on the inputs of EI pairs which determine whether that pair is inactive or has an oscillation. We then build networks of EI pairs in order to model the complex interactions among domains of the human brain. Our goal is to exploit the known properties of the single EI pairs to infer global properties of the brain network. Once formal conditions on the spreading of oscillations are derived, we develop and solve a series of optimization problems through which we can efficiently compute conditions to isolate localized oscillations from the rest of the network. We show how these optimization problems are computationally efficient and practically effective. We conclude the discussion with extensive numerical simulations on synthetically generated networks. We tie the discussion of oscillations in the brain to the the study of epilepsy; however our results can be also applied to other oscillation-related

problems in network control.

7.1 Input Conditions on EI Pairs

Consider a single EI Pair whose dynamics whose dynamics are given by

$$\dot{x}^E = -x^E + [ax^E - bx_i^I + u^E]_0^{m^E} \tag{7.1a}$$

$$\dot{x}^I = -x^I + [cx^E - dx_i^I + u^I]_0^{m^I} \tag{7.1b}$$

In Chapter 7, we characterized the fixed points and attractors in (7.1) for all possible parameter values. Here we pay attention to the following dynamical features of EI pairs: the origin being a stable fixed point (corresponding to healthy neurological behavior) and stable limit cycles (corresponding to a pathological oscillation characteristic of an epileptic seizure). The following result is a consequence of Theorem 6.2.2, and gives conditions on time-varying inputs $\mathbf{u}(t)$ resulting in trajectories converging to the origin.

Lemma 7.1.1 (Convergence to origin in EI pairs)**.** *Consider the EI pair* (7.1)*. If the input satisfies* $\mathbf{u}(t) = (u_E(t), u_I(t)) \leq 0$ *for all* $t \geq 0$*, then every trajectory converges to the origin.*

We next give conditions on time-varying inputs to (7.1) such that the corresponding

solution is oscillatory. We define the set

$$\begin{aligned}\mathcal{U} = \{(u_E, u_I) \in \mathbb{R}^2 \mid\ & u_E \geq 0, \\ & u_E \leq -(a-1)m_E + bm_I, \\ & (d+1)u_E - bu_I \geq 0, \\ & (d+1)u_E - bu_I \leq \Delta m_E\}\end{aligned} \tag{7.2}$$

where $\Delta = (bc - (a-1)(d+1))$. The next result follows as a straightforward consequence of Theorem 6.3.1.

Lemma 7.1.2 (Sufficient conditions on inputs giving rise to oscillations)**.** *Consider the EI pair* (7.1)*. Then,*

(i) $\mathcal{U}$ *is nonempty if and only if*

$$bm_I \geq (a-1)m_E, \tag{7.3a}$$

$$bc - (a-1)(d+1) \geq 0. \tag{7.3b}$$

(ii) Suppose (7.3) *holds and* $d + 1 < a - 1$*. If* $\mathbf{u}(t) \in \mathcal{U}$ *for all* $t \geq 0$*, then all solutions of* (7.1)*, except for those corresponding to equilibria, are oscillatory.*

7.2 Interconnections of EI Pairs

We consider complex networks resulting from the interconnection of EI pairs. Consider a network of N nodes, where each node corresponds to a single EI pair. For

$i \in \{1, 2, \ldots, N\}$, the parameters of the ith EI pair in the network are

$$\mathbf{W}_i = \begin{bmatrix} a_i & -b_i \\ c_i & -d_i \end{bmatrix}, \quad \mathbf{m}_i = \begin{bmatrix} m_i^E \\ m_i^I \end{bmatrix}, \quad \mathbf{u}_i = \begin{bmatrix} u_i^E \\ u_i^I \end{bmatrix}. \tag{7.4}$$

We interconnect the individual EI pairs to form a coupled network, with a $2N$-dimensional state space

$$X = \{(x_1^E, x_1^I, \ldots, x_N^E, x_N^I) \mid x_i^E \in [0, m_i^E], x_i^I \in [0, m_i^I]\}.$$

The dynamics of the network are given by (5.2), where

$$\begin{aligned} \mathbf{W} &= \operatorname{diag}(\mathbf{W}_1, \ldots, \mathbf{W}_M) && \text{(7.5a)} \\ &\quad + \mathbf{A}^{EE} \otimes \begin{bmatrix} 1 & 0 \\ 0 & 0 \end{bmatrix} + \mathbf{A}^{EI} \otimes \begin{bmatrix} 0 & -1 \\ 0 & 0 \end{bmatrix} \\ &\quad + \mathbf{A}^{IE} \otimes \begin{bmatrix} 0 & 0 \\ 1 & 0 \end{bmatrix} + \mathbf{A}^{II} \otimes \begin{bmatrix} 0 & 0 \\ 0 & -1 \end{bmatrix}, \\ \mathbf{m} &= \begin{bmatrix} \mathbf{m}_1^\top & \ldots & \mathbf{m}_M \end{bmatrix}^\top, && \text{(7.5b)} \\ \mathbf{u} &= \begin{bmatrix} \mathbf{u}_1^\top & \ldots & \mathbf{u}_M \end{bmatrix}^\top. && \text{(7.5c)} \end{aligned}$$

Here, $\mathbf{A}^{EE} \in \mathbb{R}_{\geq 0}^{N \times N}$ is a weighted adjacency matrix which characterizes the connections between the excitatory nodes of each pair in the network, $\mathbf{A}^{II} \in \mathbb{R}_{\geq 0}^{N \times N}$ models connections between the inhibitory nodes of each pair, and connections from excitatory to inhibitory nodes and from inhibitory to excitatory nodes are given by $\mathbf{A}^{EI} \in \mathbb{R}_{\geq 0}^{N}$ and $\mathbf{A}^{IE} \in \mathbb{R}_{\geq 0}^{N \times N}$, respectively. Figure 7.1 illustrates a network built by coupling EI pairs in this manner.

We seek to characterize the oscillations in the network using knowledge of the parameters of the individual pairs, as well as the interconnections $\mathbf{A}^{EE}, \mathbf{A}^{EI}, \mathbf{A}^{IE}, \mathbf{A}^{II}$. We

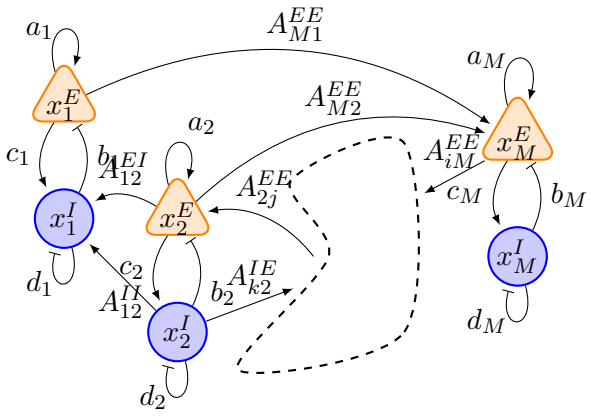

Figure 7.1: Illustration of the graph associated to a network of coupled EI pairs.

say that the ith node in the coupled network is *oscillatory* if for all solutions $\mathbf{x}(t)$ of the interconnected system, $\mathbf{x}_i(t)$ does not converge to a constant as $t \to \infty$. We say that the ith node is *inactive* if for all solutions, $\mathbf{x}_i(t) \to 0$ as $t \to \infty$. While other behaviors are of course possible, such as converging to a nonzero constant, our focus on these particular ones is driven by their relevance for neurological applications.

Determining whether a particular node in the network is oscillatory or inactive is, in general, nontrivial because of the complex effect of the interconnection on the dynamics of individual nodes. In particular, note that, if the parameters of the ith node satisfy the conditions in Lemma 7.1.1, then the ith node is not necessarily inactive in the coupled network. Likewise if the parameters of the ith node satisfy the conditions of Lemma 7.1.2, this does not necessarily mean that the ith node is necessarily oscillatory in the coupled network. We illustrate these observations in the following example. Although both cases are interesting in their own right, our focus in this chapter is on characterizing the robustness of the dynamical properties of the nodes, rather than the emergence of new features through network interconnection.

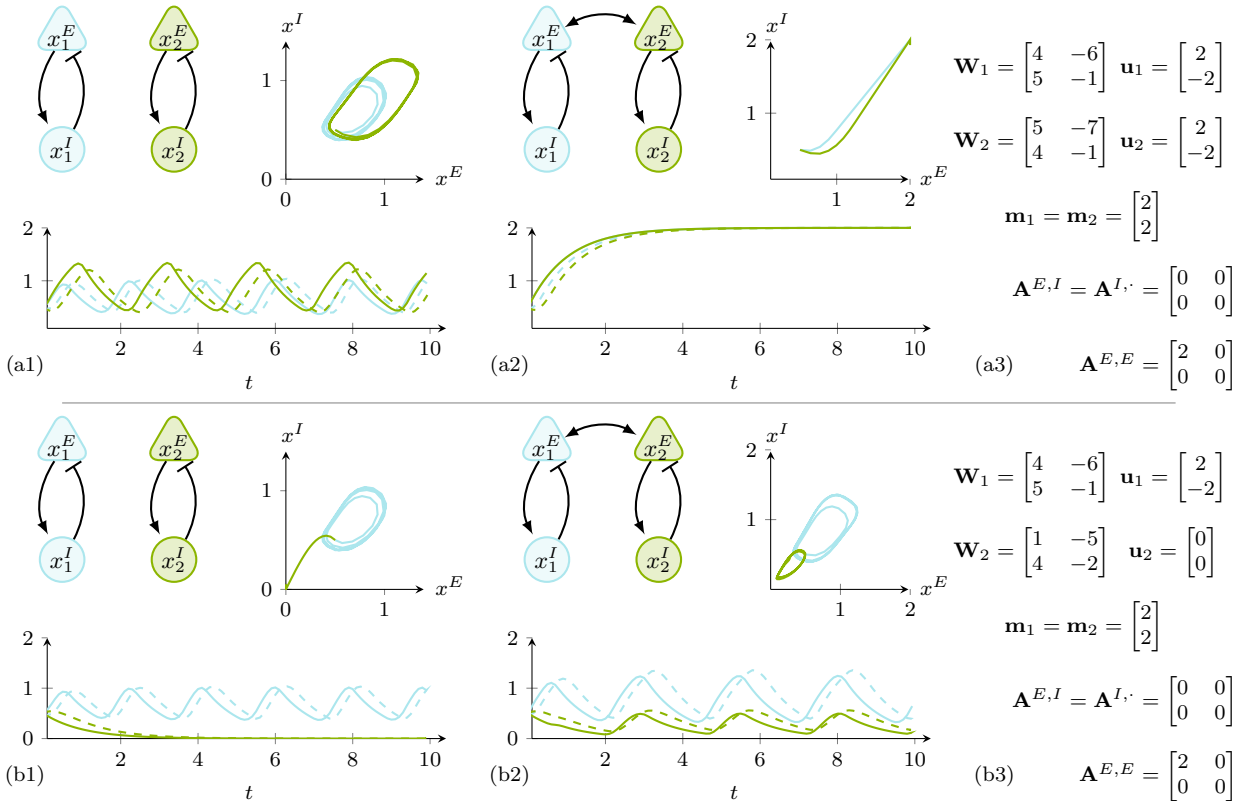

Figure 7.2: Illustration of how the dynamical properties of isolated EI pairs might significantly change when coupled with other EI pairs, as discussed in Example 7.2.1. (a) Two oscillatory EI pairs, cf. (a1), are interconnected so that, when coupled, cf. (a2), both EI pairs saturate. (b) An oscillatory EI pair and an inactive EI pair, cf. (b1), are interconnected in such a way that, in the resulting network, cf. (b2), both EI pair exhibit an oscillatory trajectory.

Example 7.2.1 (Properties of EI pairs not preserved after interconnection)**.** Consider the numerical examples in Fig 7.2. In panel (a), we study a simple network made up of two EI pairs (specific network parameters are reported in (a3)). When taken separately, each EI pair is oscillatory, cf. (a1). In panel (a2), the two EI pairs are interconnected through a simple excitatory-to-excitatory interconnection. As a result of this reciprocal excitation, the two nodes in the interconnected network become saturated.

In panel (b), we consider a network of two EI pairs (specific network parameters are

reported in (b3)), where the first node has a globally asymptotically stable limit cycle and the second node has a globally asymptotically stable fixed point at the origin, cf. (b1). After interconnecting the two EI pairs in panel (b2), the second pair becomes oscillatory as a consequence of the incoming activity from the other EI pair. □

Given these observations, this chapter has two goals. The first goal is to characterize conditions under which properties of individual pairs in the network, such as being oscillatory or inactive, are preserved when the pairs are interconnected with one another. The second goal is to develop an approach to modify the network parameters so that given sets of desired nodes are either inactive or oscillatory. We formalize both of these problems next.

Problem 7.2.2. *What are the conditions on the node parameters* $\mathbf{W}_i$, $\mathbf{u}_i$, *and* $\mathbf{m}_i$, $i \in \{1, \ldots, N\}$, *and the interconnection parameters* $\mathbf{A}^{EE}$, $\mathbf{A}^{EI}$, $\mathbf{A}^{IE}$, *and* $\mathbf{A}^{II}$ *that determine when the dynamical properties of the* i*th node are preserved after interconnection?*

Problem 7.2.3. *Consider a network whose interconnection is described by* $\hat{\mathbf{A}}^{EE}$, $\hat{\mathbf{A}}^{EI}$, $\hat{\mathbf{A}}^{IE}$, *and* $\hat{\mathbf{A}}^{II}$ *and let* $I_{oscillatory}, I_{inactive} \subset \{1, \ldots, N\}$ *be disjoint sets of nodes. How should the interconnection structure be modified so that in the resulting network every node in* $I_{oscillatory}$ *is oscillatory and every node in* $I_{inactive}$ *is inactive?*

Both problem formulations touch upon the spatio-temporal spreading (or lack of thereof) of oscillations in networks and are of general interest. Here, we are particularly motivated by the spreading of microseizures (localized pathological activity in the brain) to clinical seizures (diffused pathological activity in the brain). In this framework, one can interpret Problem 7.2.2 as studying whether a given brain network is prone to the insurgence

of a clinical seizure as a consequence of a microseizure. Consequently, Problem 7.2.3 can be viewed as the study on how interventions on the brain might target specific areas of interest.

7.3 Sufficient Conditions for Preservation of Dynamical Properties of Subsystems

We begin by introducing notation that will be useful for the proofs of the main technical results. The dynamics of the ith node in the coupled network are

$$\dot{x}_i^E(t) = -x_i^E(t) + \left[a_i x_i^E(t) - b_i x_i^I(t) + \tilde{u}_i^E(t)\right]_0^{m_i^E}, \tag{7.6a}$$

$$\dot{x}_i^I(t) = -x_i^I(t) + \left[c_i x_i^E(t) - d_i x_i^I(t) + \tilde{u}_i^I(t)\right]_0^{m_i^I}, \tag{7.6b}$$

where $(\tilde{u}_i^E(t), \tilde{u}_i^I(t))$ incorporates the combined input to the ith node from its neighbors:

$$\tilde{u}_i^E(\mathbf{x}) = u_i^E + \sum_{j=1}^{N} A_{ij}^{EE} x_j^E - \sum_{j=1}^{N} A_{ij}^{EI} x_j^I \tag{7.7a}$$

$$\tilde{u}_i^I(\mathbf{x}) = u_i^I + \sum_{j=1}^{N} A_{ij}^{IE} x_j^E - \sum_{j=1}^{N} A_{ij}^{II} x_j^I \tag{7.7b}$$

We first present sufficient conditions for the ith node in the network to be inactive. As a consequence of Lemma 7.1.1, the ith node taken individually is inactive when $(u_i^E, u_i^I) \leq 0$. The following result gives conditions which ensure that $(\tilde{u}_i^E(\mathbf{x}), \tilde{u}_i^I(\mathbf{x})) \leq 0$ for all $\mathbf{x} \in X$, so the inactivity of the ith node is robust with respect to all inputs the node receives from neighboring nodes.

Theorem 7.3.1 (Sufficient conditions for robust inactivity)**.** *Assume that for* $i \in \{1, \ldots, N\}$*,*

$$u_i^E + \sum_{j=1}^{N} A_{ij}^{EE} m_j^E \leq 0, \tag{7.8a}$$

$$u_i^I + \sum_{j=1}^{N} A_{ij}^{IE} m_j^E \leq 0. \tag{7.8b}$$

Then, the i*th node in the coupled system* (7.5) *is inactive.*

Proof. Let $\mathbf{x}(t)$ be a solution to the coupled system (7.7). Note that by (7.8),

$$\tilde{u}_i^E(\mathbf{x}(t)) \leq u_i^E + \sum_{j=1}^{N} A_{ij}^{EE} m_j^E \leq 0,$$

$$\tilde{u}_i^I(\mathbf{x}(t)) \leq u_i^I + \sum_{j=1}^{N} A_{ij}^{IE} m_j^I \leq 0.$$

Since the input to the ith EI pair is $\tilde{\mathbf{u}}_i(t) = (\tilde{u}_i^E(\mathbf{x}(t)), \tilde{u}_i^I(\mathbf{x}(t)))$, the result follows by Lemma 7.1.1. □

Note that the condition in (7.8) holds only if $(u_i^E, u_i^I) \leq 0$. In fact it is not possible for the ith node to be inactive with respect to the interconnected network, unless the ith node individually is inactive.

We now move on to discussing sufficient conditions for the ith node in the network to be oscillatory after interconnection. Our technical approach relies on the following result which formalizes the following observation: the ith node taken individually is oscillatory when $(u_i^E, u_i^I) \in \mathcal{U}_i$, where $\mathcal{U}_i$ is the set (7.2) for the parameters corresponding to the ith EI pair, so the oscillation of the ith node persists after interconnection if $(\tilde{u}_i^E(\mathbf{x}), \tilde{u}_i^I(\mathbf{x})) \in \mathcal{U}_i$

for all $\mathbf{x} \in X$.

Lemma 7.3.2 (Robustness of oscillations in coupled networks)**.** *For $i \in \{1, \dots, N\}$, assume*

$$\begin{bmatrix} \tilde{u}_i^E(\mathbf{x}) \\ \tilde{u}_i^I(\mathbf{x}) \end{bmatrix} \in \mathcal{U}_i, \text{ for all } \mathbf{x} \in X. \tag{7.9}$$

Then, the ith node in the coupled system (7.5) *is oscillatory.*

Proof. Let $\mathbf{x}(t)$ be a solution to (7.7). Then by (7.9), $\tilde{\mathbf{u}}_i(\mathbf{x}(t)) \in \mathcal{U}_i$ for all $t \geq 0$. Since $\tilde{\mathbf{u}}_i(\mathbf{x}(t))$ is the input to the ith node, the result follows by Lemma 7.1.2. □

Note that the condition (7.9) holds only if $(u_i^E, u_i^I) \in \mathcal{U}_i$, meaning that Lemma 7.3.2 characterizes only the case where a pair that is oscillatory when viewed individually remains oscillatory after being interconnected in a network. However, as shown in Example 7.2.1, it is possible for nodes $(u_i^E, u_i^I) \notin \mathcal{U}_i$ to become oscillatory after interconnection, though we do not consider such cases here.

In general, the condition in Lemma 7.3.2 is not easy to check computationally. However, as we show next, in the special case where there are no interconnections from the inhibitory neurons in each subsystem (i.e., $\mathbf{A}^{IE} = \mathbf{A}^{II} = 0$) the condition (7.9) can be expressed in terms of affine constraints on the adjacency matrices.

Corollary 7.3.3 (Affine conditions for robust oscillations without inhibitory coupling)**.** *Consider a network interconnection* (7.5) *with $\mathbf{A}^{IE} = \mathbf{A}^{II} = 0$. For $i \in \{1, \dots, N\}$, condition*

(7.9) *holds if and only if*

$$u_i^E - \sum_{j=1}^{N} A^{EI} m_j^I \geq \max\left\{0, \frac{b_i u_i^I}{d_i + 1}\right\}, \tag{7.10a}$$

$$u_i^E + \sum_{j=1}^{N} A^{EE} m_j^E \leq \min\left\{b_i m_i^I - (a_i - 1) m_i^E, \frac{\Delta_i m_i^E + b_i u_i^I}{d_i + 1}\right\}, \tag{7.10b}$$

where $\Delta_i = b_i c_i - (a_i - 1)(d_i + 1)$. *In such case, the* i*th node in the coupled system* (7.5) *is oscillatory.*

Proof. Note that

$$\begin{aligned}
\sup_{\mathbf{x} \in X}\left\{u_i^E + \sum_{j=1}^{N} A_{ij}^{EE} x_j^E - \sum_{j=1}^{N} A_{ij}^{EI} x_j^I\right\} &= u_i^E + \sum_{j=1}^{N} A_{ij}^{EE} m_j^E \\
\inf_{\mathbf{x} \in X}\left\{u_i^E + \sum_{j=1}^{N} A_{ij}^{EE} x_j^E - \sum_{j=1}^{N} A_{ij}^{EI} x_j^I\right\} &= u_i^E - \sum_{j=1}^{N} A_{ij}^{EI} m_j^I,
\end{aligned}$$

so by examining the constraints parameterizing $\mathcal{U}_i$, we see that condition (7.9) holds if and only if

$$\begin{aligned}
u_i^E - \sum_{j=1}^{N} A_{ij}^{EI} m_j^I &\geq 0, \\
(d+1)\left[u_i^E - \sum_{j=1}^{N} A_{ij}^{EI} m_j^I\right] - b u_i^I &\geq 0
\end{aligned}$$

and

$$\begin{aligned}
u_i^E + \sum_{j=1}^{N} A_{ij}^{EE} m_j^E &\leq -(a_i - 1) m_i^E + b_i m_i^I, \\
(d+1)\left[u_i^E + \sum_{j=1}^{N} A_{ij}^{EE} m_j^E\right] - b u_i^I &\leq \Delta_i m_i^E.
\end{aligned}$$

We obtain (7.10) by rearranging the above equations. □

As the following result shows, in the presence of inhibitory coupling, it is still possible

to derive checkable conditions in the form of affine constraints on the entries of the adjacency matrices given by (7.11). The conditions are valid for all interconnection structures, and are only sufficient for condition (7.9) to hold. However, in the special case where $A^{IE} = A^{II} = 0$, the equations (7.11) reduce to (7.10) and are both sufficient and necessary for (7.9) to hold.

Theorem 7.3.4 (Affine conditions for robust oscillations with inhibitory coupling)**.** *Let* $i \in \{1, \ldots, N\}$*, and suppose that*

$$u_i^E - \sum_{j=1}^{N} A_{ij}^{EI} m_j^I \geq 0, \tag{7.11a}$$

$$u_i^E + \sum_{j=1}^{N} A_{ij}^{EE} m_j^E \leq b m_i^I - (a-1) m_i^E, \tag{7.11b}$$

$$(d+1)\left[u_i^E - \sum_{j=1}^{N} A_{ij}^{EI} m_j^I\right] - b\left[u_i^I + \sum_{j=1}^{N} A_{ij}^{IE} m_j^E\right] \geq 0, \tag{7.11c}$$

$$(d+1)\left[u_i^E + \sum_{j=1}^{N} A_{ij}^{EE} m_j^E\right] - b\left[u_i^I - \sum_{j=1}^{N} A_{ij}^{II} m_j^I\right] \leq \Delta_i m_i^I, \tag{7.11d}$$

where $\Delta_i = b_i c_i - (a_i - 1)(d_i + 1)$*. Then, condition* (7.9) *holds and the* i*th node in the coupled system is oscillatory.*

Proof. Begin by observing that,

$$\begin{aligned}
&\inf_{\mathbf{x} \in X} \left\{ (d+1)\left[u_i^E + \sum_{j=1}^{N} A^{EE} x_j^E - \sum_{j=1}^{N} A_{ij}^{EI} x_j^I\right] - b\left[u_i^I + \sum_{j=1}^{N} A_{ij}^{IE} x_j^E - \sum_{j=1}^{N} A^{II} x_j^I\right] \right\} \\
&\geq \inf_{\mathbf{x}, \mathbf{y} \in X} \left\{ (d+1)\left[u_i^E + \sum_{j=1}^{N} A^{EE} x_j^E - \sum_{j=1}^{N} A_{ij}^{EI} y_j^I\right] - b\left[u_i^I + \sum_{j=1}^{N} A_{ij}^{IE} y_j^E - \sum_{j=1}^{N} A^{II} x_j^I\right] \right\} \\
&= (d+1)\left[u_i^E - \sum_{j=1}^{N} A_{ij}^{EI} m_j^I\right] - b\left[u_i^I + \sum_{j=1}^{N} A_{ij}^{IE} m_j^E\right].
\end{aligned}$$

and similarly that,

$$\begin{aligned}
&\sup_{\mathbf{x}\in X}\left\{(d+1)\left[u_i^E+\sum_{j=1}^N A^{EE}x_j^E-\sum_{j=1}^N A_{ij}^{EI}x_j^I\right]-b\left[u_i^I+\sum_{j=1}^N A_{ij}^{IE}x_j^E-\sum_{j=1}^N A^{II}x_j^I\right]\right\}\\
&\leq \sup_{\mathbf{x},\mathbf{y}\in X}\left\{(d+1)\left[u_i^E+\sum_{j=1}^N A^{EE}x_j^E-\sum_{j=1}^N A_{ij}^{EI}y_j^I\right]-b\left[u_i^I+\sum_{j=1}^N A_{ij}^{IE}y_j^E-\sum_{j=1}^N A^{II}x_j^I\right]\right\}\\
&=(d+1)\left[u_i^E+\sum_{j=1}^N A_{ij}^{EE}m_j^E\right]-b\left[u_i^I-\sum_{j=1}^N A_{ij}^{II}m_j^I\right].
\end{aligned}$$

It follows immediately that if (7.11) holds, then (7.9) holds as well. □

Remark 7.3.5 (Comparison with the literature)**.** The results presented here differ from the characterization in [NC19, NPC22, NC21a] of oscillations in linear threshold networks in two ways: first, previous results use the lack of stable equilibria as a proxy for the existence of oscillations, whereas we take a slightly different approach by showing when conditions for the existence of oscillations in the ith node are robust with respect to all inputs from neighboring nodes. Second, previous results simply ensure the existence of oscillations, while the results here allow us to determine whether a given node participates in the oscillation, or remains inactive. □

7.4 Network Design Using Sufficient Conditions

In this section we apply the results of Section 7.3 to address Problem 7.2.3, and determine how to modify the structure of a given network to control the spread of oscillations. The approach we take is to determine the network interconnection structure as the solution to an optimization problem, where the constraints of the optimization problem correspond to the

conditions in Theorems 7.3.1 and 7.3.4. We begin by presenting the proposed optimization problems, and then complement them with numerical examples.

7.4.1 Network Optimization Problems

Let $I_{\text{oscillatory}}$ and $I_{\text{inactive}} \subset \{1, \ldots, N\}$ be disjoint sets, where $I_{\text{oscillatory}}$ denotes the indices of the nodes in the network we desire to be oscillatory and I_{inactive} denotes the indices of the nodes in the network we desire to be inactive. Assume we are given a nominal network of coupled EI pairs whose interconnection is determined by $\hat{\mathbf{A}} = (\hat{\mathbf{A}}^{EE}, \hat{\mathbf{A}}^{EI}, \hat{\mathbf{A}}^{IE}, \hat{\mathbf{A}}^{II})$. The problem we address here is to modify the network parameters, so that the modified network given by $\mathbf{A} = (\mathbf{A}^{EE}, \mathbf{A}^{EI}, \mathbf{A}^{IE}, \mathbf{A}^{II})$ has oscillating and inactive nodes as determined by $I_{\text{oscillatory}}$ and I_{inactive}, respectively.

We consider two scenarios. In the first, the weights of each of the interconnection matrices can be varied continuously, as is the case with deep brain stimulation, where the magnitude of the change to the network increases with electrical stimulation. In the second scenario, we no longer have fine-grained control over the weights of each of the interconnection matrices, and the network structure can only be modified by removing edges entirely. This scenario corresponds to surgical resection, where connections between brain regions are severed to control the spread of oscillations.

A Continuous Modification of Network Weights

To find the modified network in the first scenario, we introduce the following optimization problem.

$$\begin{aligned}
&\underset{\substack{\mathbf{A}^{EE},\,\mathbf{A}^{EI}\\ \mathbf{A}^{IE},\,\mathbf{A}^{II}}}{\text{minimize}} && \sum_{k\in\{EE,EI,IE,II\}} \frac{1}{2}\left\|\mathbf{A}^k - \hat{\mathbf{A}}^k\right\|^2 \\
&\text{subject to} && \\
&\quad \mathbf{A}^{EE},\mathbf{A}^{EI},\mathbf{A}^{IE},\mathbf{A}^{II} \text{satisfy (7.8) } \forall i \in I_{\text{inactive}} && \\
&\quad \mathbf{A}^{EE},\mathbf{A}^{EI},\mathbf{A}^{IE},\mathbf{A}^{II} \text{satisfy (7.11) } \forall i \in I_{\text{oscillatory}}. &&
\end{aligned} \tag{7.12}$$

The interpretation of the optimization problem (7.12) is that it finds the minimal modification to the parameters of the nominal network that ensure they satisfy the sufficient conditions derived in Section 7.3. Because these conditions are affine with respect to $\mathbf{A}^{EE}$, $\mathbf{A}^{EI}$, $\mathbf{A}^{IE}$, and $\mathbf{A}^{II}$, (7.12) is a quadratic program and can be solved efficiently using standard convex optimization solvers. The solution, $\mathbf{A} = (\mathbf{A}^{EE},\ \mathbf{A}^{EI},\ \mathbf{A}^{IE},\ \mathbf{A}^{II})$, gives the network with the desired properties.

B Modification of Network by Removing Edges

We now consider the second scenario, where the network can only be modified by removing edges. To solve this problem, we introduce the following optimization problem:

$$\begin{aligned}
&\underset{\substack{\mathbf{S}^{EE},\mathbf{S}^{EI}\\ \mathbf{S}^{IE},\mathbf{S}^{II}\in\{0,1\}^{N\times N}}}{\text{minimize}} \sum_{k\in\{EE,EI,IE,II\}} \sum_{1\le i,j\le N} (1-S_{ij}^k)\\
&\text{subject to}\\
&\mathbf{A}^k = \mathbf{S}^k \odot \hat{\mathbf{A}}^k \qquad k\in\{EE,EI,IE,II\} \\
&\mathbf{A}^{EE},\mathbf{A}^{EI},\mathbf{A}^{IE},\mathbf{A}^{II} \text{satisfy (7.8) } \forall i\in I_{\text{inactive}}\\
&\mathbf{A}^{EE},\mathbf{A}^{EI},\mathbf{A}^{IE},\mathbf{A}^{II} \text{satisfy (7.11) } \forall i\in I_{\text{oscillatory}}.
\end{aligned} \tag{7.13}$$

Here, $\odot$ denotes element-wise multiplication. In the above problem, $\mathbf{S}^k \in \{0,1\}^{N\times N}$, where $k\in\{EE,EI,IE,II\}$ is a matrix where $S_{ij}^k = 0$ if the edge between i and j is severed, and $S_{ij}^k = 1$ if it is preserved. The interpretation of the problem is that it finds the minimum number of edges that need to be severed in order for the modified network to have the desired properties. The modified network is given by $\mathbf{A} = (\mathbf{A}^{EE}, \mathbf{A}^{EI}, \mathbf{A}^{IE}, \mathbf{A}^{II})$, where $\mathbf{A}_{ij}^k = \hat{\mathbf{A}}_{ij}^k \mathbf{S}_{ij}^k$ Unlike (7.12), the problem (7.13) is not convex, but rather a mixed-integer program (MIP), which in general is NP-complete. However, modern MIP solvers [Mak08] employ a number of heuristic techniques which allows them to solve relatively large problems efficiently.

C Feasibility and Optimality of (7.12) and (7.13)

We now give conditions for (7.12) and (7.13) to be feasible. Intuitively, both problems are feasible if, in the absence of any interconnection, every $i \in I_{\text{inactive}}$ is inactive, and every $i \in I_{\text{oscillatory}}$ is oscillatory. This intuition is formalized in the following result.

Proposition 7.4.1 (Feasibility of (7.12) and (7.13))**.** *The problems* (7.12) *and* (7.13) *are feasible if and only if for all* $i \in I_{inactive}$, $\mathbf{u}_i$ *satisfies the hypothesis of Lemma 7.1.1, and for all* $i \in I_{oscillatory}$, $\mathbf{W}_i, \mathbf{u}_i, \mathbf{m}_i$ *satisfy the hypotheses of Theorem 6.3.1.*

Proof. We begin with the forward direction. Suppose that $\mathbf{A}^k = 0$ for $k \in \{EE, EI, IE, II\}$. Then it follows immediately that these matrices satisfy the constraints in (7.12). Similarly, if $\mathbf{S}_{ij}^k = 0$ for all $1 \leq i \leq j$, then it follows immediately that the constraints of (7.13) are satisfied.

To show the reverse direction, suppose that $\mathbf{A}^k$ for $k \in \{EE, EI, IE, II\}$ is feasible for (7.12). If $i \in I_{\text{inactive}}$, then $(\tilde{u}_i^E(\mathbf{x}), \tilde{u}_i^I(\mathbf{x}))$ solve (7.8) for all $\mathbf{x} \in X$, which implies that $(u_i^E, u_i^I) \leq 0$. Likewise, if $i \in I_{\text{oscillatory}}$, then $(\tilde{u}_i^E(\mathbf{x}), \tilde{u}_i^I(\mathbf{x}))$ solve (7.11) for all $\mathbf{x} \in X$, which implies that $(u_i^E, u_i^I) \in \mathcal{U}_i$. The same argument can be applied for the constraints of (7.13). □

Finally, we show that the optimization problem (7.12) solve Problem 7.2.3. This follows as a direct consequence of Theorems 7.3.1 and 7.3.4.

Theorem 7.4.2 (Network design via optimization)**.** *Suppose that for all* $i \in I_{inactive}$, $\mathbf{u}_i$ *satisfies the hypothesis of Lemma 7.1.1, and for all* $i \in I_{oscillatory}$, $\mathbf{W}_i, \mathbf{u}_i, \mathbf{m}_i$ *satisfy the hypotheses of Theorem 6.3.1. Then*

(i) Let $\mathbf{A} = (\mathbf{A}^{EE}, \mathbf{A}^{EI}, \mathbf{A}^{IE}, \mathbf{A}^{II})$ *solve* (7.12). *Then for all* $i \in I_{oscillatory}$, *the* i*th node of coupled network determined by* $\mathbf{A}$ *will be oscillatory, and for all* $i \in I_{inactive}$, *the* i*th node will be inactive;*

(ii) Let $\mathbf{A} = (\mathbf{A}^{EE}, \mathbf{A}^{EI}, \mathbf{A}^{IE}, \mathbf{A}^{II})$ *solve* (7.13). *Then for all* $i \in I_{oscillatory}$, *the* i*th node of coupled network determined by* $\mathbf{A}$ *will be oscillatory, and for all* $i \in I_{inactive}$, *the* i*th node will be inactive.*

7.4.2 Simulations

We illustrate here how the solutions to the optimization problems (7.12) and (7.13) produce network designs that accomplish the desired controlled spread of oscillations.

A Example with Random Network

In the first example, we consider a network of $N = 10$ nodes. For $i \in \{1, \ldots, 5\}$, the ith node satisfies the hypotheses of Lemma 7.1.1, and for $i \in \{6, \ldots, 10\}$, the ith node satisfies the hypotheses of Theorem 6.3.1. The interconnections $\mathbf{A}^{EE}$ and $\mathbf{A}^{EI}$ are given by random networks, and $\mathbf{A}^{IE} = \mathbf{A}^{II} = 0$. We modify the network using the design methodology outlined in Section 7.4.1, where $I_{\text{inactive}} = \{1, 2\}$ and $I_{\text{oscillatory}} = \{6, \ldots, 10\}$, and nodes $i \in \{3, 4, 5\}$ can be either oscillatory or inactive. Figure 7.3 shows the results.

Note that the nominal network does not satisfy the desired properties since there are nodes $i \in I_{\text{inactive}}$ which oscillate, and $i \in I_{\text{oscillatory}}$ do not oscillate and instead saturate at the upper limit. We modify the network designs both by continuously modifying the network weights using (7.12), and by severing edges using (7.13). Note that with both designs, the

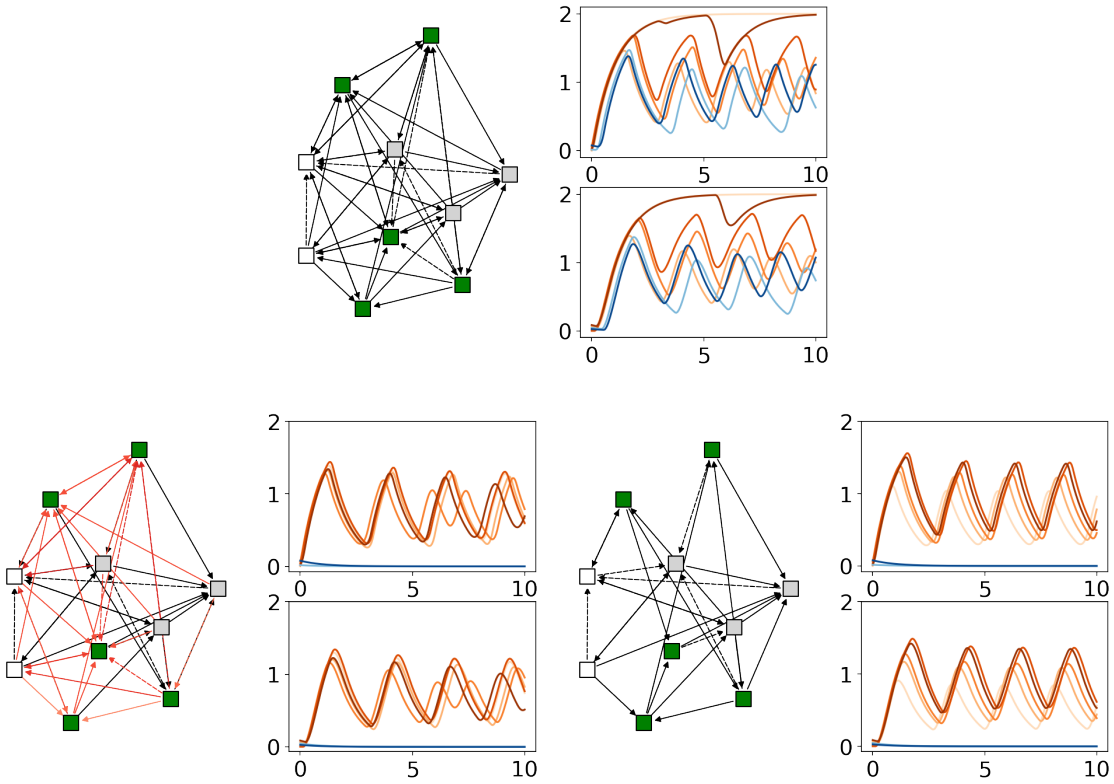

Figure 7.3: Illustration of the network design procedure. In each of the graphs, the edges given by $\mathbf{A}^{EE}$ are solid and edges given by $\mathbf{A}^{EI}$ are dashed. Each box represents a single EI pair, where the pairs in I_{inactive} are grey, the pairs in $I_{\text{oscillatory}}$ are green, and the pairs that are not in either of these sets are white. In each plot, the response of the excitatory node of each pair is on top, and the response of the inhibitory nodes are on bottom. The blue trajectories represent pairs $i \in I_{\text{inactive}}$ and orange trajectories represent pairs $i \in I_{\text{oscillatory}}$. Panel (a) displays the nominal network, where $\hat{\mathbf{A}}^{EE}$ and $\hat{\mathbf{A}}^{EI}$ are random networks. Panel (b) displays the network designed using (7.12). The red edges are those modified by the optimization, and the brightness corresponds to the magnitude of the modification. Finally, panel (c) displays the network designed using (7.13).

nodes in $i \in I_{\text{inactive}}$ are inactive, and nodes in $i \in I_{\text{oscillatory}}$ are robustly oscillatory.

B Example with Spatial Propagation

For our second example, consider a network of $N = 1230$ nodes. The first 1225 nodes in the network arranged in a 35×35 grid and satisfy the conditions in Lemma 7.1.1. The remaining 5 nodes, whose indices we denote by I_{driver}, satisfy the conditions in Lemma 6.3.1. The network has only excitatory-excitatory coupling, where each node in the grid is coupled to the nodes in the cells above, below, to the left and to the right, and the driver nodes are randomly coupled to nodes in in the grid ($\hat{\mathbf{A}}^{EE}$ denotes the adjacency matrix of the network). As shown in Figure 7.4(a), the oscillations from the 5 driver nodes spread throughout the network.

We now mark a region in the grid where we do not want the oscillations to spread. Let I_{inactive} denote the indices of these nodes. To determine how to modify the network interconnection, we use the optimization problem (7.12) to determine the interconnection weights $\mathbf{A}^{EE}$ of the modified network. As shown in Figure 7.4(b), the oscillations in the modified network spread from the driver nodes to other regions in the network while avoiding the region determines by the nodes in I_{inactive}.

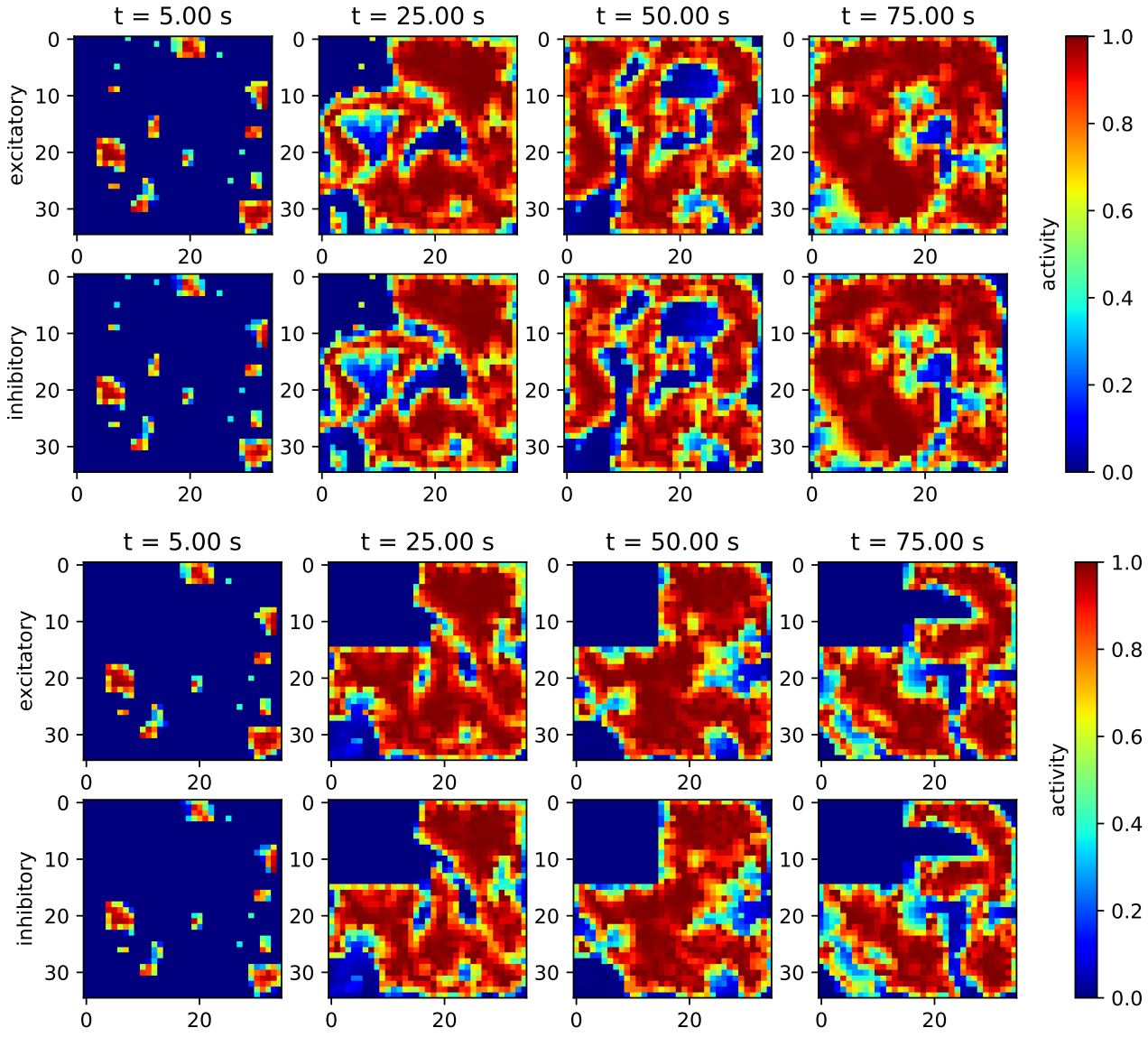

Figure 7.4: Spreading of oscillations in two 35×35 grids of EI pairs, as discussed in Section 7.4.2. Panel (a) shows four consecutive snapshots of the network activity for excitatory (top) and inhibitory (bottom) nodes in each EI pair of a randomly generated grid. We notice how oscillations originate from a subset of pairs, and spread throughout the nominal network. Panel (b) shows the network modified using (7.12), so that all pairs i in I_{inactive} are inactive. We find that 13 out of the 297 edges to nodes in I_{inactive} from nodes not in I_{inactive} have been modified (i.e., changes were made by (7.12) to less than 5% of the links between EI pairs).

7.5 Conclusions

We have studied the spreading of oscillations in complex networks of interconnected EI pairs. Such networks, modeled here with a piecewise-linear activation function, are an expressive modeling tool for oscillatory networks, with meaningful connections to brain dynamics. Motivated by the link between the spatial spread of oscillations and seizures in the brain, we have identified formal conditions on the network interconnection structure that determine which regions oscillate and which remain inactive. We have built on this understanding to propose strategies that mitigate the spread of oscillations among brain regions. These strategies formalize network design objectives by means of optimization programs with attractive numerical properties. The simulation results show that the proposed approach may be effective in practice. Future work will address the study of the emergence of oscillations through network interconnection and in particular characterize conditions for the nodes in networks of coupled EI pairs to be oscillatory without assuming that they admit oscillations individually. Further, we hope to compute tighter bounds on the sufficiency conditions for robust oscillations and to further validate these results through data-generated models of brain networks from human subjects.

Acknowledgements

This chapter, in full, is a reprint of the material [ACPC22] where it appears as "Optimal Network Interventions to Control the Spreading of Oscillations" by Ahmed Allibhoy, Federico Celi, Fabio Pasqualetti, and Jorge Cortés in IEEE Open Journal of Control Systems.

The dissertation author is one of the primary investigators and authors of this paper.

Conclusion

Chapter 8

Conclusion

This thesis addressed the control and optimization of interconnected systems. We focused on two specific instances of this challenge: (i) understanding the systems theoretic properties of optimization algorithms and using them to regulate dynamic physical processes, and modeling (ii) epileptic seizures in brain networks and optimally modifying the network structure to stop their spread. Here, we summarize the contributions of this thesis and propose directions for future work.

8.1 Summary

The first part of this thesis focuses on the systems theoretic aspects of optimization algorithms. After reviewing the literature and mathematical preliminaries in Chapter 2, we introduced the safe gradient flow in Chapter 3. The safe gradient flow is a continuous-time flow synthesized using techniques from safety-critical control that solves constrained nonlinear optimization problems while keeping the invariant set forward invariant and asymptoti-

cally stable. These properties make the system, when interpreted as an algorithm, anytime, meaning that it is guaranteed to return a feasible solution even when terminated early. This property is particularly useful for real-time applications where the algorithm might be interconnected with other physical processes, such as when the algorithm output is used to regulate a physical plant and constraints of the optimization problem ensure the safe operation of the plant.

In Chapter 4 we extended the framework developed in Chapter 3 to the setting of variational inequalities. This approach leads to reinterpretations of well-known algorithms from the lens of control theory, such as the projected monotone flow, and in other cases leads to entirely novel algorithms, such as the safe monotone flow and the recursive safe monotone flow. We thoroughly analyze the safety and stability properties of each flow, and demonstrate through numerical simulations the interconnection of the safe monotone flow with a linear dynamical system on a receding horizon linear quadratic dynamic game.

The second part of this thesis concerns modeling the human brain as a network dynamical system to understand and control epileptic seizures. We present an overview of mathematical modeling of neurological systems in Chapter 5. Next, in Chapter 6, we perform a detailed analysis of an EI Pair, a two-dimension linear threshold network that can be used to model populations of interacting neurons. We characterize all possible bifurcations of these systems, and relate the behavior of EI Pairs in different dynamical regimes to prototypical oscillations observed during epileptic seizures.

Finally, in Chapter 7 we consider networks of interconnected EI Pairs. We identify conditions which characterize the spatiotemporal spread of oscillations in the coupled net-

work. In particular, we obtain sufficient conditions that ensure harmful oscillations remain localized to certain regions of the network, and identify precisely which nodes participate in the oscillation. Once formal conditions on the spreading of oscillations are derived, we introduced an optimization-based framework to perturb the network structure so that it exhibits the desired localization of oscillations. We hope that this framework allows us to guide clinical interventions used to manage epilepsy, such as surgical resection and deep-brain stimulation.

8.2 Future Work

In this section we outline future research directions that build upon the results obtained in this thesis.

8.2.1 Interconnections of Dynamics with Optimizing Flows

A Discretization of Safe Gradient Flows

The algorithms considered in Chapter 3 and 4 are all continuous-time systems. While this makes the theoretical analysis easier, and is more natural for applications where the optimization algorithm is implemented in the form of a physical system, continuous-time algorithms are not always practical since they require continuous communication, sensor measurements, and actuation. For this reason, in the future, we would like to consider discretizations of the safe gradient flow and the safe monotone flow, which still preserve their stability and safety properties. Because Lipschitz continuity guarantees can be ob-

tained in certain cases, one approach is to use standard ODE discretization schemes like the Forward-Euler discretization, or the Runge-Kutta method. While we presented preliminary experiments on this approach in Chapter 3, a rigorous characterizing of conditions under which stability and safety are preserved can be done using tools outlined in [SH98]. Another approach would be the implementation of event-triggered discretization [HJT12], which also integrates well with the control-theoretic context in which these flows were originally derived, and for which safety and stability guarantees are known [TOCA21].

B Dynamically Varying Parameters

Another exciting frontier for future work is using optimizing flows to solve parametric optimization problems, where the parameters are varying dynamically. While the recursive safe monotone flow, and the implementation of the safe monotone flow on receding horizon dynamic games considered in Chapter 4 can be considered specific examples of this, special assumptions were needed to obtain stability and safety guarantees, such as separation of time scales and polyhedral constraint sets. However, the general case of designing optimizing flows with coupled parameter dynamics while ensuring safety, as well as convergence to the dynamically varying optimizer, is still an open problem. In the case of unconstrained problems, recent progress has been made using the framework of *sensitivity conditioning* [PBD22], where feed-forward control is used to ensure stability of the coupled system. However, this approach assumes differentiability of the dynamics, which may not hold in the presence of constraints. In the future, we hope to generalize these results to constrained systems and apply them to the flows derived in Chapter 3 and 4.

C Online Learning

As availability of data and computing power grows, the use of online learning for controlling unknown systems becomes more relevant. There are multiple ways to approach this problem. For example, this task can be formalized as an online feedback optimization problem, where the optimization problem corresponds to learning the system model, and the parameter dynamics correspond to the plant being controlled. In this case online control is enabled using the sensitivity conditioning approach [PBD22]. A second approach draws on ideas from extremum seeking control, where a dynamical system is steered to the optimizer of an unknown objective function. The key component that enables extremum seeking control approaches is the use of an oscillatory signal that allows the system to learn the gradient of the objective function. Combining this method of gradient estimation with the safe gradient flow opens the door to the possibility of optimizing flows that only need zeroth order information, making them ideal for online learning applications. To make this possible, however, we need a better understanding of the sensitivity and robustness properties of the safe gradient flow.

8.2.2 Dynamics and Control of Brain Networks

A Emergence of Oscillations Through Network Interconnection

While oscillations in LTNs were studied in Chapter 7, the analysis leveraged the idea of robustness, where individual nodes were assumed to be oscillatory, and we discussed conditions under which this property was robust to network interconnection. However, in

many cases, one is interested in the opposite situation, where individual nodes are not oscillatory, but oscillations emerge spontaneously after network interconnection. Understanding the emergence properties is key to future work in mathematically characterizing biomarkers of epilepsy, and will also inform the design of interventions to manage epileptic seizures, including through network optimization and feedback control. For example, one drawback of the optimization-based framework developed in Chapter 7 is that the designs were often overly conservative. A better understanding of the emergence of oscillations may enable network interventions which modify the network less aggressively.

B Online Control of Brain Networks

One exciting direction for future research is online control schemes for the prevention epileptic seizures. In contrast to the network interventions discussed in Chapter 7, which only modifies the parameters of the system, the goal of this line of research is controlling the dynamics of the network. Recent progress has already been made in this direction, For example vibrational control [QBP22b] has emerged as useful paradigm for controlling synchronization in brain networks. In order to control linear threshold networks to inhibit the spread of pathological oscillations, several challenges need to be addressed. First, feedback control requires access to real-time measurements from which the state of the system can be reconstructed. For neurological systems, most sensors can only acquire aggregate information of entire brain regions, and access to information about specific nodes requires invasively probing the brain. Secondly, the network can only be controlled through a sparse subset of the nodes. We hope to extend our work on LTNs to develop control strategies that can be

implemented with these limitations.

Bibliography

[AB08] V. Acary and B. Brogliato. *Numerical Methods for Nonsmooth Dynamical Systems: Applications in Mechanics and Electronics*, volume 35 of *Lecture Notes in Applied and Computational Mechanics*. Springer, New York, 2008.

[AC84] J. P. Aubin and A. Cellina. *Differential Inclusions*, volume 264 of *Grundlehren der mathematischen Wissenschaften*. Springer, New York, 1984.

[AC24] A. Allibhoy and J. Cortés. Control barrier function-based design of gradient flows for constrained nonlinear programming. *IEEE Transactions on Automatic Control*, 69(6), 2024. To appear.

[ACE+19] A. D. Ames, S. Coogan, M. Egerstedt, G. Notomista, K. Sreenath, and P. Tabuada. Control barrier functions: theory and applications. In *European Control Conference*, pages 3420–3431, Naples, Italy, 2019.

[ACPC22] A. Allibhoy, F. Celi, F. Pasqualetti, and J. Cortés. Optimal network interventions to control the spreading of oscillations. *IEEE Open Journal of Control Systems*, 1:141–151, 2022.

[ADGK+08] A. Arenas, A. Díaz-Guilera, J. Kurths, Y. Moreno, and C. Zhou. Synchronization in complex networks. *Physics Reports*, 469(3):93–153, 2008.

[AE10] A. Arsie and C. Ebenbauer. Locating omega-limit sets using height functions. *Journal of Differential Equations*, 248(10):2458–2469, 2010.

[AHU58] K. Arrow, L Hurwitz, and H. Uzawa. *Studies in Linear and Non-Linear Programming*. Stanford University Press, Stanford, CA, 1958.

[AK03] K. B. Ariyur and M. Krstić. *Real-Time Optimization by Extremum-Seeking Control*. Wiley, New York, 2003.

[AK06] P.-A. Absil and K. Kurdyka. On the stable equilibrium points of gradient systems. *Systems & Control Letters*, 55:573–577, 2006.

[AMA05] Pierre-Antoine Absil, Robert Mahony, and Benjamin Andrews. Convergence of the iterates of descent methods for analytic cost functions. *SIAM Journal on Optimization*, 16(2):531–547, 2005.

[BB03] S. P. Bhat and D. S. Bernstein. Nontangency-based Lyapunov tests for convergence and stability in systems having a continuum of equilibria. *SIAM Journal on Control and Optimization*, 42(5):1745–1775, 2003.

[BB10] S. P. Bhat and D. S. Bernstein. Arc-length-based Lyapunov tests for convergence and stability with applications to systems having a continuum of equilibria. *Mathematics of Control, Signals and Systems*, 22(2):155–184, 2010.

[BBB+12] MJ Brodie, SJE Barry, GA Bamagous, JD Norrie, and P Kwan. Patterns of treatment response in newly diagnosed epilepsy. *Neurology*, 78(20):1548–1554, 2012.

[BBCK08] M. Bernardo, C. Budd, A.R. Champneys, and P. Kowalczyk. *Piecewise-smooth Dynamical Systems: Theory and Applications*. Applied Mathematical Sciences. Springer London, 2008.

[BCPD22] G. Bianchin, J. Cortés, J. I. Poveda, and E. Dall'Anese. Time-varying optimization of LTI systems via projected primal-dual gradient flows. *IEEE Transactions on Control of Network Systems*, 9(1):474–486, 2022.

[BD95] M. J. Best and B. Ding. On the continuity of the minimum in parametric quadratic programs. *Journal of Optimization Theory & Applications*, 86(1):245–250, 1995.

[BD04] G. Buzsáki and A. Draguhn. Neuronal oscillations in cortical networks. *Science*, 304(5679):1926–1929, 2004.

[BDL06] Jérôme Bolte, Aris Daniilidis, and Adrian Lewis. A nonsmooth Morse–Sard theorem for subanalytic functions. *Journal of mathematical analysis and applications*, 321(2):729–740, 2006.

[BDL07] J. Bolte, A. Daniilidis, and A. Lewis. The Lojasiewicz inequality for nonsmooth subanalytic functions with applications to subgradient dynamical systems. *SIAM Journal on Optimization*, 17(4):1205–1223, 2007.

[BDLA06] B. Brogliato, A. Daniilidis, C. Lemaréchal, and V. Acary. On the equivalence between complementarity systems, projected systems, and differential inclusions. *Systems & Control Letters*, 55(1):45–51, 2006.

[Ber99] D. P. Bertsekas. *Nonlinear Programming*. Athena Scientific, Belmont, MA, 2nd edition, 1999.

[BF93] James V Burke and Michael C Ferris. Weak sharp minima in mathematical programming. *SIAM Journal on Control and Optimization*, 31(5):1340–1359, 1993.

[BHD10] M. Breakspear, S. Heitmann, and A. Daffertshofer. Generative models of cortical oscillations: neurobiological implications of the Kuramoto model. *Frontiers in Human Neuroscience*, 4:190, 2010.

[Bla99] F. Blanchini. Set invariance in control. *Automatica*, 35(11):1747–1767, 1999.

[BLM16] V. Bondarevsky, A. Leschov, and L. Minchenko. Value functions and their directional derivatives in parametric nonlinear programming. *Journal of Optimization Theory & Applications*, 171(2):440–464, 2016.

[BM88] E. Bierstone and P. D. Milman. Semianalytic and subanalytic sets. *Inst. Hautes Études Sci. Publ. Math.*, 67(1):5–42, 1988.

[BO99] T. Başar and G. J. Olsder. *Dynamic Noncooperative Game Theory*. SIAM, 2 edition, 1999.

[Bro91] R. W. Brockett. Dynamical systems that sort lists, diagonalize matrices, and solve linear programming problems. *Linear Algebra and Its Applications*, 146:79–91, 1991.

[Bul23] F. Bullo. *Contraction Theory for Dynamical Systems*. Kindle Direct Publishing, 1.1 edition, 2023.

[BV09] S. Boyd and L. Vandenberghe. *Convex Optimization*. Cambridge University Press, Cambridge, UK, 2009.

[CAPC21] F. Celi, A. Allibhoy, F. Pasqualetti, and J. Cortés. Linear-threshold dynamics for the study of epileptic events. *IEEE Control Systems Letters*, 5(4):1405–1410, 2021.

[CBD23] L. Cothren, F. Bullo, and E. Dall'Anese. Singular perturbation via contraction theory. *arXiv preprint arXiv:2310.07966*, 2023.

[CDB20] M. Colombino, E. Dall'Anese, and A. Bernstein. Online optimization as a feedback controller: Stability and tracking. *IEEE Transactions on Control of Network Systems*, 7(1):422–432, 2020.

[CGC17] A. Cherukuri, B. Gharesifard, and J. Cortés. Saddle-point dynamics: conditions for asymptotic stability of saddle points. *SIAM Journal on Control and Optimization*, 55(1):486–511, 2017.

[Cha96] P Chauvel. Stereoelectroencephalography. *Multimethodological Assessment of the Epileptic Forms*, 270, 1996.

[CMLC18] A. Cherukuri, E. Mallada, S. H. Low, and J. Cortés. The role of convexity in saddle-point dynamics: Lyapunov function and robustness. *IEEE Transactions on Automatic Control*, 63(8):2449–2464, 2018.

[CN19] J. Cortés and S. K. Niederländer. Distributed coordination for nonsmooth convex optimization via saddle-point dynamics. *Journal of Nonlinear Science*, 29(4):1247–1272, 2019.

[Cor08] J. Cortés. Discontinuous dynamical systems - a tutorial on solutions, nonsmooth analysis, and stability. *IEEE Control Systems*, 28(3):36–73, 2008.

[CPL22] Xin Chen, Jorge I Poveda, and Na Li. Model-free feedback constrained optimization via projected primal-dual zeroth-order dynamics. *arXiv preprint arXiv:2206.11123*, 2022.

[CVJB21] Pedro Cisneros-Velarde, Saber Jafarpour, and Francesco Bullo. A contraction analysis of primal-dual dynamics in distributed and time-varying implementations. *IEEE Transactions on Automatic Control*, 67(7):3560–3566, 2021.

[DA01] P. Dayan and L. F. Abbott. *Theoretical Neuroscience: Computational and Mathematical Modeling of Neural Systems*. Computational Neuroscience. MIT Press, Cambridge, MA, 2001.

[DB14] F. Dörfler and F. Bullo. Synchronization in complex networks of phase oscillators: a survey. *Automatica*, 50(6):1539–1564, 2014.

[DG89] G. Di Pillo and L. Grippo. Exact penalty functions in constrained optimization. *SIAM Journal on Control and Optimization*, 27(6):1333–1360, 1989.

[DJB22] A. Davydov, S. Jafarpour, and F. Bullo. Non-Euclidean contraction theory for robust nonlinear stability. *IEEE Transactions on Automatic Control*, 67(12):6667–6681, 2022.

[dSBK+03] F.H.L da Silva, W. Blanes, S.N. Kalitzin, J. Parra, P. Suffczynski, and D.N. Velis. Dynamical diseases of brain systems: different routes to epileptic seizures. *IEEE Transactions on Biomedical Engineering*, 50(5):540–548, 2003.

[DSEJ13] Hans-Bernd Dürr, Miloš S Stanković, Christian Ebenbauer, and Karl Henrik Johansson. Lie bracket approximation of extremum seeking systems. *Automatica*, 49(6):1538–1552, 2013.

[DSSPG19] F. Dörfler, S.Bolognani, J. W. Simpson-Porco, and S. Grammatico. Distributed control and optimization for autonomous power grids. In *European Control Conference*, Naples, Italy, June 2019.

[FBE21] Jan Feiling, Mohamed-Ali Belabbas, and Christian Ebenbauer. Gradient approximation and multivariable derivative-free optimization based on noncommutative maps. *IEEE Transactions on Automatic Control*, 67(12):6381–6396, 2021.

[FBM+94] T. L. Friesz, D. H. Bernstein, N. J. Mehta, R. L. Tobin, and S. Ganjlizadeh. Day-to-day dynamic network disequilibria and idealized traveler information systems. *Operations Research*, 42(6):1120–1136, 1994.

[FGW02] A. Forsgren, P. E. Gill, and M. H. Wright. Interior methods for nonlinear optimization. *SIAM Review*, 44(4):525–597, 2002.

[Fia76] A. V. Fiacco. Sensitivity analysis for nonlinear programming using penalty methods. *Mathematical Programming*, 10(1):287–311, 1976.

[Fit61] Richard FitzHugh. Impulses and physiological states in theoretical models of nerve membrane. *Biophysical Journal*, 1(6):445–466, 1961.

[FM90] A. V. Fiacco and G. P. McCormick. *Nonlinear Programming: Sequential Unconstrained Minimization Techniques*, volume 4 of *Classics in Applied Mathematics*. SIAM, Philadelphia, PA, 1990.

[FP03] F. Facchinei and J.-S. Pang. *Finite-Dimensional Variational Inequalities and Complementarity Problems*. Springer, 2003.

[FP10] D. Feijer and F. Paganini. Stability of primal-dual gradient dynamics and applications to network optimization. *Automatica*, 46:1974–1981, 2010.

[FSRV20] Guilherme França, Jeremias Sulam, Daniel P Robinson, and René Vidal. Conformal symplectic and relativistic optimization. *Journal of Statistical Mechanics: Theory and Experiment*, 2020(12):124008, 2020.

[FZB16] A. Fornito, A. Zalesky, and E. Bullmore. *Fundamentals of Brain Network Analysis*. Academic Press, 2016.

[FZE18] J. Feiling, A. Zeller, and C. Ebenbauer. Derivative-free optimization algorithms based on non-commutative maps. *IEEE Control Systems Letters*, 2(4):743–748, 2018.

[FZL20] Han Feng, Haixiang Zhang, and Javad Lavaei. A dynamical system perspective for escaping sharp local minima in equality constrained optimization problems. In *IEEE Conf. on Decision and Control*, pages 4255–4261, Jeju Island, Republic of Korea, December 2020.

[GCB06] A. Ganguli, J. Cortés, and F. Bullo. Maximizing visibility in nonconvex polygons: Nonsmooth analysis and gradient algorithm design. *SIAM Journal on Control and Optimization*, 45(5):1657–1679, 2006.

[GCC+21] Katharina Glomb, Joana Cabral, Anna Cattani, Alberto Mazzoni, Ashish Raj, and Benedetta Franceschiello. Computational models in electroencephalography. *Brain Topography*, pages 1–20, 2021.

[GM79] Leon Glass and Michael C Mackey. Pathological conditions resulting from instabilities in physiological control systems. *Annals of the New York Academy of Sciences*, 316(1):214–235, 1979.

[GZE18] Victoria Grushkovskaya, Alexander Zuyev, and Christian Ebenbauer. On a class of generating vector fields for the extremum seeking problem: Lie bracket approximation and stability properties. *Automatica*, 94:151–160, 2018.

[HBD21] A. Hauswirth, S. Bolognani, and F. Dörfler. Projected dynamical systems on irregular, non-Euclidean domains for nonlinear optimization. *SIAM Journal on Control and Optimization*, 59(1):635–668, 2021.

[HBHD21] A. Hauswirth, S. Bolognani, G. Hug, and F. Dörfler. Optimization algorithms as robust feedback controllers. *arXiv preprint arXiv:2103.11329*, 2021.

[HC08] W. Haddad and V. S. Chellaboina. *Nonlinear Dynamical Systems and Control: A Lyapunov-Based Approach*. Princeton University Press, Princeton, NJ, 2008.

[HE15] J. Harris and B. Ermentrout. Bifurcations in the Wilson-Cowan equations with nonsmooth firing rate. *SIAM Journal on Applied Dynamical Systems*, 14(1):43–72, 2015.

[HH52] A. L. Hodgkin and A. F. Huxley. A quantitative description of membrane current and its application to conduction and excitation in nerve. *The Journal of Physiology*, 117(4):500–544, 1952.

[HJT12] W. P. M. H. Heemels, K. H. Johansson, and P. Tabuada. An introduction to event-triggered and self-triggered control. In *IEEE Conf. on Decision and Control*, pages 3270–3285, Maui, HI, 2012.

[HM94] U. Helmke and J. B. Moore. *Optimization and Dynamical Systems*. Springer, 1994.

[HSB+18] Adrian Hauswirth, Irina Subotić, Saverio Bolognani, Gabriela Hug, and Florian Dörfler. Time varying projected dynamical systems with applications to feedback optimization of power systems. In *IEEE Conf. on Decision and Control*, pages 3258–3263, Nice, France, 2018. IEEE.

[HSW00] W. P. M. H. Heemels, J. M. Schumacher, and S. Weiland. Projected dynamical systems in a complementarity formalism. *Operations Research Letters*, 27:83–91, 2000.

[Iof09] Alexander D Ioffe. An invitation to tame optimization. *SIAM Journal on Optimization*, 19(4):1894–1917, 2009.

[Izh00] Eugene M Izhikevich. Neural excitability, spiking and bursting. *International Journal of Bifurcation and Chaos*, 10(6):1171–1266, 2000.

[Izh07] E. M. Izhikevich. *Dynamical Systems in Neuroscience*. MIT Press, Cambridge, MA, 2007.

[Jit84] K. Jittorntrum. Solution point differentiability without strict complementarity in nonlinear programming. In *Sensitivity, Stability and Parametric Analysis*, pages 127–138. Springer, 1984.

[JLvdB09] A. Jokic, M. Lazar, and P. J. van den Bosch. On constrained steady-state regulation: Dynamic KKT controllers. *IEEE Transactions on Automatic Control*, 54(9):2250–2254, 2009.

[JR95] Ben H Jansen and Vincent G Rit. Electroencephalogram and visual evoked potential generation in a mathematical model of coupled cortical columns. *Biological Cybernetics*, 73(4):357–366, 1995.

[KA18] S. Kolathaya and A. D. Ames. Input-to-state safety with control barrier functions. *IEEE Control Systems Letters*, 3(1):108–113, 2018.

[KG21] Suad Krilašević and Sergio Grammatico. An extremum seeking algorithm for monotone nash equilibrium problems. In *IEEE Conf. on Decision and Control*, pages 1232–1237. IEEE, 2021.

[KLA+21] Joachim K Krauss, Nir Lipsman, Tipu Aziz, Alexandre Boutet, Peter Brown, Jin Woo Chang, Benjamin Davidson, Warren M Grill, Marwan I Hariz, Andreas Horn, et al. Technology of deep brain stimulation: current status and future directions. *Nature Reviews Neurology*, 17(2):75–87, 2021.

[Kos56] T. Kose. Solutions of saddle value problems by differential equations. *Econometrica*, 24(1):59–70, 1956.

[KTG+10] Corey J Keller, Wilson Truccolo, John T Gale, Emad Eskandar, Thomas Thesen, Chad Carlson, Orrin Devinsky, Ruben Kuzniecky, Werner K Doyle, Joseph R Madsen, Donald L Schomer, Ashesh D Mehta, Emery N Brown, Leigh R Hochberg, István Ulbert, Eric Halgren, and Sydney S Cash. Heterogeneous neuronal firing patterns during interictal epileptiform discharges in the human cortex. *Brain*, 133(6):1668–1681, 2010.

[Kur98] Krzysztof Kurdyka. On gradients of functions definable in o-minimal structures. *Annales de l'institut Fourier*, 48(3):769–783, 1998.

[KW00] M. Krstić and H-H. Wang. Stability of extremum seeking feedback for general nonlinear dynamic systems. *Automatica*, 36(4):595–601, 2000.

[Lag07] Christian Lageman. Pointwise convergence of gradient-like systems. *Mathematische Nachrichten*, 280(13-14):1543–1558, 2007.

[Leb22] Maurice Leblanc. Sur l'electrification des chemins de fer au moyen de courants alternatifs de frequence elevee. *Revue générale de l'électricité*, 12(8):275–277, 1922.

[Liu95] J. Liu. Sensitivity analysis in nonlinear programs and variational inequalities via continuous selections. *SIAM Journal on Control and Optimization*, 33(4):1040–1060, 1995.

[LJJ20] Tianyi Lin, Chi Jin, and Michael I Jordan. Near-optimal algorithms for minimax optimization. In *Conference on Learning Theory*, pages 2738–2779. PMLR, 2020.

[LMNK20] Dominic Liao-McPherson, Marco M Nicotra, and Ilya V Kolmanovsky. Time-distributed optimization for real-time model predictive control: Stability, robustness, and constraint satisfaction. *Automatica*, 117:108973, 2020.

[Loj82] Stanislaw Lojasiewicz. Sur les trajectoires du gradient d'une fonction analytique. *Seminari di geometria*, 1983:115–117, 1982.

[LPD02] S. H. Low, F. Paganini, and J. C. Doyle. Internet congestion control. *IEEE Control Systems*, 22(1):28–43, 2002.

[LS02] Tzon-Tzer Lu and Sheng-Hua Shiou. Inverses of 2×2 block matrices. *Computers & Mathematics with Applications*, 43(1-2):119–129, 2002.

[LSPM21] L. S. P. Lawrence, J. W. Simpson-Porco, and E. Mallada. Linear-convex optimal steady-state control. *IEEE Transactions on Automatic Control*, 66(11):5377–5384, 2021.

[Mak08] Andrew Makhorin. GLPK (GNU linear programming kit), 2008. `http://www.gnu.org/s/glpk/glpk.html`.

[MBBP19] T. Menara, G. Baggio, D. S. Bassett, and F. Pasqualetti. A framework to control functional connectivity in the human brain. In *IEEE Conf. on Decision and Control*, pages 4697–4704, Nice, France, 2019. IEEE.

[MEK+15] Hil GE Meijer, Tahra L Eissa, Bert Kiewiet, Jeremy F Neuman, Catherine A Schevon, Ronald G Emerson, Robert R Goodman, Guy M McKhann, Charles J Marcuccilli, Andrew K Tryba, et al. Modeling focal epileptic activity in the wilson–cowan model with depolarization block. *Journal of Mathematical Neuroscience*, 5:1–17, 2015.

[MG77] Michael C Mackey and Leon Glass. Oscillation and chaos in physiological control systems. *Science*, 197(4300):287–289, 1977.

[MJ21] M. Muehlebach and M. I. Jordan. Optimization with momentum: Dynamical, control-theoretic, and symplectic perspectives. *Journal of Machine Learning Research*, 22(73):1–50, 2021.

[MJ22] M. Muehlebach and M. I. Jordan. On constraints in first-order optimization: A view from non-smooth dynamical systems. *Journal of Machine Learning Research*, 23:1–47, 2022.

[MWMM19] Bharat Monga, Dan Wilson, Tim Matchen, and Jeff Moehlis. Phase reduction and phase-based optimal control for biological systems: a tutorial. *Biological Cybernetics*, 113(1-2):11–46, 2019.

[NAY62] Jinichi Nagumo, Suguru Arimoto, and Shuji Yoshizawa. An active pulse transmission line simulating nerve axon. *Proceedings of the IRE*, 50(10):2061–2070, 1962.

[NC19] E. Nozari and J. Cortés. Oscillations and coupling in interconnections of two-dimensional brain networks. In *American Control Conference*, pages 193–198, Philadelphia, PA, July 2019.

[NC21a] E. Nozari and J. Cortés. Hierarchical selective recruitment in linear-threshold brain networks. Part I: Intra-layer dynamics and selective inhibition. *IEEE Transactions on Automatic Control*, 66(3):949–964, 2021.

[NC21b] E. Nozari and J. Cortés. Hierarchical selective recruitment in linear-threshold brain networks. Part II: Inter-layer dynamics and top-down recruitment. *IEEE Transactions on Automatic Control*, 66(3):965–980, 2021.

[NdS05] Ernst Niedermeyer and FH Lopes da Silva. *Electroencephalography: Basic Principles, Clinical Applications, and Related Fields*. Lippincott Williams & Wilkins, 2005.

[Nes83] Y. E. Nesterov. A method of solving a convex programming problem with convergence rate $O(1/k^2)$. *Soviet Mathematics Doklady*, 27(2):372–376, 1983.

[NLMK18] Marco M Nicotra, Dominic Liao-McPherson, and Ilya V Kolmanovsky. Embedding constrained model predictive control in a continuous-time dynamic feedback. *IEEE Transactions on Automatic Control*, 64(5):1932–1946, 2018.

[NPC22] E. Nozari, R. Planas, and J. Cortés. Structural characterization of oscillations in brain networks with rate dynamics. *Automatica*, 146:110653, 2022.

[NW06] J. Nocedal and S.J. Wright. *Numerical optimization*. Springer, Berlin, Heidelberg, 2006.

[NZ96] A. Nagurney and D. Zhang. *Projected Dynamical Systems and Variational Inequalities with Applications*, volume 2 of *International Series in Operations Research and Management Science*. Kluwer Academic Publishers, Dordrecht, The Netherlands, 1996.

[PBD22] M. Picallo, S. Bolognani, and F. Dörfler. Sensitivity conditioning: Beyond singular perturbation for control design on multiple time scales. *IEEE Transactions on Automatic Control*, 68(4):2309–2324, 2022.

[PP10] M. Pachter and K. D. Pham. Discrete-time linear-quadratic dynamic games. *Journal of Optimization Theory & Applications*, 146:151–179, 2010.

[QBP22a] Y. Qin, D. S. Bassett, and F. Pasqualetti. Vibrational control of cluster synchronization: Connections with deep brain stimulation. In *IEEE Conf. on Decision and Control*, Cancún, Mexico, December 2022. Submitted.

[QBP22b] Yuzhen Qin, Danielle S Bassett, and Fabio Pasqualetti. Vibrational control of cluster synchronization: Connections with deep brain stimulation. In *IEEE Conf. on Decision and Control*, pages 655–661. IEEE, 2022.

[RF10] H. L. Royden and P. Fitzpatrick. *Real Analysis*. Prentice Hall, 2010.

[RL01] Felix Rosenow and Hans Lüders. Presurgical evaluation of epilepsy. *Brain*, 124(9):1683–1700, 2001.

[RM09] J. B. Rawlings and D. Q. Mayne. *Model predictive control: theory and design*. Nob Hill Pub. cop., Madison, WI, 2009.

[Rob75] S. M. Robinson. Stability theory for systems of inequalities. Part I: Linear systems. *SIAM Journal on Numerical Analysis*, 12(5):754–769, 1975.

[Rob80] S. M. Robinson. Strongly regular generalized equations. *Mathematics of Operations Research*, 5(1):43–62, 1980.

[Rob83] S. M. Robinson. Generalized equations. In *Mathematical Programming The State of the Art: Bonn 1982*, pages 346–367. Springer, 1983.

[Roc70] R. T. Rockafellar. *Convex Analysis*. Princeton University Press, 1970.

[RW98] R. T. Rockafellar and R. J. B. Wets. *Variational Analysis*, volume 317 of *Comprehensive Studies in Mathematics*. Springer, New York, 1998.

[SBB+10] M. Stead, M. Bower, B.H. Brinkmann, K. Lee, W.R. Marsh, F.B. Meyer, B. Litt, J. Van Gompel, and G.A. Worrell. Microseizures and the spatiotemporal scales of human partial epilepsy. *Brain*, 133(9):2789–2797, 2010.

[SBC16] W. Su, S. Boyd, and E.J. Candès. A differential equation for modeling Nesterov's accelerated gradient method: theory and insights. *Journal of Machine Learning Research*, 17(1):5312–5354, 2016.

[SBS22] Raphael Schmetterling, Thiago B Burghi, and Rodolphe Sepulchre. Adaptive conductance control. *Annual Reviews in Control*, 2022.

[SDJS22] B. Shi, S. S. Du, M. I. Jordan, and W. J. Su. Understanding the acceleration phenomenon via high-resolution differential equations. *Mathematical Programming*, 195:79–148, 2022.

[SDSJ19] B. Shi, S. S. Du, W. Su, and M. I. Jordan. Acceleration via symplectic discretization of high-resolution differential equations. In H. Wallach, H. Larochelle, A. Beygelzimer, F. d'Alché Buc, E. Fox, and R. Garnett, editors, *Conference on Neural Information Processing Systems*, pages 5744–5752. Curran Associates, Inc., 2019.

[SH98] A. Stuart and A. R. Humphries. *Dynamical systems and numerical analysis*, volume 2. Cambridge University Press, 1998.

[SH08] Susan Spencer and Linda Huh. Outcomes of epilepsy surgery in adults and children. *The Lancet Neurology*, 7(6):525–537, 2008.

[Sha85] Alexander Shapiro. Second order sensitivity analysis and asymptotic theory of parametrized nonlinear programs. *Mathematical Programming*, 33(3):280–299, 1985.

[Sma00] S. Smale. Mathematical problems for the next century. In *Mathematics: frontiers and perspectives*, pages 271–294. American Mathematical Society, Providence, RI, 2000.

[Spe02] S.S. Spencer. Neural networks in human epilepsy: evidence of and implications for treatment. *Epilepsia*, 43(3):219–227, 2002.

[SS00] J. Schropp and I. Singer. A dynamical systems approach to constrained minimization. *Numerical functional analysis and optimization*, 21(3-4):537–551, 2000.

[SS06] Matti Sillanpää and Dieter Schmidt. Natural history of treated childhood-onset epilepsy: prospective, long-term population-based study. *Brain*, 129(3):617–624, 2006.

[Str00] S. H. Strogatz. *Nonlinear Dynamics and Chaos: With Applications to Physics, Biology, Chemistry, and Engineering*. Perseus Books Group, 2000.

[SVW+21] Nirit Sukenik, Oleg Vinogradov, Eyal Weinreb, Menahem Segal, Anna Levina, and Elisha Moses. Neuronal circuits overcome imbalance in excitation and inhibition by adjusting connection numbers. *Proceedings of the National Academy of Sciences*, 118(12):e2018459118, 2021.

[SW99] Marcin Studniarski and Doug E Ward. Weak sharp minima: characterizations and sufficient conditions. *SIAM Journal on Control and Optimization*, 38(1):219–236, 1999.

[Tan80] K. Tanabe. A geometric method in nonlinear programming. *Journal of Optimization Theory & Applications*, 30(2):181–210, 1980.

[TDH+11] Wilson Truccolo, Jacob A Donoghue, Leigh R Hochberg, Emad N Eskandar, Joseph R Madsen, William S Anderson, Emery N Brown, Eric Halgren, and Sydney S Cash. Single-neuron dynamics in human focal epilepsy. *Nature Neuroscience*, 14(5):635–641, 2011.

[TOCA21] A. J. Taylor, P. Ong, J. Cortés, and A. Ames. Safety-critical event triggered control via input-to-state safe barrier functions. *IEEE Control Systems Letters*, 5(3):749–754, 2021.

[TWCF11] Jonathan Touboul, Fabrice Wendling, Patrick Chauvel, and Olivier Faugeras. Neural mass activity, bifurcations, and epilepsy. *Neural Computation*, 23(12):3232–3286, 2011.

[VdDM96] Lou Van den Dries and Chris Miller. Geometric categories and o-minimal structures. *Duke Mathematical Journal*, 84(2):497–540, 1996.

[WC72] H. R. Wilson and J. D. Cowan. Excitatory and inhibitory interactions in localized populations of model neurons. *Biophysical Journal*, 12(1):1–24, 1972.

[WGTB14] Yujiang Wang, Marc Goodfellow, Peter Neal Taylor, and Gerold Baier. Dynamic mechanisms of neocortical focal seizure onset. *PLoS computational biology*, 10(8):e1003787, 2014.

[WKS23] A. Williams, M. Krstic, and A. Scheinker. Semi-global practical extremum seeking with practical safety. *arXiv preprint arXiv:2309.15401*, 2023.

[WM22] Dan Wilson and Jeff Moehlis. Recent advances in the analysis and control of large populations of neural oscillators. *Annual Reviews in Control*, 54:327–351, 2022.

[WRJ21] Ashia C Wilson, Ben Recht, and Michael I Jordan. A lyapunov analysis of accelerated methods in optimization. *The Journal of Machine Learning Research*, 22(1):5040–5073, 2021.

[WSH+23] A. Williams, A. Scheinker, E. Huang, C. Taylor, and M. Krstic. Experimental safe extremum seeking for accelerators. *arXiv preprint arXiv:2308.15584*, 2023.

[WWJ16] A. Wibisono, A. C. Wilson, and M. I. Jordan. A variational perspective on accelerated methods in optimization. *Proceedings of the National Academy of Sciences*, 113(47):E7351–E7358, 2016.

[XW00] Y. S. Xia and J. Wang. On the stability of globally projected dynamical systems. *Journal of Optimization Theory & Applications*, 106(1):129–150, 2000.

[Yam80] H. Yamashita. A differential equation approach to nonlinear programming. *Mathematical Programming*, 18(1):155–168, 1980.

[Yen95] N. D. Yen. Lipschitz continuity of solutions of variational inequalities with a parametric polyhedral constraint. *Mathematics of Operations Research*, 20(3):695–708, 1995.